CSIRO MARINE & ATMOSPHERIC RESEARCH
www.csiro.au

Upper Hunter Valley Particle Characterization Study

Final Report

17 September 2013

Mark Hibberd, Paul Selleck, Melita Keywood

CSIRO Marine & Atmospheric Research

David Cohen, Eduard Stelcer and Armand Atanacio

Institute for Environmental Research, ANSTO

Prepared for
NSW Office of Environment and Heritage (Contact: Matt Riley)
NSW Department of Health (Contact: Wayne Smith)

ISBN: 978-1-4863-0170-6

Citation

Hibberd MF, Selleck, PW, Keywood MD, Cohen DD, Stelcer E and Atanacio, AJ (2013). Upper Hunter Particle Characterisation Study. CSIRO, Australia.

Contact addresses:

CSIRO Marine & Atmospheric Research
Private Bag 1
Aspendale, Vic 3195
Australia

Institute for Environmental Research, ANSTO
Locked Bag 2001
Kirrawee DC, NSW 2232
Australia

Copyright and disclaimer

Important disclaimer

-

Contents

Executive Summary

This study provides an analysis of the composition of $PM_{2.5}$ (particulate matter with a diameter of less than 2.5 micrometres) in the two main population centres in the Upper Hunter, namely Muswellbrook and Singleton, during 2012.The finer $PM_{2.5}$ particles have been studied because they are of greatest concern owing to their impact on health.

Samples were collected for 24 hours every third day and analysed for the components of $PM_{2.5}$, specifically twenty elements, fourteen soluble ions, two anhydrous sugars (levoglucosan and mannosan) that are found in woodsmoke, organic carbon (OC), and black carbon (BC), as well as gravimetric mass.

The chemical composition of all the samples from each site was analysed using a mathematical technique called Positive Matrix Factorisation (PMF), which is widely used in air pollution source apportionment studies. This identified eight factors (also called 'fingerprints') which represent the mix of components that tend to vary together in time. Further analysis, using information about known sources and knowledge of atmospheric chemistry as well as wind sector and seasonal analysis, was undertaken to identify the most likely source of emissions for each factor and hence the contribution that each source makes to the measured $PM_{2.5}$ concentrations.

The veracity of the final results was confirmed by the good agreement between separate analyses using two different PMF techniques (EPA PMF 3.0 and PMF2 DOS). The differences between them provide an indication of the uncertainties in apportioning source contributions, which was typically 10% of each source contribution. The results for the whole year from the CSIRO PMF analysis are summarised in Table 1. At Singleton the dominant factors during the year were identified as:

- Factor 3 (Secondary Sulfate), 20 ± 2%
- Factor 5 (Industry Aged Sea Salt), 18 ± 3%
- Factor 2 (Vehicle/Industry), 17 ± 2%
- Factor 1 (Woodsmoke), 14 ± 2%
- Factor 6 (Soil), 12 ± 2%.

At Muswellbrook the dominant factors were identified as:

- Factor 1 (Woodsmoke), 30 ± 3%
- Factor 3 (Secondary Sulfate), 17 ± 2%
- Factor 5 (Industry Aged Sea Salt), 13 ± 2%
- Factor 4 (Biomass Smoke), 12 ± 2%
- Factor 6 (Soil), 11 ± 1%.

Table 1 lists the PMF factors, their names based on the dominant sources identified in their fingerprints, and the contribution of each factor to the total $PM_{2.5}$ concentrations in Singleton and Muswellbrook.

The identification of most of the Factors is reasonably clear-cut because of the use of either unique tracer species, e.g. levoglucosan for Factor 1 (Woodsmoke), or two or more species whose ratios are defined by a particular source, e.g. Si and Al in Factor 6 (Soil), Na^+ and Mg^{2+} in Factor 7 (Sea Salt), and NH_4^+ and SO_4^{2-} in Factor 3 (Secondary Sulfate). However in the case of Factor 2 (Vehicle/Industry) and Factor 4 (Biomass Smoke), the identification of the source is less definitive.

Factor 1 (Woodsmoke) dominates at both sites during the winter, while Factor 3 (Secondary Sulfate) and Factor 5 (Industry Aged Sea Salt) make higher contributions during summer months. The seasonal variations in the contributions from each factor are shown in Figure 1 and Figure 2.

Table 1 Summary of the PMF factors (from the EPA PMF 3.0 analysis), main species, contributions of these factors at each site and potential sources

Factor	Main Species in Factor	Contribution of the factor to total annual $PM_{2.5}$ mass at:		Potential Sources
		Singleton	Muswellbrook	
Factor 1 Woodsmoke	levoglucosan, mannosan, OC1	14 ± 2%	30± 3%	Domestic woodheaters
Factor 2 Vehicle/Industry	BC, OC1, OC2, SO_4^{2-} Fe, Zn, Mn, Cu	17 ± 2%	8 ± 1%	Vehicles, industry
Factor 3 Secondary Sulfate	NH_4^+, SO_4^{2-}	20 ± 2%	17 ± 2%	Local and regional sources of SO_2 such as power stations
Factor 4 Biomass Smoke	OC2, OC3, OC4, K, SO_4^{2-}, Al, Si, Ti, BC	8 ± 2%	12 ± 2%	Wildfires, hazard reduction burns
Factor 5 Industry Aged Sea Salt	Na^+, Mg^{2+}, SO_4^{2-} and with almost no Cl^-	18 ± 3%	13 ± 2%	Sea salt, local and regional sources of SO_2 such as power stations
Factor 6 Soil	Al, Si, Ca, Ti and Fe	12 ± 2%	11 ± 1%	Soil dust, fugitive coal dust
Factor 7 Sea Salt	Na^+, Cl^-, and Mg^{2+}	8 ± 1%	3 ± 1%	Sea salt
Factor 8 Secondary Nitrate	NO_3^- and includes some NH_4^+, Cl^-, Na^+, OC	3 ± 2%	6 ± 1%	Motor vehicle NO_2, power station NO_2

Notes: Al – aluminium; BC – black carbon; Ca – calcium; Cl^- – chloride; Cu – copper; Fe – iron; K – potassium; Mg^{2+} – magnesium; Mn – manganese; Na^+ – sodium; NH_4^+ – ammonium; NO_3^- – nitrate; OC1-OC4 – fractions of organic carbon distinguished by the volatility of the organic compounds, OC1 is the most volatile, as organic aerosol ages its OC becomes less volatile; Si – silicon; SO_4^{2-} – sulfate; Ti – titanium; Zn – zinc.

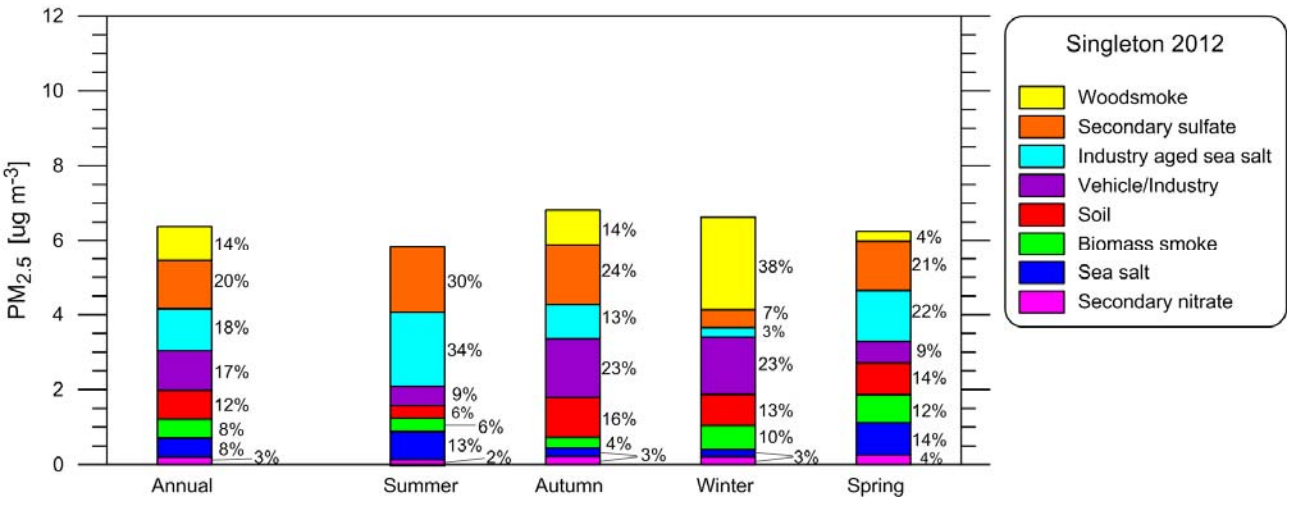

Figure 1 Annual and seasonal contributions of the PMF factors to $PM_{2.5}$ in Singleton

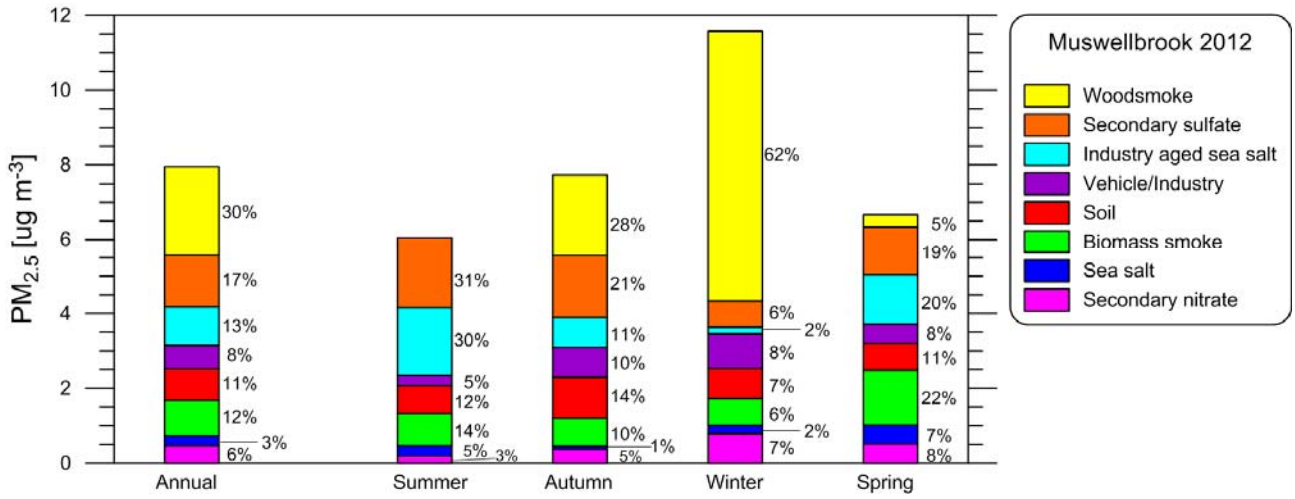

Figure 2 Annual and seasonal contributions of the PMF factors to $PM_{2.5}$ in Muswellbrook

Acknowledgments

This is a CSIRO co-investment project funded by

NSW Office of Environment & Heritage

NSW Department of Health

CSIRO Climate & Atmosphere Theme

We acknowledge the assistance provided by OEH staff in organising, setting up and running the sampling equipment – Chris Eiser, Melinda Hale, Scott Thompson, Matt Flack and John Kirkwood.

We acknowledge the contributions of the ANSTO project team: Peter Drewer who assisted with the sampling program and the ANSTO accelerator staff involved in the IBA analyses.

We acknowledge the contributions of the CSIRO project team: Kate Boast, Fabienne Reisen and Mahendra Buhjel for the analyses.

1 Introduction

1.1 Aim of Study

The objective of the Upper Hunter Valley Particle Characterization Study was to determine the major components and sources of particulate matter (as $PM_{2.5}$ – particles with a diameter of less than 2.5 micrometres) in the two main population centres in the Upper Hunter Valley, namely Singleton and Muswellbrook (Figure 3, see also Figure 35).

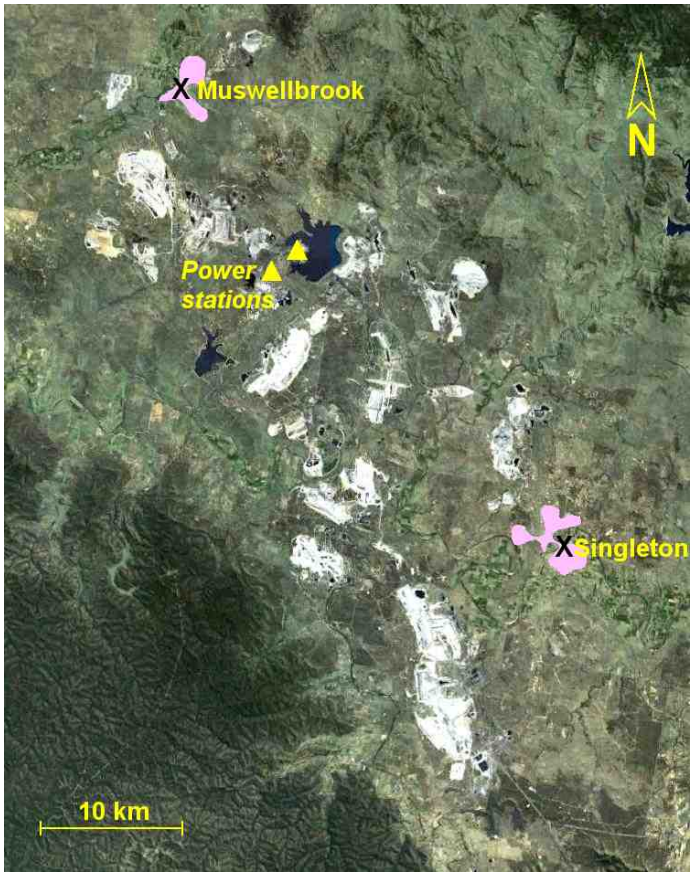

Figure 3 Overview of the Upper Hunter showing the locations of the measurement sites used in this study at Singleton and Muswellbrook (urban areas shaded pink) as well as the location of the two coal-fired power stations.

1.2 Project description

This project collected $PM_{2.5}$ samples in the two main population centres in the Upper Hunter, namely Muswellbrook and Singleton during the full calendar year of 2012. Two different types of samplers were used to collect 24-hour samples from midnight to midnight every third day. Two samplers were required since different chemical analyses require different filter media. One sampler collected particles on quartz fibre filters for the analysis of organic carbon, elemental carbon, soluble ions, and anhydrous sugars, while the second sampler collected particles on stretched Teflon filters for the analysis of elemental composition, soluble ions, black carbon and gravimetric mass. A range of analysis techniques was employed to determine the concentrations of these species. The chemical composition of all the samples from each site was then

analysed using Positive Matrix Factorisation to determine source fingerprints and the contribution that each source makes to the total $PM_{2.5}$ concentrations. This analysis provides:

- a description of the contributors to fine particles in the Upper Hunter
- an estimate of which sources are important and their relative contribution to fine particles in the Upper Hunter
- an indication of seasonal changes in the relative importance of the various sources to $PM_{2.5}$ in the Upper Hunter.

2 Sampling methodology

2.1 Measurement sites

Figure 3 shows the location of the monitoring sites in Singleton and Muswellbrook in the Upper Hunter valley of NSW, Australia. The many open-cut coal mines show up as white areas. There are two major power stations (Bayswater and Liddell) situated between the two towns with a total installed generating capacity of 5.6 GW. The axis of the valley is aligned approximately north-west to south-east with Singleton located about 70 km from the coast.

Figure 4 shows the location of the Singleton site with respect to rest of the town, the surrounding agricultural land and the nearest mine sites. Figure 6 shows a photograph of the monitoring station with the view towards the north.

The equivalent information for the Muswellbrook site is given in Figure 5 and Figure 6, with latter showing the view towards the south-east.

Figure 4 Location maps for Singleton monitoring site (X) at 32.5575°S, 151.1769°E

Figure 5 Location maps for Muswellbrook monitoring site (X) at 32.2717°S, 150.8858°E

Figure 6 Monitoring stations at Singleton (left) and Muswellbrook (right), which are part of the Upper Hunter Air Quality Monitoring Network (UHAQMN)

At both sites the equipment was located on the roof platforms of the NSW Office of Environment and Heritage (OEH) Upper Hunter Air Quality Monitoring Network (UHAQMN) sites. These sites include equipment to make routine measurements of $PM_{2.5}$ concentrations using a BAM (beta attenuation mass monitor) and PM_{10} measurements using a TEOM (tapered element oscillating microbalance) as well as NO_2 and SO_2 concentrations and meteorological measurements of temperature, relative humidity, wind speed and wind direction using an ultrasonic anemometer.

2.2 Sampling equipment

Two types of sampling equipment were used in this study that enabled the analysis of a wide range of constituents. These were:

- Ecotech HiVol 3000 high volume samplers with a $PM_{2.5}$ size selective inlet. These $PM_{2.5}$ samples were collected on quartz tissue filters and analysed by CSIRO.
- ANSTO ASP (Aerosol Sampling Program) $PM_{2.5}$ particulate Cyclone samplers with 25mm stretched Teflon filters. These samples were analysed by ANSTO and CSIRO.

Both types of samplers were installed at each site on the roof-top sampling platform about 4 m above the ground.

Note that different filters were required for the various analyses. The method for determining OC (organic carbon) and EC (elemental carbon) involves combusting the sample, hence a filter substrate that includes organic material (such as Teflon) is not appropriate because it will have very high blank concentrations. Similarly the fibrous nature of the quartz filters means that their gravimetric mass is not stable, so that quartz filters cannot be used for the determination of gravimetric mass. The ultra thin stretched Teflon filters together with the low volume sampling are optimised for IBA techniques at ANSTO. Finally, quartz filters cannot be used for ion beam analysis (such as PIXE) because they are typically too thick and have high blank elemental concentrations.

2.2.1 HIGH VOLUME SAMPLER

An Ecotech 3000 high volume sampler with a $PM_{2.5}$ size-selective inlet was used (Figure 7). The ambient flow rate through the inlet is 67.8 m^3 hr^{-1}. The flow rate is controlled with a mass flow controller, and the ambient temperature and pressure are monitored during sampling so that both the ambient volumetric and standard flow rates can be determined. The flow rate was audited and calibrated using a calibration orifice plate every 3-6 months. Samples were collected on 250 mm x 200 mm quartz membrane filters (Pall-Gelman; prebaked at 600°C for 4 hours to minimize for adsorbed organic vapours). Samples were collected

for 24 hours from midnight to midnight (Australian Eastern Standard time) on a 1-day-in-3-cycle. The filters were stored in sealed containers within a freezer before and after the sampling.

One field blank sample was collected once per month at each site by placing a pre-baked filter into the sample holder and running the sampler for 1 minute (total of 24 field blank samples). The field blank filters were then subject to the same filter handling and analysis procedures as the sample filters. In addition for the collection of 50% of the samples, two filters were placed in the filter holder in sequence (front filter and back filter) to correct for sampling artefacts on the OC and EC concentrations. Positive artefacts arise from the adsorption of volatile gases onto the filter material and negative artefacts arise from the degassing of semi-volatile compounds from the collected aerosol on the front filter which may be then absorbed onto the back filter.

The sample collection rate was 100% in that all samples were returned to CSIRO for analysis.

Figure 7 CSIRO high volume sampler at Singleton with flow rate calibration being carried out

2.2.2 ANSTO $PM_{2.5}$ ASP SAMPLER

The ANSTO built ASP sampling unit is a $PM_{2.5}$ cyclone type sampler based on the US EPA IMPROVE system used across North America in their National Parks air monitoring program. The cyclone operates at a flow rate of 22 L min^{-1} using a mass flow controller which results in a $PM_{2.5}$ particle size cut-off. The particles are collected on a 25mm diameter thin stretched Teflon filter masked to 17 mm diameter to increase sample thickness and improve deposit uniformity. The filters and the sampling regime are specifically designed for the ANSTO ion beam analysis (IBA) system described below. Samples were collected over the same time period and on the same days as the high volume sampler to enable comparison of data.

The sample collection rate was 100% in that all samples were returned to ANSTO for analysis.

Figure 8 ANSTO ASP sampler with cover open for filter changing

3 Analysis techniques

3.1 Mass measurements

The mass of $PM_{2.5}$ on the 25 mm Teflon filters was determined gravimetrically. The filters were weighed before and after the sampling period to determine the particulate mass collected and then divided by the total volume of air that passed through the filter to obtain the $PM_{2.5}$ concentration. The weighing was performed under controlled conditions of 22 ± 2°C and 50 ±10% relative humidity.

3.2 Ion beam analysis (IBA) techniques

The 25 mm Teflon filters were analysed non-destructively on the ANSTO STAR 2MV accelerator using nuclear IBA techniques.

The simultaneous IBA techniques applied are:

- Proton induced X-ray emission (PIXE) – for analysis of elements from aluminium to lead in concentrations from a few ng m^{-3} upwards, as described in Cohen (1993).
- Proton induced gamma-ray emission (PIGE) – for analysis of light elements such as fluorine and sodium in concentrations above 100 ng m^{-3}, as described in Cohen (1998).
- Proton elastic scattering analysis (PESA) – for analysis of hydrogen at levels down to 20 ng m^{-3}, as described in Cohen (1996).

A full description of these methods and how they are used can be found on the ANSTO web page at www.ansto.gov.au/environment/iba together with key publications describing other fine particle studies at ANSTO.

The elements whose concentrations were determined are:

- Hydrogen (H)
- Sodium (Na)
- Aluminium (Al)
- Silicon (Si)
- Phosphorous (P)
- Sulfur (S)
- Chlorine (Cl)
- Potassium (K)
- Calcium (Ca)
- Titanium (Ti)
- Vanadium (V)
- Chromium (Cr)
- Manganese (Mn)
- Iron (Fe)
- Cobolt (Co)
- Nickel (Ni)
- Copper (Cu)
- Zinc (Zn)
- Bromine (Br)
- Lead (Pb)

3.3 Ion chromatography

A 6.25 cm^2 portion of each quartz filter was analysed for major water soluble ions by suppressed ion chromatography (IC) and for anhydrous sugars including levoglucosan by high-performance anion-exchange chromatography with pulsed amperometric detection (HPAEC-PAD). The filter portions were extracted in 10 ml of 18.2 mΩ de-ionized water. The sample is then preserved using 1% chloroform. The ANSTO teflon filter was also analysed for water soluble ions by IC after IBA was carried out by ANSTO. The Teflon filter was first wetted with 100 µl of methanol, extracted in 5 ml of 18.2 mΩ de-ionized water and then preserved with 1% chloroform.

Anion and cation concentrations were determined with a Dionex ICS-3000 reagent free ion chromatograph. Anions were separated using a Dionex AS17c analytical column (2 x 250 mm), an ASRS-300 suppressor and a gradient eluent of 0.75 mM to 35 mM potassium hydroxide. Cations were separated using a Dionex CS12a column (2 x 250 mm), a CSRS-300 suppressor and an isocratic eluent of 20 mM methanesulfonic acid.

Anhydrous sugar concentrations were determined by HPAEC-PAD with a Dionex ICS-3000 chromatograph with electrochemical detection. The electrochemical detector utilizes disposable gold electrodes and is operated in the integrating (pulsed) amperometric mode using the carbohydrate (standard quad) waveform. Anhydrous sugars are separated using a Dionex CarboPac MA 1 analytical column (4 x 250mm) with a gradient eluent of 300 mM to 550 mM sodium hydroxide.

The species whose concentrations were determined are:

- Chloride (Cl^-)
- Nitrate (NO_3^-)
- Sulfate (SO_4^{2-})
- Oxalate ($C_2O_4^-$)
- Formate ($HCOO^-$)
- Acetate (CH_3COO^-)
- Phosphate (PO_4^{3-})
- Methanosulfonate (MSA^-)
- Sodium (Na^+)
- Ammonium (NH_4^+)
- Magnesium (Mg^{2+})
- Calcium ($Ca^{2+)}$
- Potassium (K^+)
- Levoglucosan ($C_6H_{10}O_5$, an anhydrous sugar - woodsmoke tracer)
- Mannosan ($C_6H_{10}O_5$, an anhydrous sugar - woodsmoke tracer)

3.4 Organic carbon (OC) and Elemental carbon (EC) analysis

The carbon in $PM_{2.5}$ is analysed to obtain two separate components – organic carbon and elemental carbon – because different sources emit different types of carbon. Elemental carbon is principally emitted during the combustion of fossil fuels as small, sooty particles often with other chemicals attached to their surface.

Organic carbon is the carbon in organic compounds in $PM_{2.5}$. In practice this includes most compounds that contain carbon, excluding particles that are just elemental carbon. Sources of organic carbon include traffic and industrial combustion

Elemental and organic carbon analysis was performed using a DRI Model 2001A Thermal-Optical Carbon Analyzer following the IMPROVE-A temperature protocol (Chow et al., 2007). Laser reflectance is used to correct for charring, since reflectance has been shown to be less sensitive to the composition and extent of primary organic carbon. Prior to analysis of filter samples, the sample is baked in an oven to 910°C for 10 minutes to remove residual carbon. System blank levels are then tested until < 0.20 μg C cm^{-2} is reported (with repeat oven baking if necessary). Twice daily calibration checks are performed to monitor possible catalyst degeneration. The analyser is reported to effectively measure carbon concentrations between 0.05 – 750 μg C cm^{-2}, with uncertainties in OC and EC of ± 10%.

The IMPROVE-A carbon method measures four OC fractions at four non-oxidizing heat ramps (OC1 at 140°C, OC2 at 280°C, OC3 at 480°C, OC4 at 580°C) and three EC fractions at three oxidizing heat ramps (EC1 at 580°C, EC2 at 740°C, EC3 at 840°C). The quartz filter sample is held at the target temperature until all carbon is desorbed at that fraction. During the non-oxidizing heat ramps some of the OC can be pyrolyzed and will not desorb until the oxidized stages. The quantity of OC that was pyrolyzed (OCpyro) during the non-oxidizing heat ramps is determined based on the time the reflectance of the filter rises back up to its initial value. Total OC is then calculated from the addition of all the OC fractions plus OCpyro. Total EC is calculated from the addition of all the EC fractions minus OCpyro.

As discussed in Appendix A, analysis of the initial results showed that EC was overestimated, and for the results presented in this report did not include OCpyro in the OC fraction.

3.5 Black carbon (BC) analysis

ANSTO measured black carbon (BC) on their 25 mm Teflon filters using a light absorption technique called the Laser Integrated Plate Method (LIPM). Black carbon concentrations generally agree well with elemental carbon concentrations (USEPA 2012) but differences arise because the two techniques each measure different but related properties of the carbon. As discussed in Appendix A because of problems identified in the EC measurements, the BC results were used in the PMF analysis.

For LIPM measurements, light from a HeNe laser (wavelength 633 nm) is diffused and collimated to give a uniform beam across the Teflon filter. The transmitted signal intensity is measured using a photodiode detector on each filter before and after exposure. The BC concentration is estimated from these two transmission measurements assuming a mass absorption coefficient value of 7 $m^2 g^{-1}$ for carbon particles. Full details can be found in a publication by Taha et al. (2007).

3.6 Positive matrix factorisation (PMF)

Positive Matrix Factorisation (PMF) is a multivariate factor analysis tool that decomposes a matrix of speciated sample data into two matrices – factor contributions and factor profiles. These factors are then interpreted to determine what sources are represented by these factors. This is done using measured source profile information, wind direction analysis, and emissions inventories (Norris et al., 2008). The method is described in greater detail by Paatero (1997).

PMF is widely used in air pollution studies for source apportionment, including in Australia (e.g. Chan et al., 2008; Cohen et al., 2011; Cohen et al., 2012). The US EPA has developed a software package to implement this technique and EPA PMF 3.0 (Norris et al., 2008). Analysis was also undertaken by ANSTO using PMF2 DOS and these results are reported in Appendix C

In the main analysis for this study, the chemical composition data of all the samples from each site was analysed using the EPA PMF software. This identified a number of factors. Each factor has a 'fingerprint' which represent a mix of components that generally occur together in the data. To understand what this means, consider a simplified example of fine particles of sea salt in the air formed from sea spray. The ratio of the concentrations of the main elements in sea water is well known – the ratio of [Na:Cl:Mg:Ca] is equal to [1:1.8:0.12:0.04]. Thus on days when there are fine sea salt particles in the $PM_{2.5}$, the chemical analysis of the filters will show these elements occurring together in the above proportions. On some days, the concentrations will all be higher and on other days lower but the proportions will stay the same. It is this principal that underlies PMF. In practice, there are many potential sources of $PM_{2.5}$ but PMF does not require or use any *a priori* information about the chemical composition of possible $PM_{2.5}$ sources. Rather it uses a mathematical technique to identify the factors. Indeed an advantage of the PMF over other source apportionment techniques is that it is able to identify the presence of particles which are not directly emitted as particles (primary particles) but form by chemical reactions in the atmosphere and gas-to-particle conversions (secondary particles).

Once the factors are obtained, further analysis is undertaken to identify the sources in each factor. This uses information about known sources and other knowledge of atmospheric chemistry as well as wind sector and seasonal analysis to identify the most likely source of emissions for each factor and hence the contribution that each source makes to the total $PM_{2.5}$ concentrations. In many cases, there is a single dominant source in a factor and this has been used to name the factors in Section 6. However, if sources are co-located or otherwise correlated, they can appear together in a single factor or across several factors. This is discussed in Section 6.

3.7 Wind sector analysis

To determine the directions from the sampling site which are likely to include the locations of the sources, the conditional probability function (CPF) technique was used. This couples the source contribution

estimates from PMF with the wind directions measured at the sampling site (e.g. Kim and Hopke, 2004). The CPF estimates the probability that a given source contribution from a given wind direction will exceed a pre-determined criterion. It is defined as

$$CPF = m_{\Delta\theta}/n_{\Delta\theta}$$

where $m_{\Delta\theta}$ is the number of occurrences from wind sector $\Delta\theta$ that exceed the criterion and $n_{\Delta\theta}$ is the total number of data from the same wind sector. In this study, the optimum value of the size of the wind sector $\Delta\theta$ was found to be 20°. Wind speeds below 0.5 m s^{-1} were excluded from the analysis as these were considered to represent calm conditions.

Daily fractional mass contribution from each source was used rather than the absolute source contribution. The criterion was set as the upper 25^{th} percentile of the fractional contribution from each source. The same daily fraction was assigned to each hour of a given day to match the hourly wind data. Although it might seem more appropriate to match the (24-hour average) $PM_{2.5}$ data with the corresponding 24-hour average wind direction, the loss of information in averaging the wind directions produces poorer results from the CPF analysis than using the method outlined above.

4 Monitoring results

4.1 $PM_{2.5}$ time series

Figure 9 shows the time series of 24-hour average $PM_{2.5}$ concentrations measured at Singleton by the OEH Beta Attenuation Mass (BAM) monitor for 2012. The red symbols highlight the days when 1-in-3-day sampling was carried out by CSIRO and ANSTO for the current study. It shows that these are representative of the full period, including days with both high and low $PM_{2.5}$ concentrations. The equivalent time series for Muswellbrook is given in Figure 10.

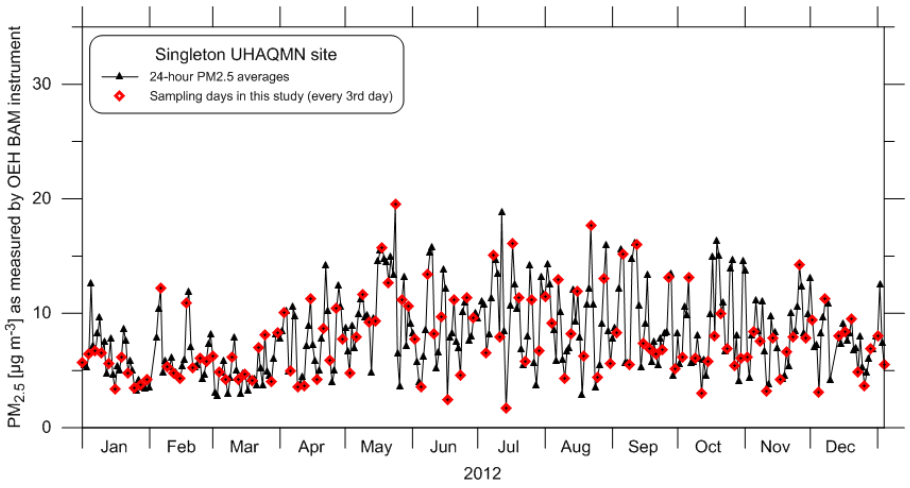

Figure 9 Time series of 24-hour average $PM_{2.5}$ concentrations measured by the OEH BAM (Beta Attenuation Mass) monitor at Singleton. The red symbols show the days when sampling for the current study was carried out.

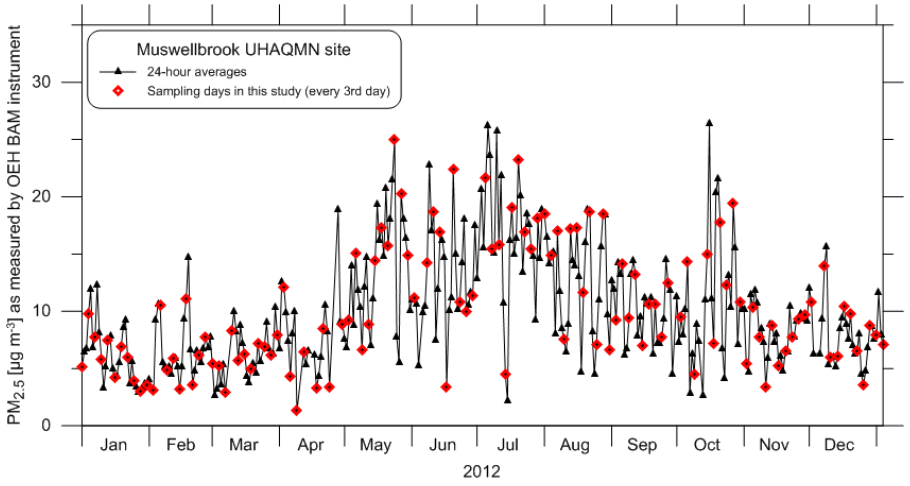

Figure 10 Time series as in previous figure but for Muswellbrook.

By plotting the time series as running averages in Figure 11, it is easier to compare the $PM_{2.5}$ levels at the two sites and identify the elevated levels during the cooler months from May to October.

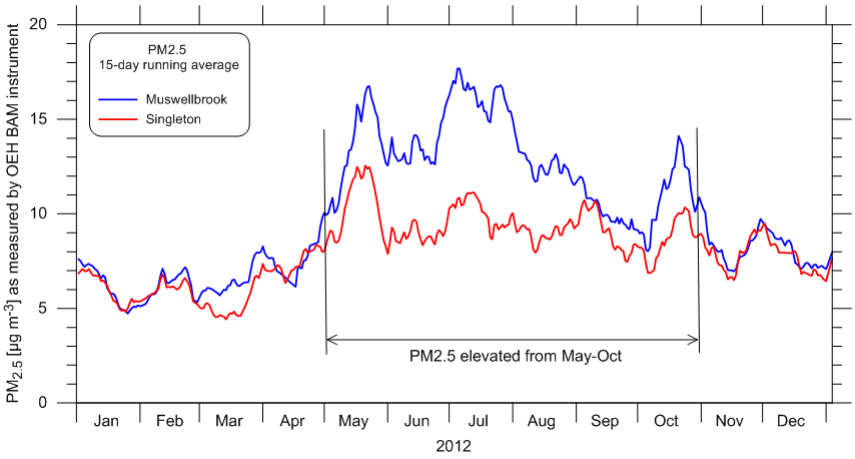

Figure 11. Running averages of $PM_{2.5}$ to show the seasonal trends more clearly with elevated levels from May to October at both sites.

Comparison in Figure 12 between the OEH $PM_{2.5}$ results and the gravimetric mass determination of $PM_{2.5}$ from the ANSTO sampler shows that apart from a few outliers, the gravimetric mass is on average close to but about 16 – 18% lower than the BAM measurement – probably due to slight differences in the measurement techniques – but the agreement is considered to be good.

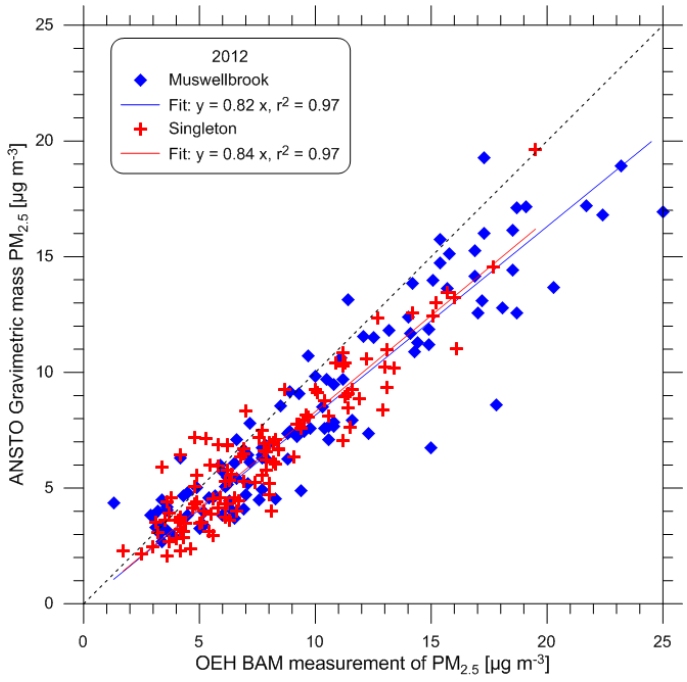

Figure 12 Comparison of $PM_{2.5}$ measured on ANSTO filters and by OEH BAM instrument.

4.2 Wind

Both sites include wind direction and wind speed measurements as part of the routine measurements by OEH. The winds are generally aligned along the valley on a north-west to south-east axis. The 2012 seasonal wind roses for Singleton are shown in Figure 13 and for Muswellbrook in Figure 14. Summer winds are almost all from the south-east whereas in winter most of the winds are from the north-west, particularly in Singleton. The other seasons include a mix of these directions with a very infrequent north-easterlies or south-westerlies. The winds speeds measured at Singleton are higher because of its more exposed location.

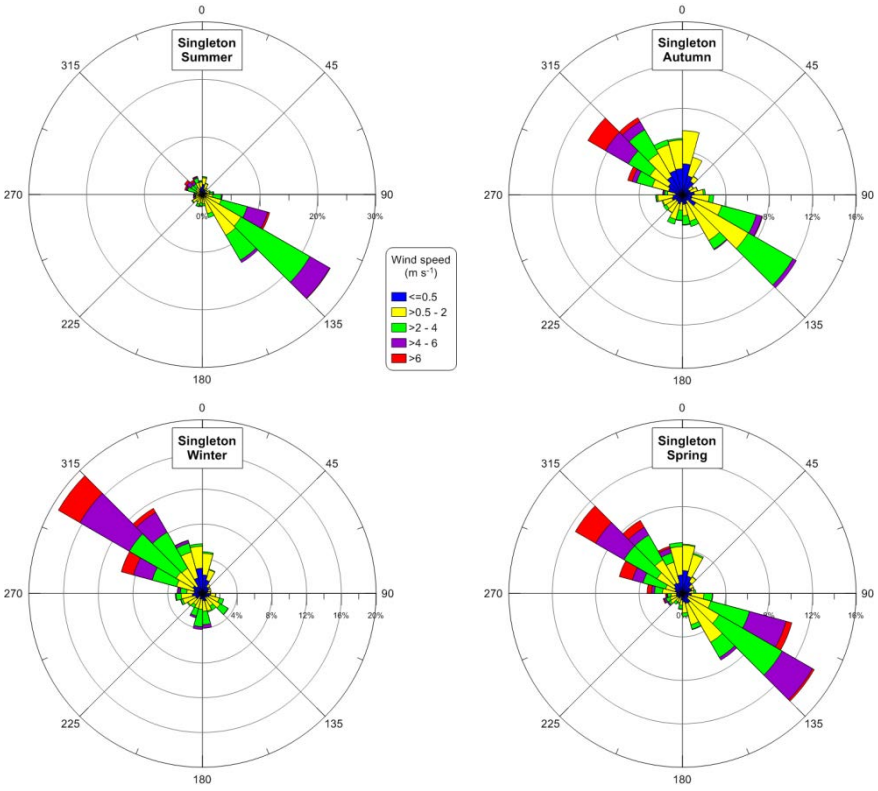

Figure 13. Seasonal wind roses for 2012 at the Singleton sampling site from 1-hour average OEH data

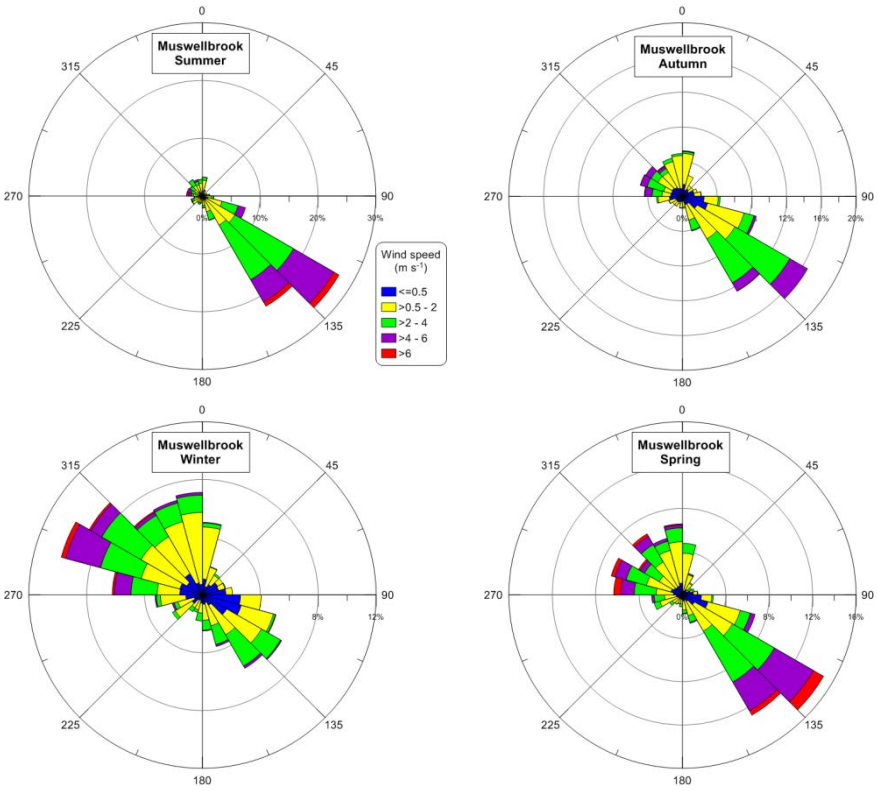

Figure 14. Seasonal wind roses for 2012 at the Muswellbrook sampling site from 1-hour average OEH data

4.3 Singleton $PM_{2.5}$ speciation

Table 2 lists the species measured in the Singleton samples with their median concentration, minimum detection limit (MDL) and uncertainty. The table shows that OC (sum of OC1, OC2, OC3 and OC4) is the dominant component (OC includes the contributions from levoglucosan, mannosan and oxalate which are also resolved separately). The next most important species are black carbon/elemental carbon and sulfate.

Table 2 Median concentrations for species measured at Singleton using either ion chromatography(IC), ion beam analysis (IBA), LIPM (laser integrated plate method (LIPM), or thermal-optical carbon analyser (TA)

Species	Median Conc.	MDL	% of values <MDL	Uncert.	Species	Median Conc.	MDL	% of values <MDL	Uncert.
	(ng m^{-3})	(ng m^{-3})		(%)		(ng m^{-3})	(ng m^{-3})		(%)
Na^+ (IC)	219	0.6	0%	9	**OC1 (TA)**	223	13.9	0%	10
Na (IBA)	200	77	27%	14	**OC2 (TA)**	397	36.1	0%	10
NH_4^+ (IC)	141	0.3	0%	8	**OC3 (TA)**	821	63.7	0%	10
Mg^{2+} (IC)	26	0.14	0%	9	**OC4 (TA)**	409	1	0%	10
Cl^- (IC)	46	0.7	0%	5	**Mn (IBA)**	1.1	0.4	6%	20
Cl (IBA)	52	1.9	8%	6	**Cu (IBA)**	0.6	0.4	31%	25
NO_3^- (IC)	126	0.6	0%	6	**Zn (IBA)**	3.0	0.4	2%	15
SO_4^{2-} (IC)	765	0.6	0%	7	**Br (IBA)**	2.0	1.4	25%	40
S (IBA)	255	1.5	0%	6	**Pb (IBA)**	1.4	2.6	77%	40
$C_2O_4^{2-}$ (IC)	53	0.3	0%	9	**Mass**	6108	160	0%	5
Levoglucosan	48.5	3	0%	5	**NO_2^- (IC)**	0.4	0.8	100%	9
Mannosan	1.3	2	18%	5	**Br^- (IC)**	0.3	0.5	94%	9
Al (IBA)	45	4	12%	7	**PO_4^{3-} (IC)**	3.3	0.6	0%	9
Si (IBA)	143	2	0%	6	**P (IBA)**	0.2	2	92%	35
K (IBA)	37	1	0%	6	**F^- (IC)**	0.1	0.2	58%	9
K^+ (IC)	35	0.35	0%	10	**Acetic (IC)**	3.2	6.4	77%	12
Ca (IBA)	23	1.2	0%	6	**Formic (IC)**	3.5	1.8	38%	9
Ca^{2+} (IC)	25	1.4	0%	8	**HCO_3^- (IC)**	20	0.2	0%	5
Ti (IBA)	3.4	0.7	15%	11	**H (IBA)**	161	6.6	0%	6
Fe (IBA)	53	0.5	0%	6	**V (IBA)**	0.3	0.7	88%	33
BC (LIPM)	857	29	0	8	**Cr (IBA)**	0.2	0.5	98%	30
EC (TA)	1273	5	0%	10	**Co (IBA)**	0.3	1.6	100%	-
MSA^- (IC)	14	0.7	0%	19	**Ni (IBA)**	0.2	0.6	82%	18

Figure 15 shows the time series of the these species concentrations, many of which show a seasonal variation, some with peaks in winter such as levoglucosan, mannosan, and others with a minimum in winter such as sulfate, sodium and MSA.

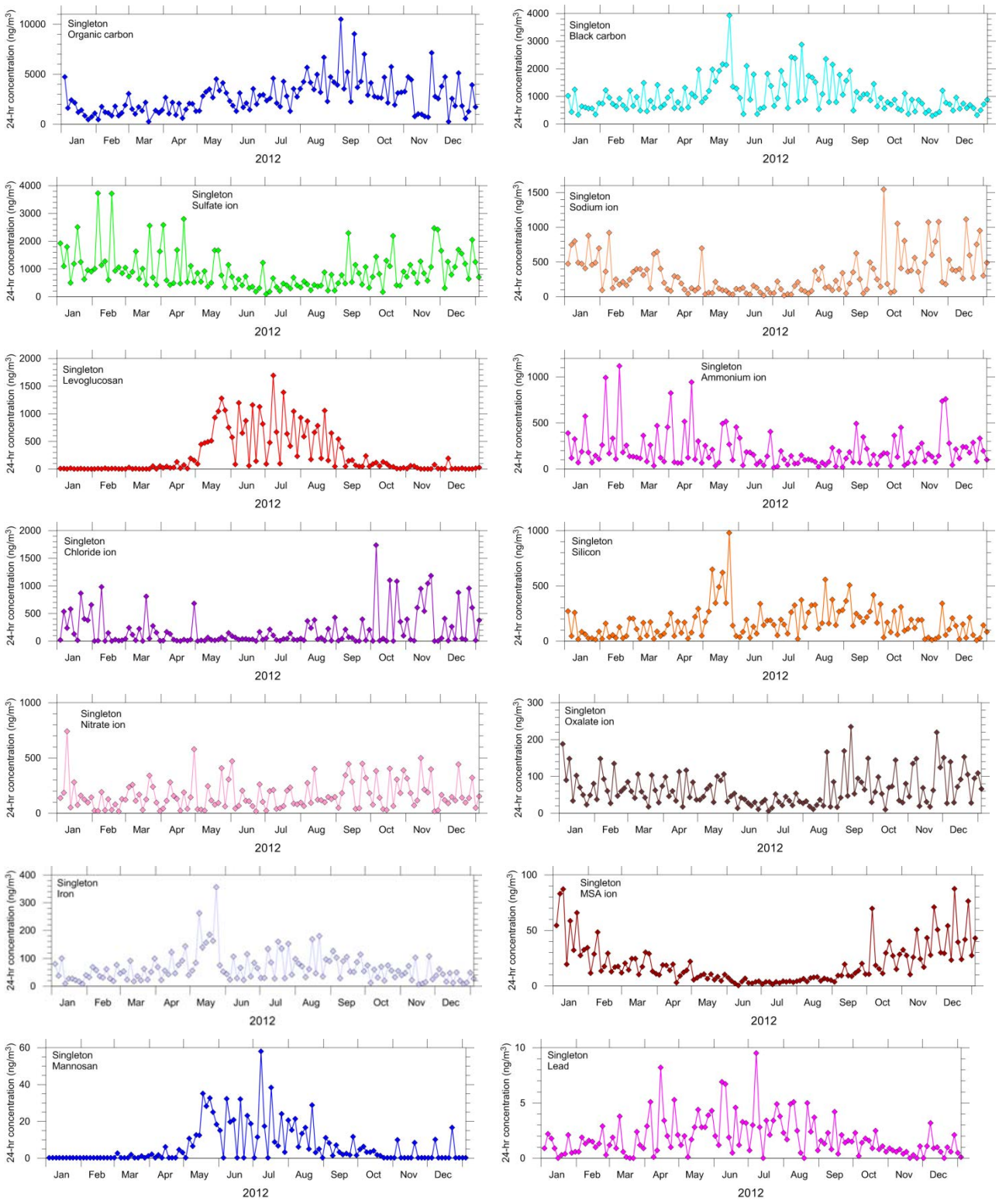

Figure 15. Time series of selected constituents of the Singleton samples during 2012

4.4 Muswellbrook $PM_{2.5}$ speciation

Table 3 lists some of the properties of the species measured in the Muswellbrook samples. In most case the median concentrations are very similar to those in Singleton. The table shows that as in Singleton, the dominant component is organic carbon but its concentration is about 30% higher than in Singleton. The next most important species are black carbon/elemental carbon and sulfate, followed by levoglucosan which is 70% higher than in Singleton.

Table 3. Median concentrations for species measured at Muswellbrook using either ion chromatography(IC), ion beam analysis (IBA), LIPM (laser integrated plate method (LIPM), or thermal-optical carbon analyser (TA)

Species	Median Conc.	MDL	% of values <MDL	Uncert ainty	Species	Median Conc.	MDL	% of values <MDL	Uncert ainty
	(ng m^{-3})	(ng m^{-3})		(%)		(ng m^{-3})	(ng m^{-3})		(%)
Na^+ (IC)	158	0.6	0%	9	**OC1 (TA)**	325	13.9	0%	10
Na (IBA)	140	73	35%	14	**OC2 (TA)**	618	36.1	0%	10
NH_4^+ (IC)	204	0.28	0%	8	**OC3 (TA)**	1142	63.7	0%	10
Mg^{2+} (IC)	20.5	0.14	0%	9	**OC4 (TA)**	567	1	0%	10
Cl^- (IC)	64	0.7	0%	5	**Mn (IBA)**	1.1	0.4	11%	20
Cl (IBA)	66	1.8	18%	6	**Cu (IBA)**	0.6	0.4	27%	25
$NO3^-$ (IC)	120	0.6	0%	6	**Zn (IBA)**	2.8	0.4	1%	15
SO_4^{2-} (IC)	846	0.6	0%	7	**Br (IBA)**	2.3	1.4	16%	40
S (IBA)	277.30	1.4	0%	6	**Pb (IBA)**	1.2	2.5	70%	40
$C_2O_4^{2-}$ (IC)	50	0.3	0%	9	**Mass**	7081	160	0%	5
Levoglucosan	82	3	0%	5	**NO_2^- (IC)**	0.4	0.8	99%	9
Mannosan	2.6	2	18%	5	**Br^- (IC)**	0.27	0.5	84%	9
Al (IBA)	33	3.6	1%	7	**PO_4^{3-} (IC)**	3.8	0.6	0%	9
Si (IBA)	118	1.9	0%	6	**P (IBA)**	0.2	1.9	89%	35
K (IBA)	40	1	0%	6	**F^- (IC)**	0.1	0.2	86%	9
K^+ (IC)	36	0.4	0%	10	**Acetic (IC)**	3.2	6.4	58%	12
Ca (IBA)	16	1.2	0%	6	**Formic (IC)**	6.5	1.8	6%	9
Ca^{2+} (IC)	17	1.4	0%	8	**HCO_3^- (IC)**	15	0.2	0%	5
Ti (IBA)	3	0.7	5%	11	**H (IBA)**	242	7.2	0%	6
Fe (IBA)	46	0.4	0%	6	**V (IBA)**	0.2	0.7	95%	33
BC (LIPM)	1046	29	0%	8	**Cr (IBA)**	0.2	0.5	96%	30
EC (TA)	1447	5	0%	5	**Co (IBA)**	0.2	1.4	100%	-
MSA^- (IC)	15	0.7	0%	19	**Ni (IBA)**	0.2	0.5	84%	18

Figure 16 shows the time series of these species concentrations with similar seasonal variations as in Singleton.

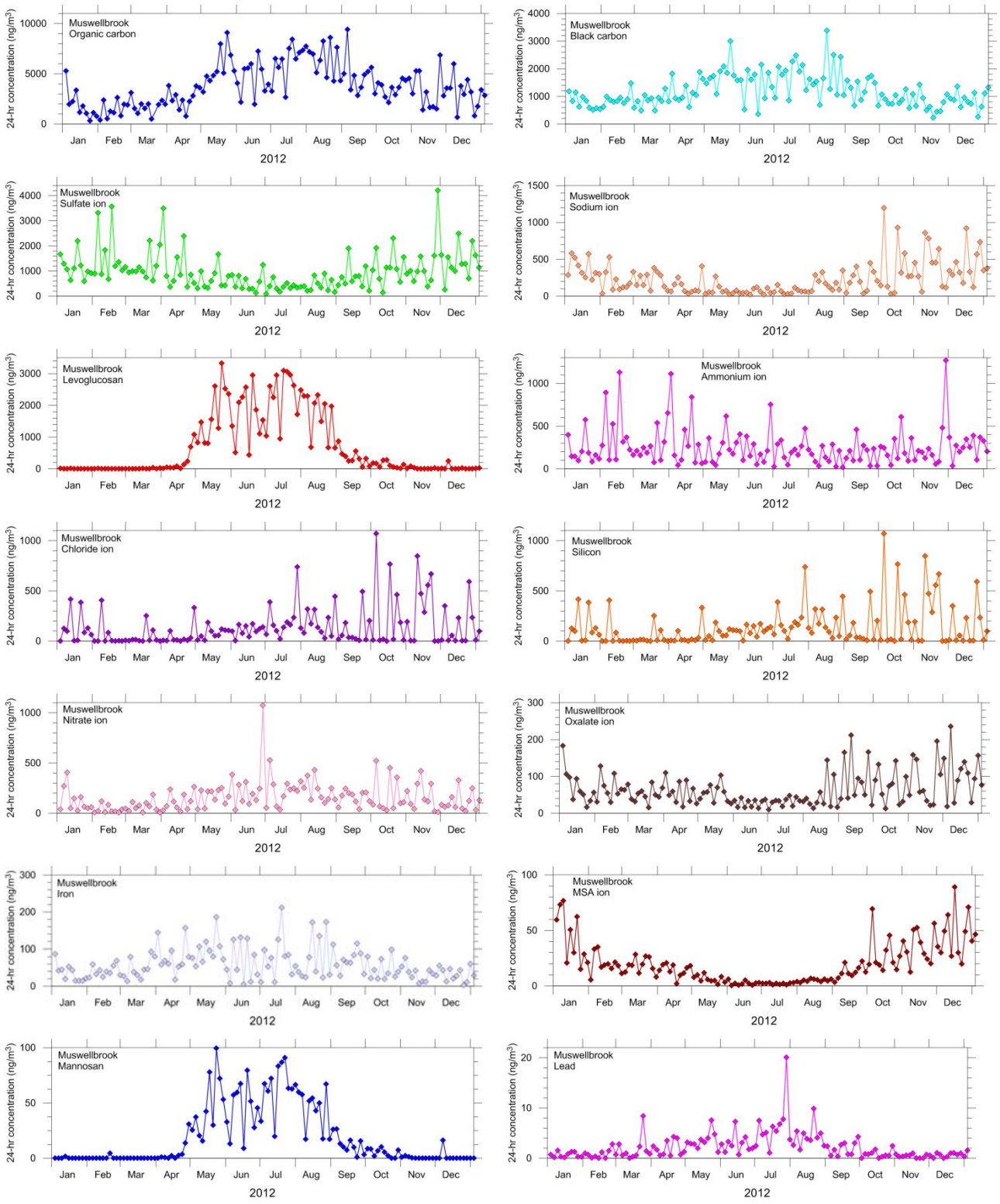

Figure 16 Time series of selected constituents of the Muswellbrook samples during 2012

4.5 Correlations

Figure 17 displays the linear relationships between a number of key species that indicate the sources of these species. The Na^{+} versus Mg^{2+} shows that at both sites the slope of the lines is close to that of the ratio

[Na^+/Mg^{2+}] found in sea salt; the Si versus Al plot shows the slope at both sites is similar to the [Si/Al] ratio observed in crustal material. The linear relationships between $nssSO_4^{2-}$ versus NH_4^+ and levoglucosan versus OC1 indicate these species are related in their sources.

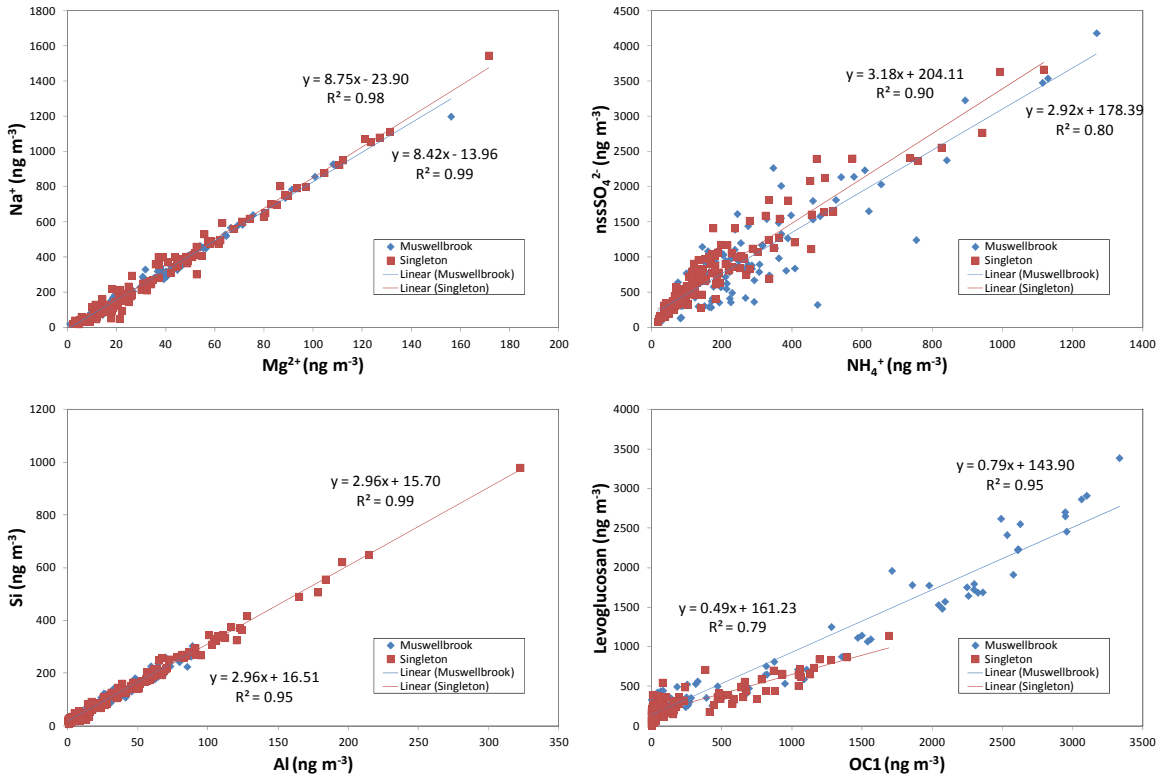

Figure 17 Scatter plots showing linear relationships between key species which provide an indication of the sources of the species.

4.6 $PM_{2.5}$ mass closure

Figure 18 compares the $PM_{2.5}$ from the gravimetric measurement on the 25 mm Teflon filter against the sum of the species concentrations (with appropriate oxygen added) measured on the 25 mm Teflon filter and the OC fractions measured on the quartz filters. Although the average shows good agreement, there is considerable scatter. This arises from uncertainty in conversion of the measurement of organic carbon to organic mass. Russell (2003) reported conversion factors of 1.2 to 1.6 depending on the number of functional groups in the organic compounds. We used a value of 1.2 to match the average, but the large scatter remains unexplained.

Figure 19 compares the $PM_{2.5}$ gravimetric measurement against the ANSTO reconstructed mass (RCM), where this is computed using the method reported by Malm, Sisler et al. (1994) as

RCM = Salt + Ammonium Sulfate + Soil + Smoke + Organics + BC

where:

Salt = 2.54 [Na]

Ammonium sulfate = 4.125 [S]

Soil = 2.20 [Al] + 2.49 [Si] + 1.63 [Ca] + 1.94 [Ti] + 2.42 [Fe]

Smoke = [K] – 0.6 [Fe]

Organics = 11 [H] – 0.25 [S] assuming the average organic material is 9% hydrogen.

The RCM is smaller than the gravimetric mass (by about 25%) because it does not include nitrates or water vapour. This proportion is typical for other ANSTO studies (e.g. (Cohen, Crawford et al. 2010)).

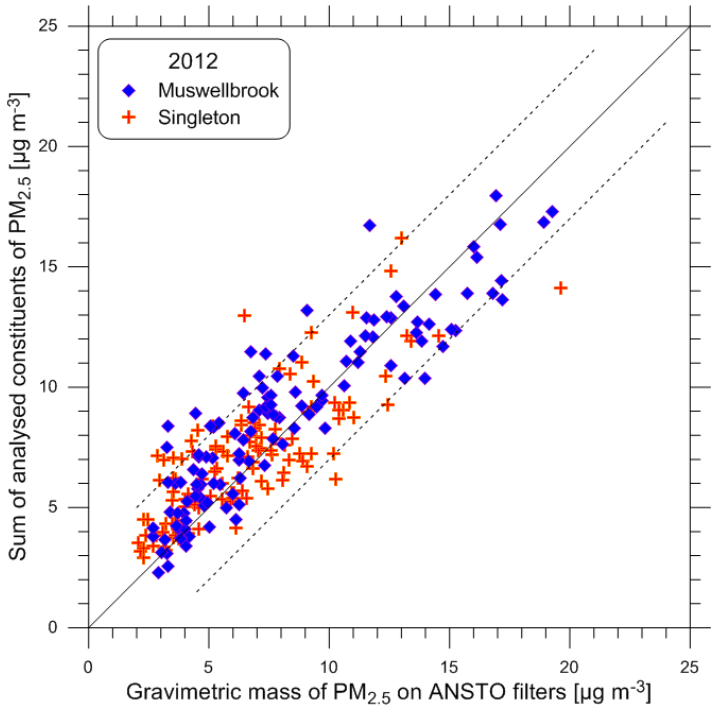

Figure 18 Comparison between the sum of the masses of the constituents of $PM_{2.5}$ with the gravimetric mass measurements on the ANSTO $PM_{2.5}$ filters. The solid line is 1:1 correspondence, the dashed lines are ± 3 µg m^{-3}.

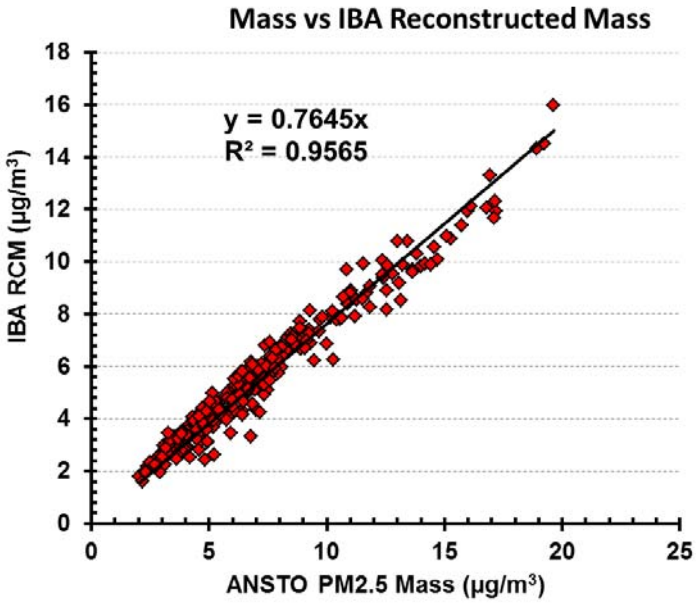

Figure 19 Comparison between the sum of the reconstructed mass from the ANSTO IBA constituents of $PM_{2.5}$ with the gravimetric mass measurements on the ANSTO $PM_{2.5}$ Teflon filters

5 Data analysis by PMF

5.1 Selection of species

The selection of species for inclusion in PMF analysis requires some discussion. The analytical methods used for the analysis of samples in this project have produced data sets for 46 species. In a number of cases different methods have measured the same or similar species (e.g. SO_4^{2-} by IC and S by PIXE, EC by thermal desorption and BC by integrated plate method). In these cases one of these species has been selected for PMF. This has resulted in the removal of H, Na, S, Cl measured by PIXE, EC measured by thermal desorption and K^+ and Ca^{2+} measured by IC (Table 4).

Table 4 Species excluded from the PMF analysis

Species Excluded	Reason
H by PIXE	Duplicate, so used OC1, OC2, OC3 and OC4 by thermal desorption
Na by PIXE	Duplicate, so used Na^+ by IC
S by PIXE	Duplicate, so used SO_4^{2-} by IC
Cl by PIXE	Duplicate, so used Cl^- by IC
EC by thermal desorption	EC data quality poor (see Appendix A), so replaced by BC
K^+ by IC	Duplicate, so used K by PIXE
Ca^{2+} by IC	Duplicate, so replaced by Ca by PIXE
Cr, Co by PIXE, NO_2^-, Br^- by IC P, V, Ni, by PIXE	> 95% of data below MDL > 75% of data below MDL and poor fit
MSA, F, acetate, formate by IC	PMF model fit poor ($r^2 < 0.6$)

In a number of cases a large proportion of the concentrations were below the MDL. The EPA PMF 3 Users Manual (Norris et al., 2008) recommends the exclusion of species if more than 95% of samples have concentrations less than the MDL. In addition species with more than 75% of samples less than the MDL were examined closely and their inclusion was dependent on how well the modelled time series fit the observational data. In other PMF analyses all species have been used in PMF regardless of whether they are consistently below the MDL (Cohen et al., 2012) or data below MDL concentrations are replaced with values of half the MDL (Poirot et al., 2001). The species removed from the PMF analysis due to the MDL criteria adopted for this work were P, V, Cr, Co, Ni, and Br (Table 4).

We also used the criteria of the signal-to-noise (S/N) ratios to assign an uncertainty weighting to the species. Variables were initially defined to be good, weak or bad depending on their S/N ratio. Species with S/N ratios less than 0.2 were excluded (although all data had S/N ratios > 0.2). Species with S/N ratios between 0.2 and 2 were considered weak variables and by flagging them as such their estimated uncertainties were increased by a factor of 3 to reduce their weight in the solution. We also set the mass variable to weak assigning it as a totalising variable.

Finally we evaluated the ability of PMF to model each species. PMF was unable to model MSA, F, acetate, formate so these species were removed from the PMF analysis.

Table 5 and Table 6 list the strength of the various species used in the PMF analysis at Singleton and Muswellbrook respectively. There were a total of 123 samples from each site, each with 25 species included in the PMF analysis.

Table 5 Species included in PMF analysis at Singleton.

Species	PMF Categorization	S/N	Median Concentration (ng m^{-3})	MDL (ng m^{-3})	% of values <MDL	Uncertainty (%)
Na^+	Strong	10.3	219	0.6	0%	9
NH_4^+	Strong	11.3	141	0.3	0%	8
Mg^{2+}	Strong	9.9	26	0.14	0%	9
Cl^-	Strong	18.0	46	0.7	0%	5
NO_3^-	Strong	15.1	126	0.6	0%	6
SO_4^{2-}	Strong	12.7	765	0.6	0%	7
$C_2O_4^{2}$-	Strong	9.8	53	0.3	0%	9
Levoglucosan	Strong	19.0	48.5	3	0%	5
Mannosan	Strong	7.9	1.3	2	18%	5
Al	Strong	14.8	45	4	11%	7
Si	Strong	16.1	143	2	0%	6
K	Strong	15.9	37	1	0%	6
Ca	Strong	14.9	23	1.2	0%	6
Ti	Strong	10.3	3.4	0.7	15%	11
Fe	Strong	15.8	53	0.5	0%	6
BC	Strong	12.0	857	29	0%	8
OC1	Strong	12.5	223	13.9	0%	10
OC2	Strong	10.6	397	36.1	0%	10
OC 3	Strong	13.7	821	63.7	0%	10
OC4	Strong	18.9	409	1	0%	10
Mn	Strong	6.0	1.1	0.4	7%	20
Cu	Strong	3.8	0.6	0.4	30%	25
Zn	Strong	7.7	3.0	0.4	2%	15
Pb	Weak	1.2	1.4	2.6	76%	40
Mass	Weak Total Variable	0.8	6108	160	0%	5

Table 6 Species included in PMF analysis at Muswellbrook.

Species	PMF Categorization	S/N	Median Concentration (ng m^{-3})	MDL (ng m^{-3})	% of values <MDL	Uncertainty (%)
Na^+	Strong	10.3	158	0.6	0%	9
NH_4^+	Strong	11.0	204	0.28	0%	8
Mg^{2+}	Strong	9.9	20.5	0.14	0%	9
Cl^-	Strong	11.9	64	0.7	0%	5
NO_3^-	Strong	10.9	120	0.6	0%	6
SO_4^{2-}	Strong	12.7	846	0.6	0%	7
$C_2O_4^{2}$-	Strong	9.8	50	0.3	0%	9
Levoglucosan	Strong	17.4	82	3	0%	5
Mannosan	Strong	15.1	2.6	2	18%	5
Al	Strong	13.2	33	3.6	1%	7
Si	Strong	16.0	118	1.9	0%	6
K	Strong	14.1	40	1	0%	6
Ca	Strong	14.3	16	1.2	0%	6
Ti	Strong	7.8	3	0.7	5%	11
Fe	Strong	15.7	46	0.4	0%	6
BC	Strong	12.0	1046	29	0%	8
OC1	Strong	17.8	325	13.9	0%	10
OC2	Strong	14	618	36.1	0%	10
OC 3	Strong	15.1	1142	63.7	0%	10
OC4	Strong	18.9	567	1	0%	10
Mn	Strong	6.4	1.1	0.4	11%	20
Cu	Strong	4.3	0.6	0.4	26%	25
Zn	Strong	9.8	2.8	0.4	1%	15
Pb	Weak	1.8	1.2	2.5	68%	40
Mass	Weak Total Variable	0.8	7081	160	0%	5

5.2 PMF model diagnostics

The model was executed with 40 runs, a random seed, with various numbers of factors and an extra modelling uncertainty of 5%. The best fit with factors that could be explained physically was obtained using 8 factors. Examination of the scaled residuals and the ability to model the observed time series of the species concentrations were used in arriving at the final solution. The G-space plots showed little rotation and F_{peak} was not used. The G-space plots are shown in Appendix B At Muswellbrook, this produced values of Q_{robust} = 2876 and Q_{true} = 2928 indicating very little influence from outliers. At Singleton the values were Q_{robust} = 2425 and Q_{true} = 2448. All runs converged and the Q values were stable.

6 Source apportionment

Eight factors were identified in the PMF analysis at each site. These are summarised in Figure 20 which shows the average portion of $PM_{2.5}$ explained by each factor at each site over the 2012 period. These factors are discussed in detail in the following sections. Figure 21 shows that the PMF solution is able to resolve close to 100% of the mass weighed on the 25 mm Teflon filters.

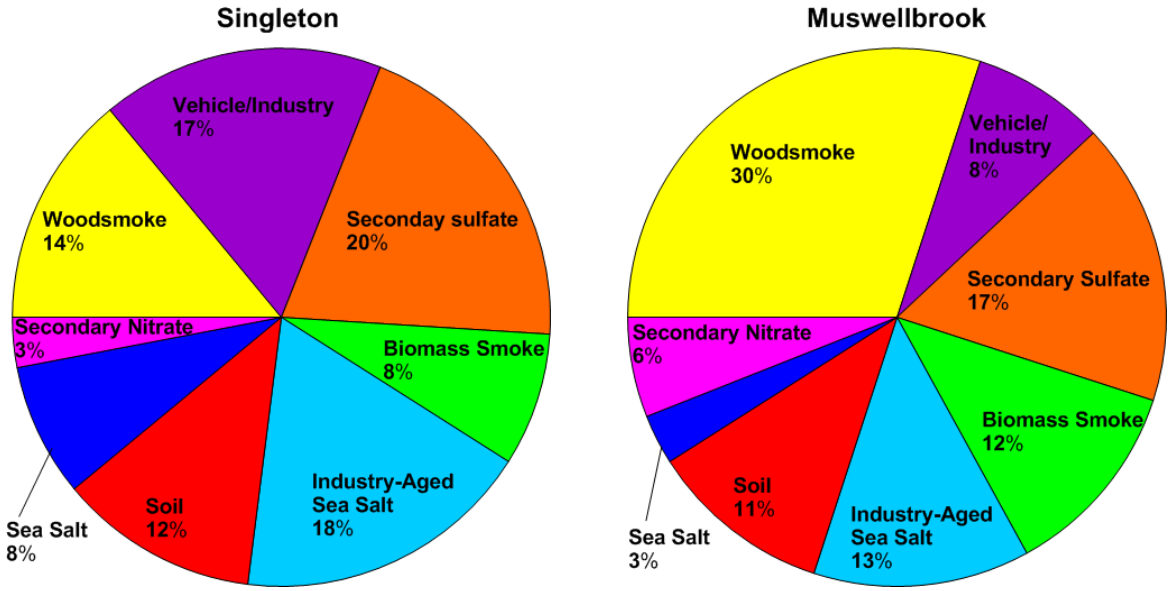

Figure 20 Average portion of $PM_{2.5}$ mass explained by each factor in the PMF solution.

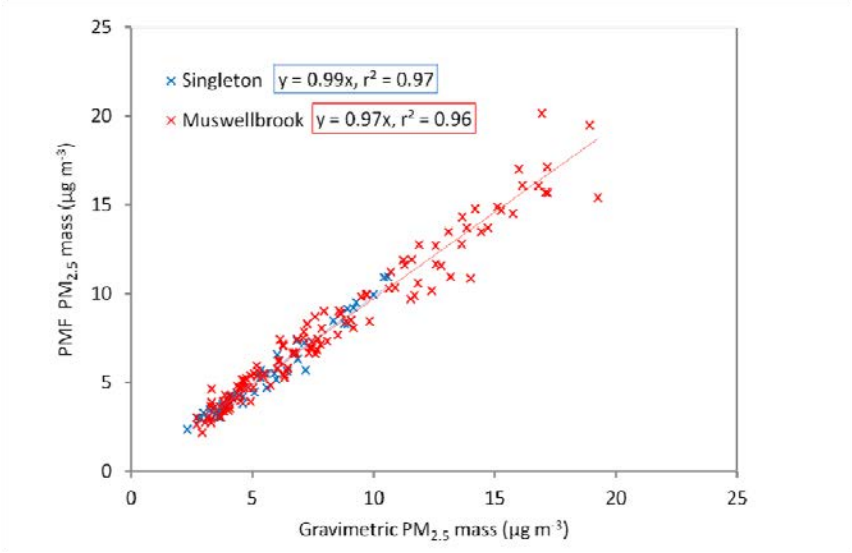

Figure 21 Gravimetric $PM_{2.5}$ mass measured on the 25 mm Teflon filter versus mass determined by the EPA PMF solution.

Each of the factors is characterised by a chemical 'fingerprint' which is a unique pattern of chemical species and their concentrations. Before considering each factor in turn, we describe here the interpretation of the three types of figures presented for each factor – the fingerprints, the time series and the CPF plots – using the figures for Factor 1 in Section 6.1.

Interpretation of the fingerprints, time series and CPF plots

Figure 22 shows an example of the 'fingerprint' of the factor, so called because it shows a unique pattern of species concentrations. The fingerprint shows the relative amounts of the various species in the factor. It does this in two ways. Firstly, the vertical blue bars show the species concentrations, e.g. in Factor 1 at Singleton, the levoglucosan concentration is 210 ng m^{-3} and the mass (second bar from the right) is 920 ng/m^3 = 0.92 µg m^{-3}. Secondly, the dark red squares show the percentage of the species that occurs in the factor, e.g. Factor 1 at Singleton includes 86% of the levoglucosan measured in the samples and 14% of the mass. Both of these pieces of information (concentrations and percentages) are shown because both are important in analysing and interpreting the factors.

Figure 23 shows how the contribution of the factor to total $PM_{2.5}$ varies during the year. Factor 1 only makes a significant contribution from May to August with almost no contribution from November to March. The figure shows that in Singleton there are some days in winter when up to 60% of the $PM_{2.5}$ is in this factor. These time series provide additional evidence that is used in deciding on the source of the emissions. For example, the cooler weather from May to August corresponds to the period when domestic woodheaters are used, and this agrees with the fingerprint analysis indicating woodsmoke. Smoke is also produced by bushfires and hazard reduction burns, but the time series of these in Figure 34 is quite different from the time series for Factor 1, indicating that bushfires and hazard reduction burns are not the sources of the woodsmoke in Factor 1 from May to August.

Figure 24 shows the wind sector plot from the conditional probability function (CPF) analysis described in Section 3.7. In simple terms, the distance of the yellow line from the central yellow dot shows the percentage of time that sources in that wind direction contribute to the factor. Because of limitations of the analysis discussed in Section 3.7, attention should focus on the gross features and not the fine detail. Thus Figure 24 for Singleton shows roughly similar contributions from most wind directions except south-easterly, which indicates a disperse local source, which is consistent with what is known about this factor from Figure 23 and Figure 24.

The differences between the gross features in the CPF plots for the various factors can be seen by comparing Figure 24 with the CPF figure for Factor 7 (Figure 44), which shows the strongest lobe for south-easterlies, i.e. for winds from the coast moving inland along the Hunter Valley. This is consistent with the sea salt source for this factor.

6.1 Factor 1 – Woodsmoke

The first factor (Factor 1) identified as the woodsmoke factor makes up 30% of the $PM_{2.5}$ mass at Muswellbrook and 14% of the mass at Singleton. It is characterised by high levels of levoglucosan, mannosan and organic carbon (OC1) (Figure 22). Levoglucosan and mannosan are unique tracers for the combustion of cellulose found in trees and plants (Iinuma et al, 2007). The ratio of levoglucosan to mannosan is an indication of the type of wood combusted. The correlation between levoglucosan and mannosan in the samples was extremely high (r^2 = 0.99) and the ratio of 36 is close to the value for eucalyptus of 34.9 ± 1.9 measured by Goncalves et al. (2010).

Levoglucosan shows a clear linear relationship with OC1 (Figure 17). OC1 is the most volatile OC fraction measured by the IMPROVE-A method (since it is the lowest temperature fraction). Generally as organic aerosol ages the organic compounds present become less volatile. Thus the good correlation between OC1 and levoglucosan indicates the smoke is fairly fresh, as we would expect considering the proximity of the sampling sites to houses.

This factor accounts for 30% of the annual average organic carbon (sum of OC1, OC2, OC3 and OC4) in Muswellbrook and 8% in Singleton. It also includes 22% of the BC in Muswellbrook and 4% in Singleton.

The time series (Figure 23) show that the factor is only present during the cooler months of the year with significant contributions from May to August in both towns. In Muswellbrook it contributes up to two-thirds of the $PM_{2.5}$ during the middle of winter and in Singleton up to one-third. The CPF plots (Figure 24) show the direction of the sources being the urban areas with good consistency between the directions of

the CPF lobes and the urban lobes except for south-easterly winds. The Muswellbrook site is closer to houses (Figure 5) than the Singleton site (Figure 4), where the closest houses are to the south.

This is similar to the Smoke factor identified by Cohen et al. (2012) in an analysis of 10 years of data from the Sydney Basin (2001 to 2011 at Richmond). In the absence of the unique woodsmoke tracer levoglucosan the species H, K and BC were used as the indicators. This factor grouped smoke from woodheaters and bushfire smoke together. At Richmond this factor contributed 37% on average to the $PM_{2.5}$ loading. A strong seasonal cycle was observed with maximum contributions occurring during winter.

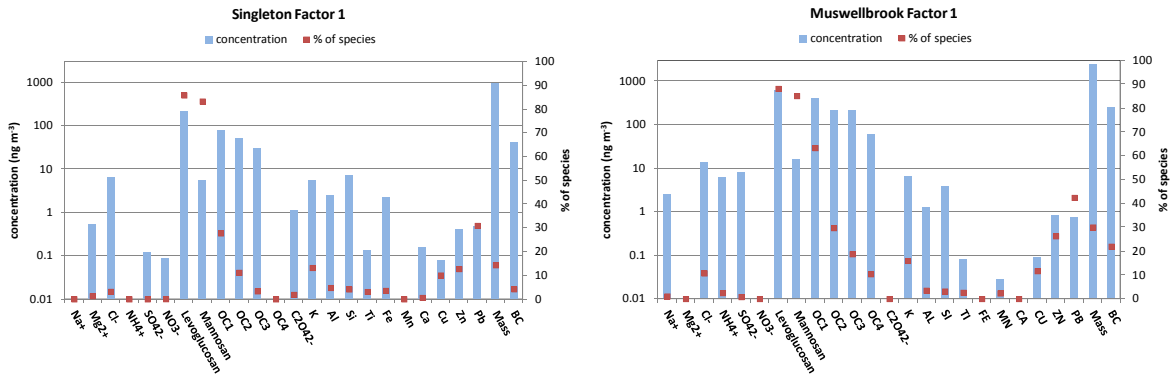

Figure 22 Fingerprint of Factor 1 (Woodsmoke) at Singleton (left) and Muswellbrook (right)

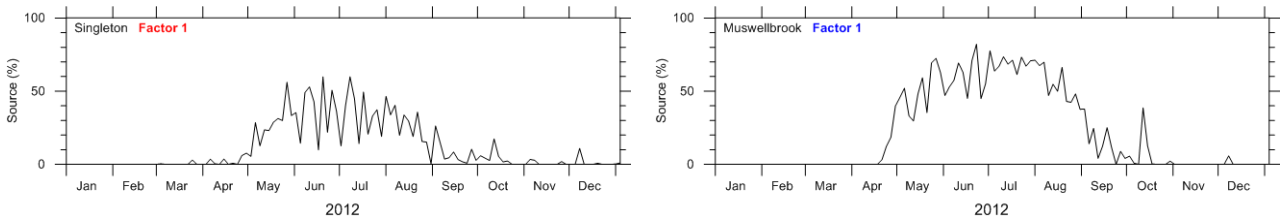

Figure 23 Time series of percentage that Factor 1 (Woodsmoke) contributes to $PM_{2.5}$ in Singleton and Muswellbrook; only contributes significantly during the cooler months May-August.

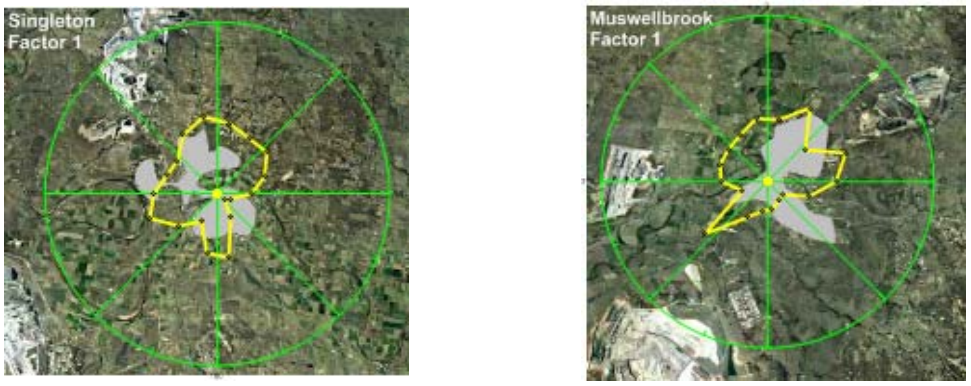

Figure 24 CPF plot of Factor 1 (Woodsmoke) at Singleton (left) and Muswellbrook (right). At both sites highest Woodsmoke source contributions at Singleton (left) were associated with winds from the north and south, while at Muswellbrook they were associated with winds from the southwest.

This factor includes 42% of the lead detected in the samples at Muswellbrook and 31% at Singleton, and the time series for lead (bottom right panel of Figure 15 and Figure 16) are most similar to those for the

levoglucosan and mannosan. It should be noted that the maximum 24-hour average lead concentrations were extremely low – 9.5 ng m^{-3} in Singleton and 20.1 ng m^{-3} in Muswellbrook – compared to the NEPM (National Environmental Protection Measure) of 500 ng m^{-3} for the annual average lead concentration. It is postulated that the lead originates from the burning of small amounts of painted wood in domestic wood heaters, in spite of advice to the contrary by NSW EPA (1999).

Only a very small amount of lead needs to be released by burning to produce the observed low concentrations. For example 1 g of lead released into and thoroughly mixed over an area 1 km x 1 km and to a depth of 100 m would produce an average concentration of 10 ng m^{-3}. If the volume of air were smaller, then a smaller amount of lead would be needed to reach 10 ng m^{-3}, and vice versa. Although modern paint is restricted to a maximum of 0.1% lead, prior to 1992 the limit was 1%, and prior to 1965 it could be up to 50% lead. Based on a typical paint coverage rate of 10 m^2 $litre^{-1}$, a 20 cm^2 piece of fifty year old painted wood could release about 1 g lead when burnt.

6.2 Factor 2 – Vehicle/Industry (Fe and BC)

Factor 2 makes up 8% of the $PM_{2.5}$ mass at Muswellbrook and 16% of the $PM_{2.5}$ mass at Singleton. This factor explains most of the variation in Fe at both sites (44% of Fe at Singleton and 55% at Muswellbrook) and explains 21% of BC at Muswellbrook and 58% of BC at Singleton. This factor also explains significant fractions of Cu, Mn and Zn in the samples (Figure 25). OC is also present.

We have named this a Vehicle/Industry factor as the species present are found in both of these sources.

The vehicle component could include direct vehicle emissions from the combustion of petrol and diesel, as well as emissions from brakes and tyre wear or resuspension of paved road dust. We discount the latter since the factor would be dominated by Si and Al if resuspension of roadside dust was the main contributor to the vehicle factor. Vehicle use in coal mining could contribute to this factor.

The profile of species presented by Chow et al. (2004) for vehicle emission composite samples collected during the Big Bend Regional Aerosol Visibility and Observational Study is similar to the profiles of the species that make up most of the mass of the Factor 2 at both Singleton and Muswellbrook (Table 7).

The wear of motor vehicle engines results in the emission of Fe, the wear of brakes in the emissions of Cu and tyres in the emission of Zn (Sternbeck et al., 2002). Thus the Fe and Zn present in this factor may be due to these processes. Calcium is used as in lubricating oil for diesel vehicles (Cheung et al., 2010). Manganese may be indicative of the fuel additive methylcyclopentadienyl manganese tricarbonyl (MMT), which during combustion releases inorganic Mn species (Joly et al. 2011). MMT has been used as a fuel additive in Australia since 2000 (NICNAS 2003).

This factor could also be similar to an Auto factor identified by Cohen et al. (2011) based on 10 years (1999 to 2009) of data at Liverpool in NSW. The dominant species were H, BC and Fe. Factor7-Auto identified by Cohen et al. (2012), based on 10 years (2001 to 2011) of data at Richmond in NSW was dominated by H, BC and trace elements associated with motor vehicles such as Zn from tyre wear, P and Ca from engine oils and small amounts of Pb and Br associated with historic leaded petrol use. The contribution to the total mass from this fingerprint was also consistent with the motor vehicle use in the vicinity of the Richmond site (11%). Note that the Auto factor identified by Cohen et al. (2011) does not include Fe.

Table 7 Dominant species in motor vehicle factors

Location	Species	Reference
Big Bend Regional Aerosol Visibility and Observational Study Vehicle composite	Each > 10% OC1, OC2, OC3, OC, EC1, EC2, EC Each > 1% S, OC4	Chow et al., 2004
Richmond, Sydney (2001-2011)	H, BC, Zn, P, Ca	Cohen et al., 2012
Liverpool Sydney (1999 -2009)	BC, Fe and H	Cohen et al., 2011

This factor could be similar to the Industry factor identified by Cohen et al. (2012) at Richmond where BC, Fe and Zn were used as the indicators and the likely industries were metal smelting or processing. At Richmond this factor only contributed 2% on average to the $PM_{2.5}$ loading consistent with it being a suburban site.

In another source apportionment study, this time in Hanoi, Cohen et al. (2010) identified a factor dominated with BC, Fe and H and significant V and Ni tracers as an iron smelting source, which was supported by the presence of several such smelting operations within 24 km of the sampling site probably contributing to this source. However in the Upper Hunter Valley, Fe smelting is not carried out.

The CPF plots (Figure 27) for this factor suggest that highest contributions from this source occurs with winds from the north and northwest at Singleton i.e. in the direction of the coal mines and most sectors at Muswellbrook but with significant contributions from a range of directions it probably includes local sources. It is interesting to note that the Singleton site is located closer to the mines than the Muswellbrook site and this factor makes a greater contribution to $PM_{2.5}$ at Singleton.

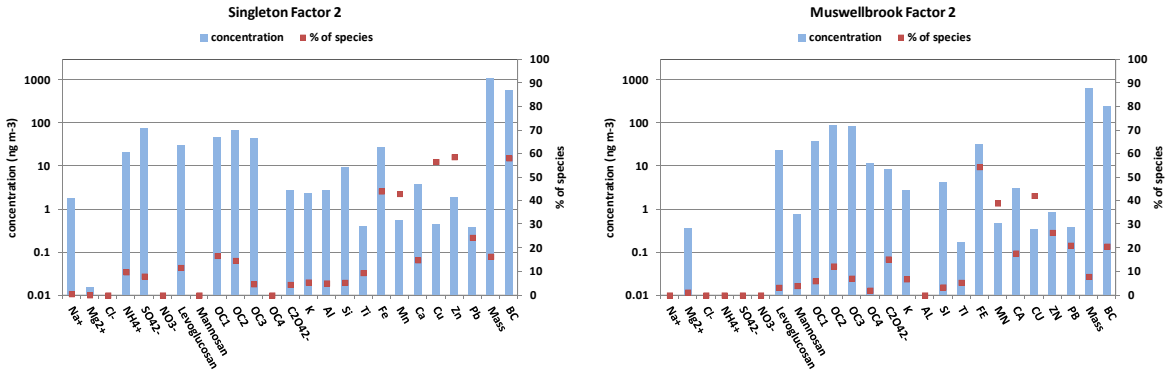

Figure 25 Fingerprint of Factor 2 (Vehicle/Industry) at Singleton (left) and Muswellbrook (right)

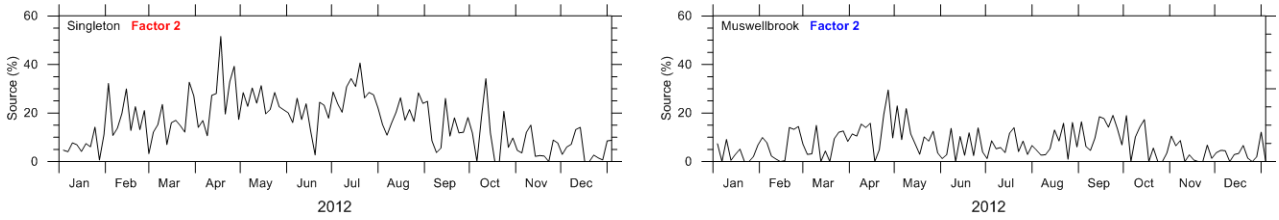

Figure 26 Time series of percentage that Factor 2 (Vehicle/Industry) contributes to $PM_{2.5}$ in Singleton and Muswellbrook; weak seasonal variation but different at the two sites.

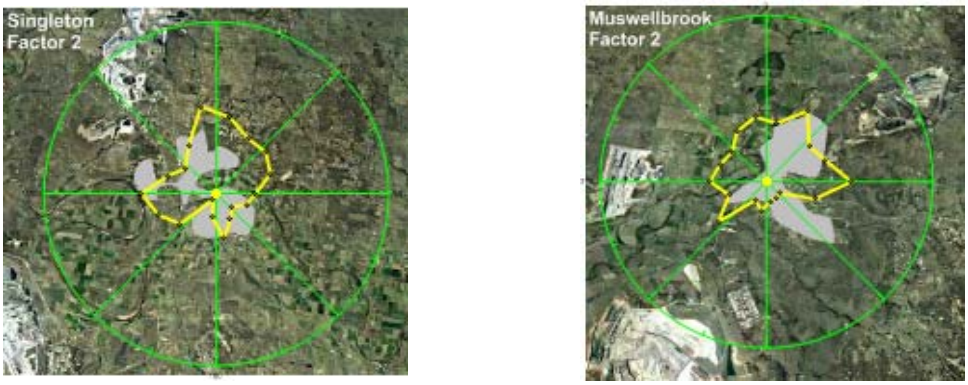

Figure 27 CPF plot of Factor 2 (Vehicle/Industry) at Singleton (left) and Muswellbrook (right). The highest Vehicle/Industry contributions at Singleton (left) were associated with winds from the north and west i.e. in the direction of the coal mines and most sectors at Muswellbrook (right) but there are contributions from most other wind directions indicating local sources.

6.3 Factor 3 – Secondary Sulfate

Factor 3 contributes 17% to the $PM_{2.5}$ mass at Muswellbrook and 20% at Singleton. The factor is dominated by secondary ammonium sulfate with the factor accounting to 60% of the sulfate and 85% of the ammonium in the samples.

Ammonium and sulfate occur in atmospheric particles as a result of photochemical reactions in the atmosphere. Gaseous sulfur dioxide (SO_2) is emitted to the atmosphere during combustion of fossil fuels (e.g. in power stations or motor vehicles) and in the presence sunlight will oxidise to form sulfuric acid (H_2SO_4), which is a strong acid. The seasonal cycle displayed by the contribution of this factor to $PM_{2.5}$ mass in Figure 29 of higher contributions during the summer months represents the greater time for photochemical reactions to occur during the summer months. The only significant gaseous base in the atmosphere is ammonia which is globally derived from biological production, such livestock wastes and fertiliser. It plays an important role in neutralising acids in the atmosphere, hence readily neutralises the sulfuric acid to produce ammonium sulfate aerosol.

The CPF plots (Figure 30) both have lobes to the north and south. This does not correspond to the major source of SO_2 in the region (the power stations) but reflects the fact that the chemical reactions to form the $(NH_4)_2SO_4$ take time to occur.

This is similar to Secondary Sulfate (2ndryS) identified by Cohen et al. (2012) at Richmond, although in that data set H was used as a surrogate for NH_4^+. At Richmond this factor contributed 27% on average to the $PM_{2.5}$ loading. A strong seasonal cycle was observed with maximum contributions occurring during summer. A similar factor was identified at Liverpool (Cohen et al., 2011), where again S, H and BC were the dominant species.

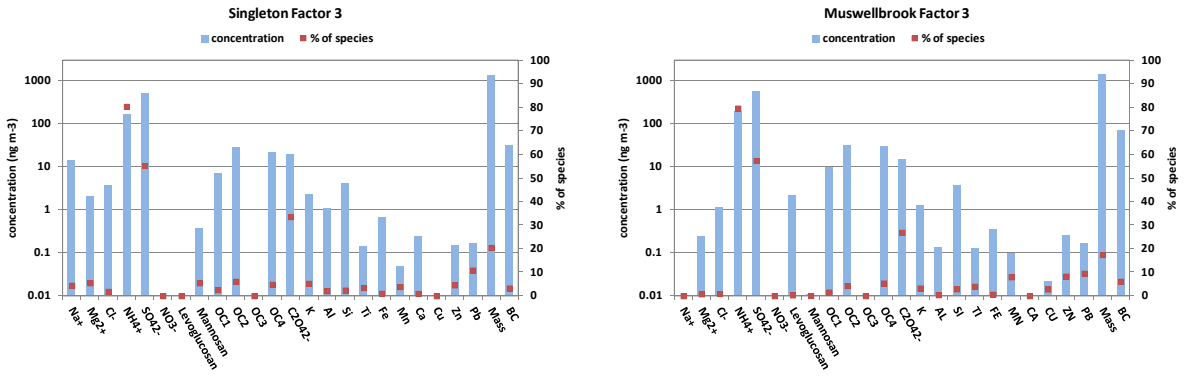

Figure 28 Fingerprint of Factor 3 (Secondary Sulfate) at Singleton (left) and Muswellbrook (right)

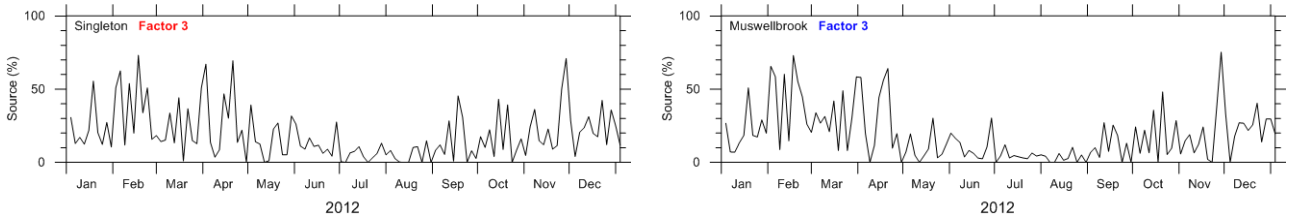

Figure 29 Time series of percentage that Factor 3 (Secondary Sulfate) contributes to $PM_{2.5}$ in Singleton and Muswellbrook; minimum during winter months.

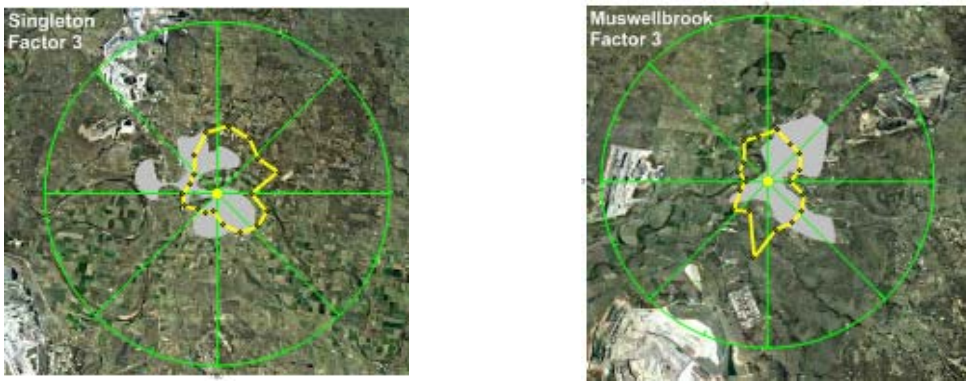

Figure 30 CPF plot of Factor 3 (Secondary Sulfate) at Singleton (left) and Muswellbrook (right). Both plots show lobes to the north and south. This does not correspond to the major source of SO_2 in the region (the power stations) but reflects the fact that the chemical reactions take time to occur.

6.4 Factor 4 – Biomass Smoke

The average contribution of Factor 4 to $PM_{2.5}$ is 8% at Singleton and 12% at Muswellbrook. It consists of the four OC fractions (OC1 to OC4) with the contribution OC4 having the greatest contribution and OC1 the lowest. Other species contributing to this factor include K (20% of K at Singleton and 30% at Muswellbrook), 10% of BC, 10% of the soil elements (Al, Si and Ti) and about 3% SO_4^{2-}. We have named this the Biomass Smoke factor as the available evidence indicates that principal source is biomass burning in bushfires and hazard reduction burns, with smaller contributions from vehicles and a small amount of soil dust (about a fifth of that in the Soil Factor).

The presence of K in this source is indicative of a biomass burning source. However the woodsmoke tracer levoglucosan is absent from the factor at Singleton and present in low concentration at Muswellbrook (less than 10 ng m^{-3}). Hennigan, Sullivan et al. (2010) showed under experimental conditions the decay of

levoglucosan after reaction with hydroxyl radicals. Thus the low concentrations of levoglucosan in these fingerprints may have resulted from the loss of levoglucosan due to hydroxyl reactions as the smoke plume ages.

Iinuma et al. (2007) showed that the type of fuel burned determines the emission rates of most species. Table 8 compares the emissions factors (EF) of K^+, levogluosan, mannosan and several other groups of organic compounds measured for burning pine logs and savannah grass measured by Iinuma et al. (2007). The pine logs show greater EFs than the savannah grass for levoglucosan and mannosan, while the savannah grass has higher EFs for K^+. Also shown are the molecular weights of the compound with the largest EF in each group of organic compounds. The EFs for PAH, n-alkanes, n-alkenes are greater for the savannah grasses than the pine logs and the molecular weight for the compound with the highest EF in these groups is also greater for the savannah smoke.

If we assume for this case that the savannah most closely represents the scrub and grasses burned during prescribed burning activities in the Upper Hunter region and the pine logs represent fuel used in woodheaters (acknowledging that in fact hardwood is burnt in woodheaters in the Upper Hunter region), we would expect to see higher K^+, lower levoglucosan and mannosan concentrations and higher proportions of high molecular weight species in smoke associated with prescribed burning than burning logs in woodheaters.

The time series (Figure 32) show elevated levels during spring into early summer and slightly elevated levels during autumn (more distinct at Muswellbrook). The CPF plots show the main direction of the source to be to the north-west, which is different from the patterns for the woodsmoke factor (Figure 33).

Data from the NSW Rural Fire Service in Figure 34 shows that there were many wildfires and hazard reduction burns from August to December 2012. The locations of the fires in Figure 35 show that not many of the fires were north-west of Muswellbrook, but back trajectories have not been calculated and it is likely that widespread burning around the region would contribute to elevated smoke levels in Singleton and Muswellbrook. Medium-range transport of the smoke would also explain the observed low levoglucosan concentrations as Hennigan, Sullivan et al. (2010) showed that levoglucosan has an atmospheric lifetime of 0.7-2.2 days in typical summertime conditions (exposed to sunlight and OH).

Table 8 Emission factors (EF) of K^+, levoglucosan, mannosan and several groups of organic compounds (and the molecular weight (MW) of the species with the highest concentration in each group), from burning pine logs and savannah grasses. Adapted from Iiunma et al. (2007). EF units are mg kg^{-1}

	Pine logs		Savannah grass	
	max MW	EF	max MW	EF
K+	39	5	39	25
Levoglucosan	162	1200	162	500
Mannosan	162	320	162	23
Lignin decomp products	178	66	112	59
Nitrophenols	169	14	169	4
PAH	166	1.4	226	5.6
n-alkanes	338	0.38	464	4.5
n-alkenes	336	0.45	420	1.5
Resin Acids	300	110	300	0.2

The agreement between the timing of the elevated levels of Factor 4 and the wildfire and hazard reduction burn data provides strong evidence of the importance of biomass burning as a major source for this Factor, however the CPF plots for this factor are similar to those for Factor 2 (Vehicle/Industry) and Factor 6 (Soil Dust). The profile of vehicle emissions is also similar to that for Factor 4. As discussed in Section 6.2 Chow et al. (2004) present the profile of a vehicle emission composite collected during the Big Bend Regional

Aerosol Visibility and Observational to include OC1, OC2, OC3, OC, EC1, EC2, EC (each comprising > 10% of the chemical mass for the profile) and S, OC4 (comprising > 1%). The organic aerosol profile for Singleton and Muswellbrook is similar and includes OC2, OC3, OC4 making up > 10% of the chemical mass and BC, Na and OC1 making up > 1% of the mass. However Chow et al. (2004) also present a profile of a vegetative burning composite where OC1, OC2, OC3, OC, EC1, EC each individually contribute to > 10% of the chemical mass and SO_4 , K, Cl, OC4 make up > 1% of the chemical mass. There is insufficient data to fully explain the sources for this factor, but the weight of evidence indicates that wildfire and hazard reduction burns are the dominant sources for this Factor.

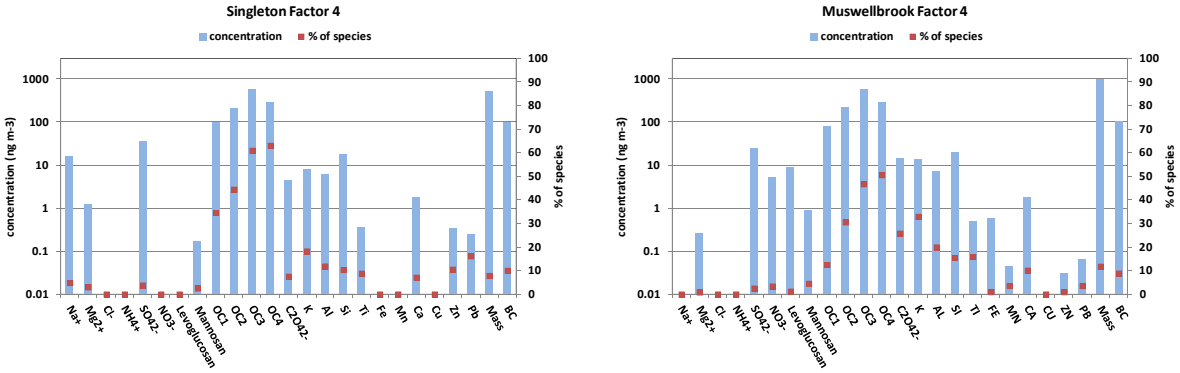

Figure 31 Fingerprint of Factor 4 (Biomass Smoke) at Singleton (left) and Muswellbrook (right)

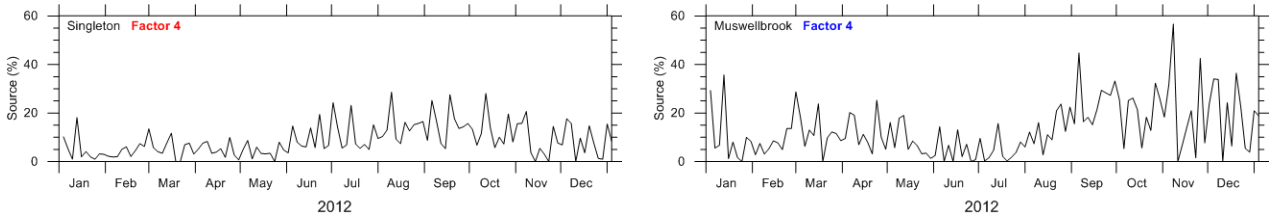

Figure 32. Time series of percentage that Factor 4 (Biomass Smoke) contributes to $PM_{2.5}$ in Singleton and Muswellbrook; elevated values in spring and slightly elevated in autumn.

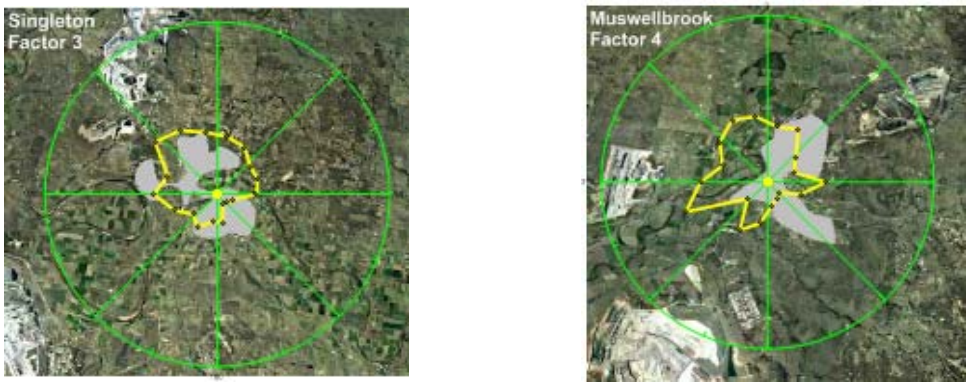

Figure 33. CPF plot of Factor 4 (Biomass Smoke) at Singleton (left) and Muswellbrook (right). At Singleton (left) and Muswellbrook (right) highest concentrations of the Biomass Smoke factor are associated with winds from the northwest.

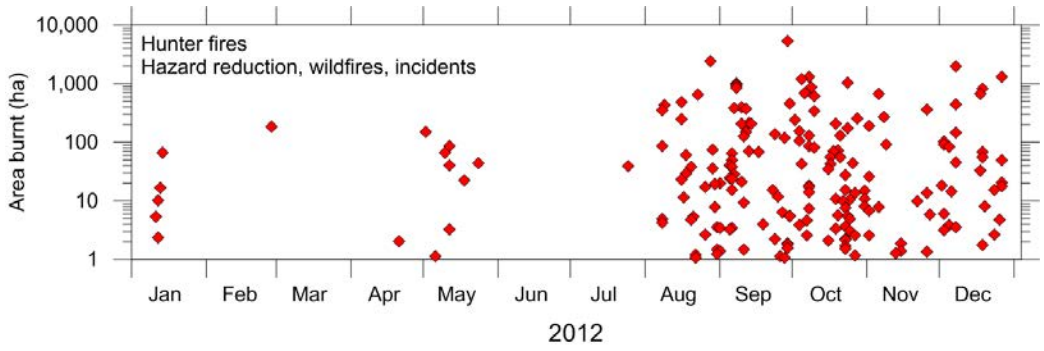

Figure 34 Occurrence of wildfires and hazard reduction burns in the Hunter region during 2012 (data from Rural Fire Service). The vertical axis shows the area burnt, which is representative of the amount of smoke generated.

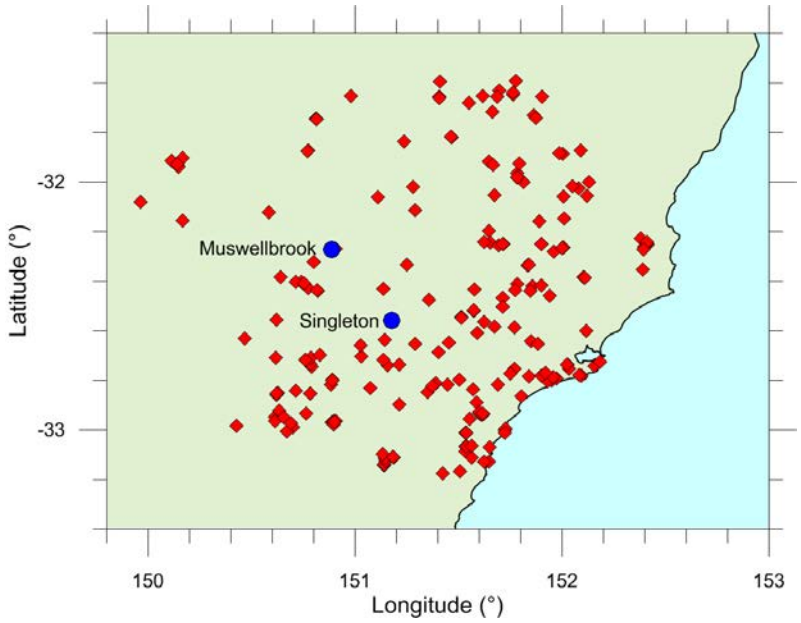

Figure 35 Spatial distribution of fires in the Hunter region during 2012.

6.5 Factor 5 – Industry Aged Sea Salt

The average contribution of Factor 5 to $PM_{2.5}$ is 18% at Singleton and 13% at Muswellbrook. This factor consists of Na^+, Mg^{2+}, SO_4^{2-} and with almost no Cl^-. This source is identified as industry aged sea salt as the $[Na^+/Mg^{2+}]$ ratio is the same as that of sea salt with the Cl^- displaced as HCl mostly by the acid H_2SO_4 and to a lesser extent nitric acid (HNO_3). As discussed in Section 6.3, the source of H_2SO_4 the oxidation of SO_2 emitted from fossil fuel combustion, so the seasonal cycle displayed by the contribution of this factor to $PM_{2.5}$ mass in Figure 37 of higher contributions during the summer months represents the greater time for photochemical reactions to occur during the summer months. In this case however, H_2SO_4 is neutralised by the weak base of the sea salt particles resulting in the replacement of Cl^- by SO_4^{2-}.

The CPF (Figure 38) show the main direction to be from the south-east (both of these are similar for Factor 7 (sea salt) in section 6.7). The lower contribution of this factor at Muswellbrook is consistent with Muswellbrook being a greater distance from the coast than Singleton.

This is similar to the Aged Industrial Sulfate (IndSaged) identified by Cohen et al. (2012) at Richmond, where Na, S and BC were used to identify the factor at Richmond. This factor contributed 12% on average to the $PM_{2.5}$ loading and a strong seasonal cycle was observed with maximum contributions occurring during summer. A similar factor was identified at Liverpool (Cohen et al., 2011) with Na, S, and BC and the absence of Cl being the determining species.

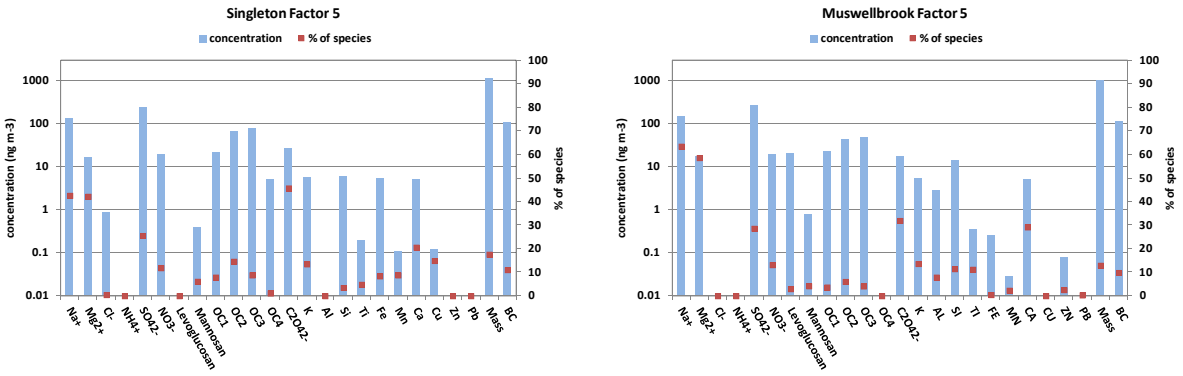

Figure 36 Fingerprint of Factor 5 (industry aged sea salt) at Singleton (left) and Muswellbrook (right)

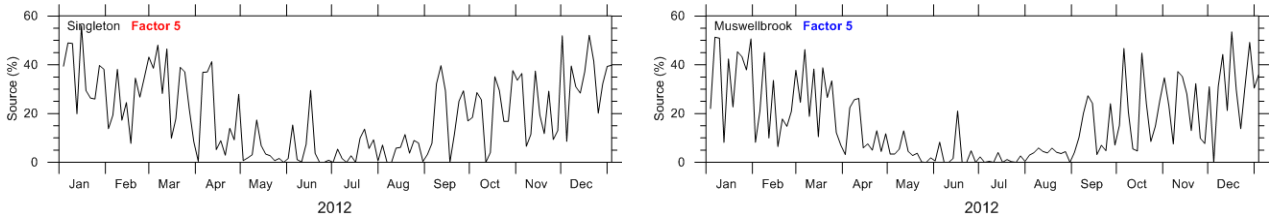

Figure 37. Time series of percentage that Factor 5 (Industry Aged Sea Salt) contributes to $PM_{2.5}$ in Singleton and Muswellbrook; strong seasonal variation with minimum in winter.

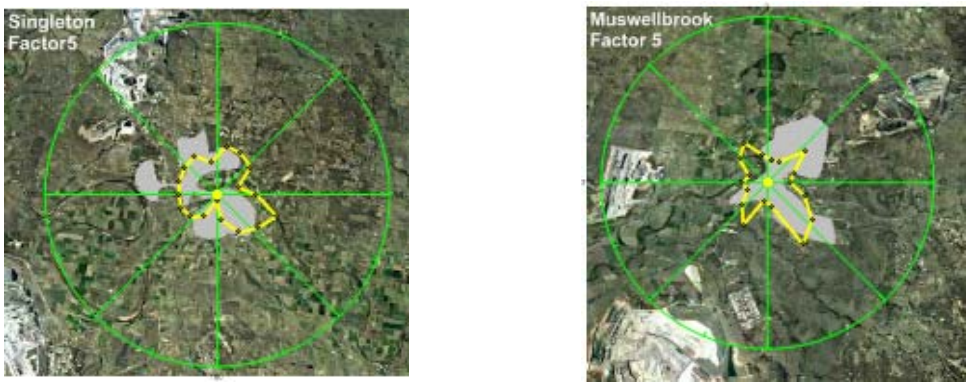

Figure 38. CPF plot of Factor 5 (Industry Aged Sea Salt) at Singleton (left) and Muswellbrook (right). At Singleton (left) and Muswellbrook (right) highest concentrations of the Industry Aged Sea Salt factor are associated with winds from the southeast (the direction of the coast).

6.6 Factor 6 – Soil

The average contribution of Factor 6 to $PM_{2.5}$ is 12% at Singleton and 11% at Muswellbrook. This factor is identified as soil dust because it includes the key elements associated with crustal dust – Al, Si, Ca, Ti and Fe. There is a very strong correlation (r^2 = 0.97) between Al and Si in all samples and the [Si/Al] ratio of 3.1 matches that of soil dust. There is a similar strong correlation for aluminium and titanium with an [Al/Ti] ratio of 14.

The soil factor accounts for 29% of the BC at Muswellbrook and 8% of the BC at Singleton. The time series at Muswellbrook displays a faint seasonal cycle with a minimum during the winter months (Figure 40).

The CPF plot (Figure 41) at Muswellbrook shows a strong lobe towards the southwest in the direction of an open cut mine site closest to the town. Thus the possibility exists that the higher contribution of BC to the soil factor at Muswellbrook may be due to emission from the open cut coal mine site to the southwest of the town.

This is similar to the Soil factor identified by Cohen et al. (2012) at Richmond where the same five key elements were used (Al, Si, Ca, Ti and Fe). At Richmond this factor contributed 5% on average to the $PM_{2.5}$ loading. At Liverpool a similar factor was also identified (Cohen et al., 2011) dominated by Al, Si, K, Ca, Ti, Mn and Fe and low in H, BC and S.

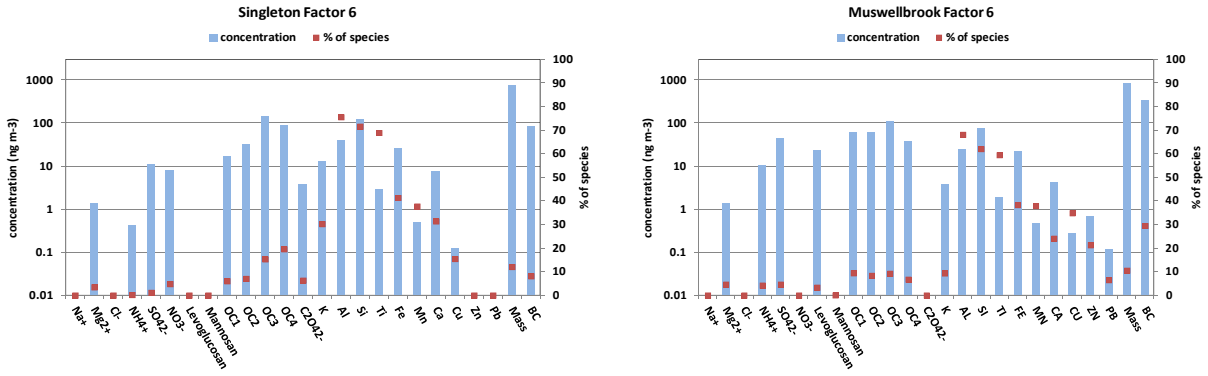

Figure 39 Fingerprint of Factor 6 (Soil) at Singleton (left) and Muswellbrook (right)

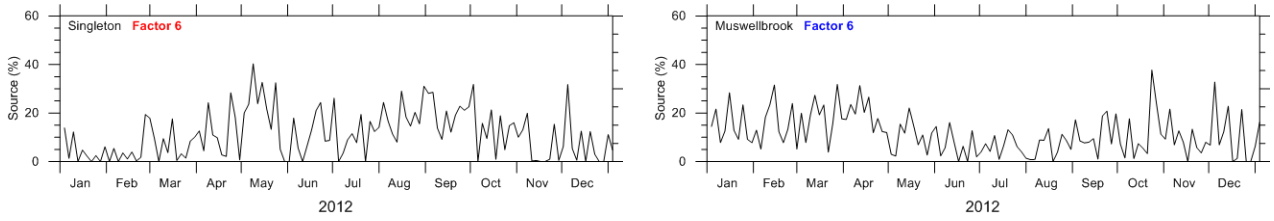

Figure 40. Time series of percentage that Factor 6 (Soil) contributes to $PM_{2.5}$ in Singleton and Muswellbrook; weak seasonal variation but with different phase at the two sites – low in summer in Singleton but low in winter in Muswellbrook.

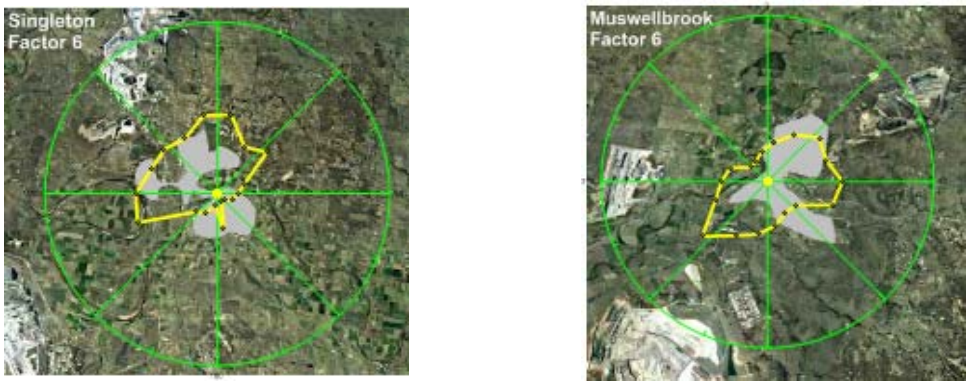

Figure 41 CPF plot of Factor 6 (Soil) at Singleton (left) and Muswellbrook (right). At Singleton (left) highest contributions from the Soil factor are associated with winds from the northwest (in the direction of an open cut coal mine) and Muswellbrook (right) highest concentrations of the Soil factor are associated with winds from the southwest (also in the direction of an open cut coal mine).

6.7 Factor 7 –Sea salt

The average contribution of Factor 7 to $PM_{2.5}$ is 8% at Singleton and 3% at Muswellbrook. This factor is dominated by the sea water elements of Na^+, Cl^-, and Mg^{2+} as well as lower levels of Ca and K. The constituent data shows a very tight correlation between Na^+ and Mg^{2+} with the same [Na^+/Mg^{2+}] ratio as that for standard sea water (8.2:1). Similarly the [Mg^{2+}/Ca^{2+}] ratio is within 10% of that for standard sea water (3.1:1). The average [Cl^-/Na^+] ratio (1.3 at Singleton and 1.2 at Muswellbrook) is lower than the value for standard sea water (1.8) but this factor, at both sites, also contains some nss SO_4^{2-} and NO_3^- which accounts for a slight Cl^- loss.

The CPF plots in Figure 44 both show a dominant south-east wind component, which is the direction of the coast. The extreme spikiness in the time series in Figure 43 reflects the fact that occasionally meteorological conditions are conducive to the transport of coastal air direct to these sites with much higher than average sea salt concentrations. The lower contribution of this factor at Muswellbrook is consistent with Muswellbrook being a greater distance from the coast than Singleton.

This is similar to the Sea salt factor identified by Cohen et al. (2012) at Richmond where Na and Cl, with small amounts of Br were used to indicate sea spray. In our analysis however Br was removed from the PMF analysis since the concentration of this species was below the MDL for more than 95% of the time. Cohen et al. (2012) explain the higher than the expected of [Cl/Na] to an excess of Cl in this source possibly from Cl sources such as motor vehicle exhaust. This factor contributed to 5% of the $PM_{2.5}$ mass at Richmond. At Liverpool high Na and Cl with traces of H and Ca, and no sulfate were indicators of a seaspray factor (Cohen et al. 2011).

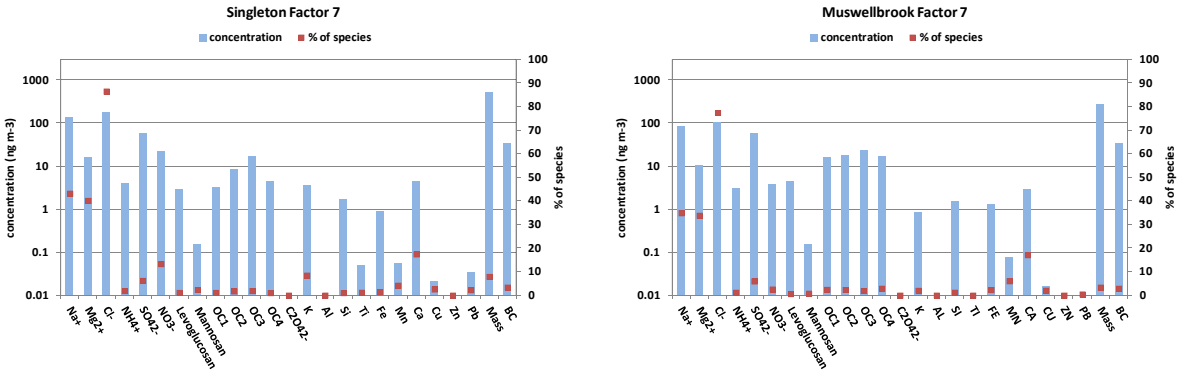

Figure 42 Fingerprint of Factor 7 (Sea Salt) at Singleton (left) and Muswellbrook (right).

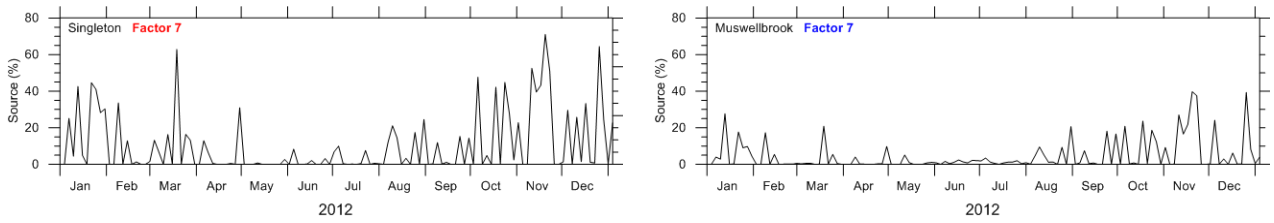

Figure 43. Time series of percentage that Factor 7 (Sea Salt) contributes to $PM_{2.5}$ in Singleton and Muswellbrook; large day-to-day variations but seasonal variation with low values during winter.

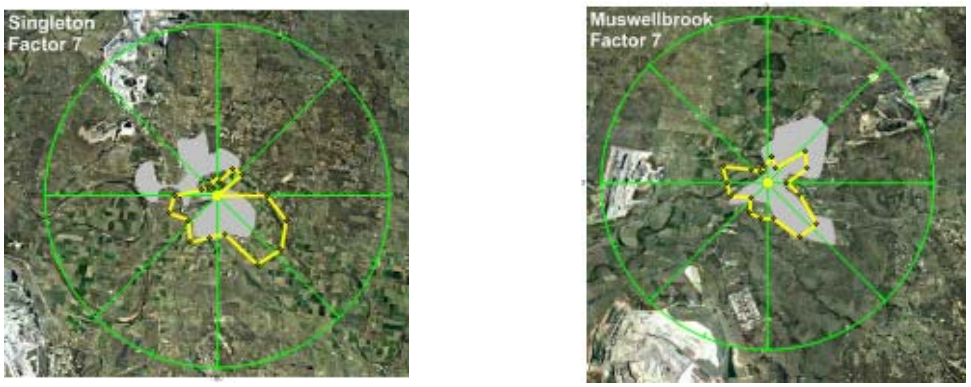

Figure 44. CPF plot of Factor 7 (Sea Salt) at Singleton (left) and Muswellbrook (right). At Singleton (left) and Muswellbrook (right) highest concentrations of the Sea Salt factor are associated with winds from the southeast (the direction of the coast).

6.8 Factor 8 – Secondary Nitrate

The average contribution of Factor 8 to $PM_{2.5}$ is 3% at Singleton and 8% at Muswellbrook. This factor contains most of the NO_3^- and includes some NH_4^+, Cl^-, Na^+, and OC. Nitrate occurs in atmospheric particles as a result of photochemical reactions in the atmosphere. NO_2 is emitted to the atmosphere during combustion of fossil fuels (e.g. in power stations or motor vehicles) and in the presence sunlight will oxidise to form HNO_3 (nitric acid). Nitrate is neutralised by the gaseous base ammonia.

The CPF plots (Figure 47) both show the dominant directions to be from the urban areas of the towns, indicating that it is likely to be vehicle exhaust. The local nature of this source is also indicated by the lack of seasonal variation in the time series (Figure 46).

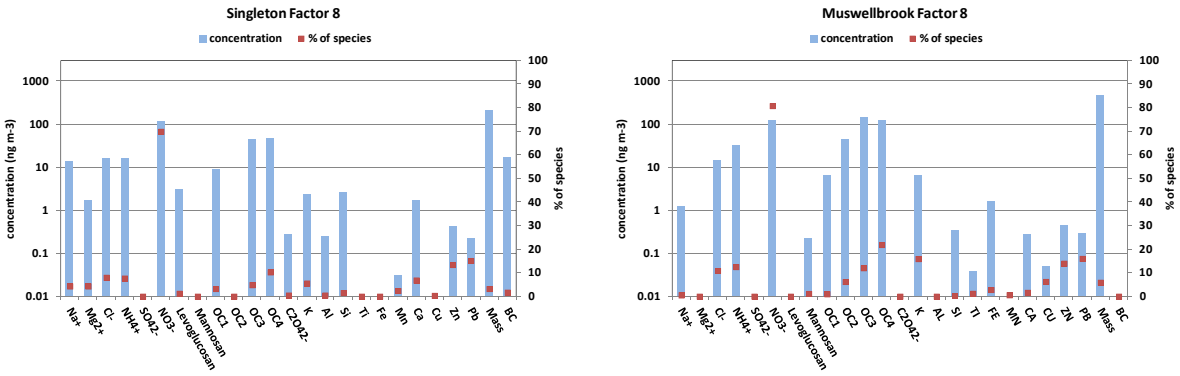

Figure 45 Fingerprint of Factor 8 (Secondary Nitrate) at Singleton (left) and Muswellbrook (right)

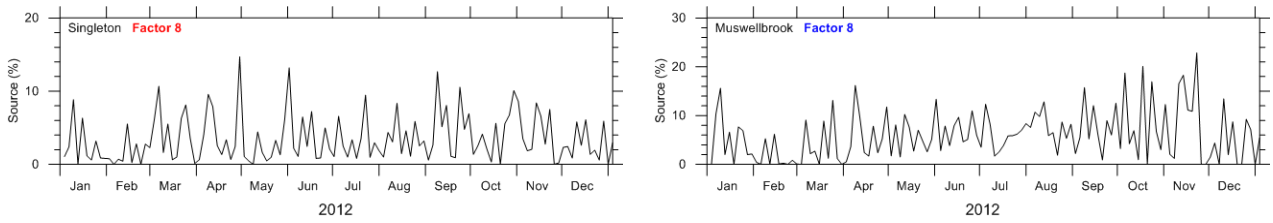

Figure 46. Time series of percentage that Factor 8 (Secondary Nitrate) contributes to $PM_{2.5}$ in Singleton; negligible seasonal variation.

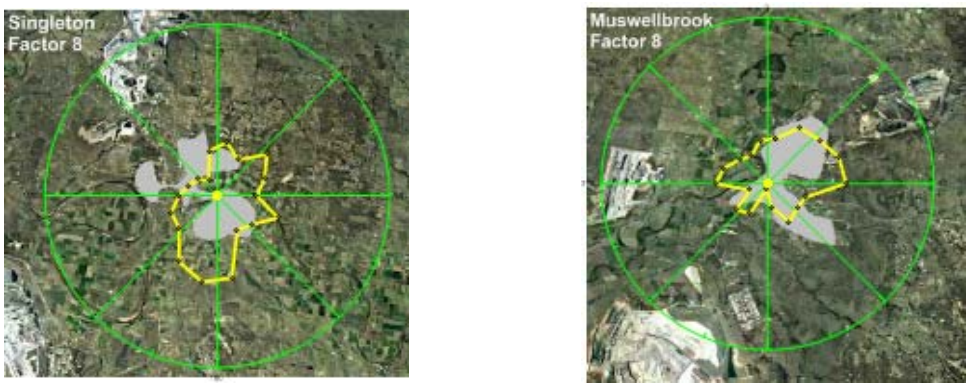

Figure 47. CPF plot of Factor 8 (Secondary Nitrate) at Singleton (left) and Muswellbrook (right). At Singleton (left) the highest contributions are in broad lobes to the south and north-east, and at Muswellbrook (right) the highest contributions are associated with winds from the northeast, which is the main activity area of the town.

6.9 Seasonal variability

The contribution during the year of the various factors to the total $PM_{2.5}$ concentration is shown for Singleton in Figure 48 and for Muswellbrook in Figure 49. Figure 50 shows bar charts of the annual and seasonal contributions of the various factors to the $PM_{2.5}$ loadings. Woodsmoke is clearly the dominant source of $PM_{2.5}$ during the winter, particularly at Muswellbrook. Secondary Sulfate and Industry Aged Sea Salt make higher contributions during the summer months at both sites.

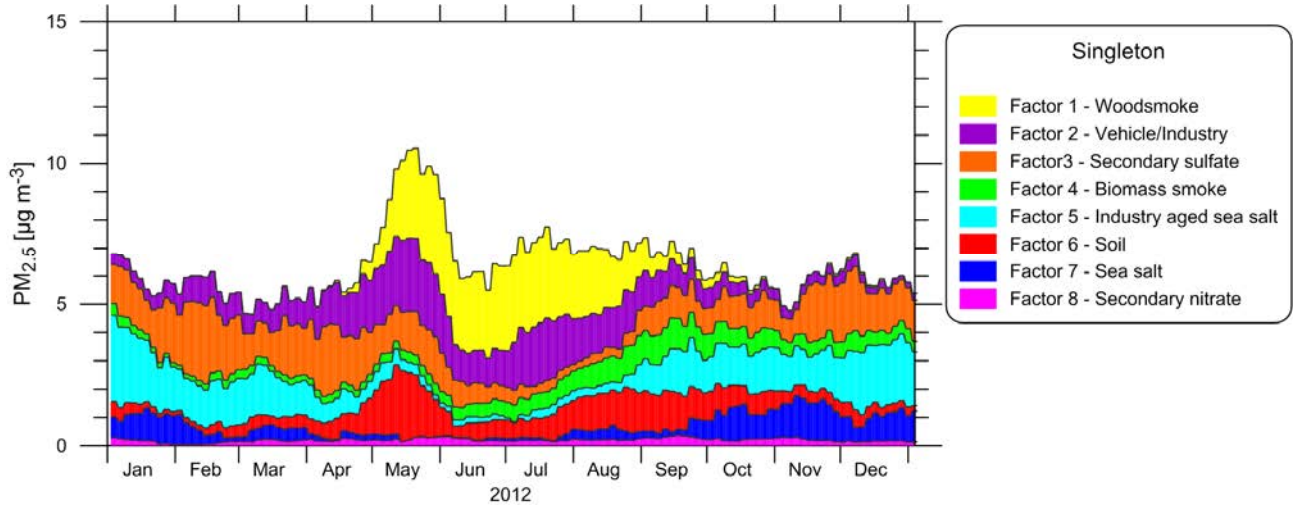

Figure 48. Time series (smoothed with 31-day running window) of the contribution of each factor to the total $PM_{2.5}$ in Singleton.

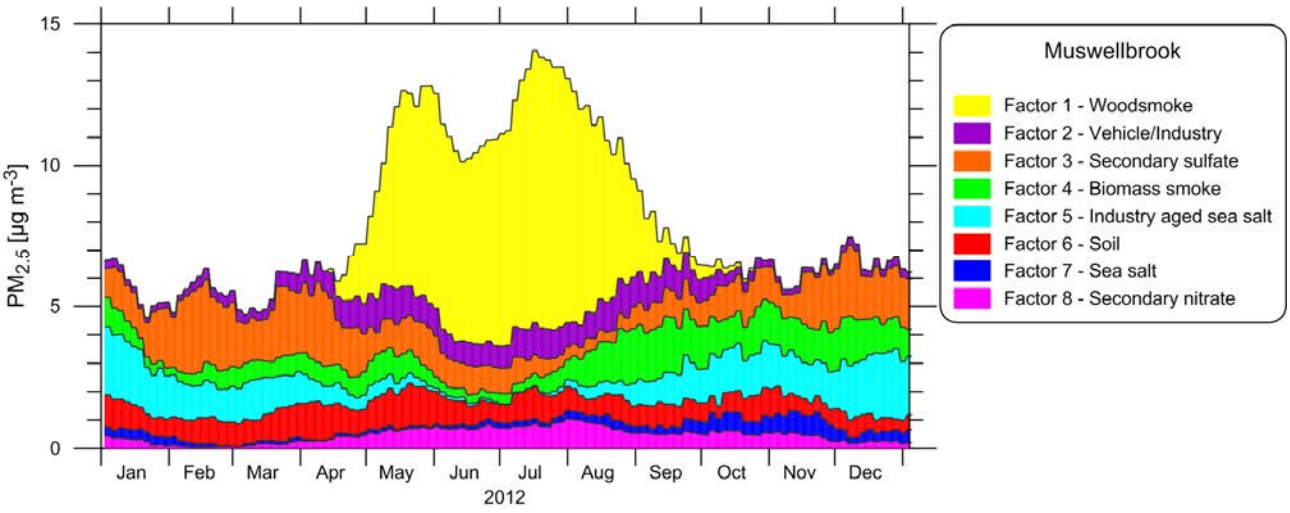

Figure 49. Time series (smoothed with 31-day running window) of the contribution of each factor to the total $PM_{2.5}$ in Muswellbrook

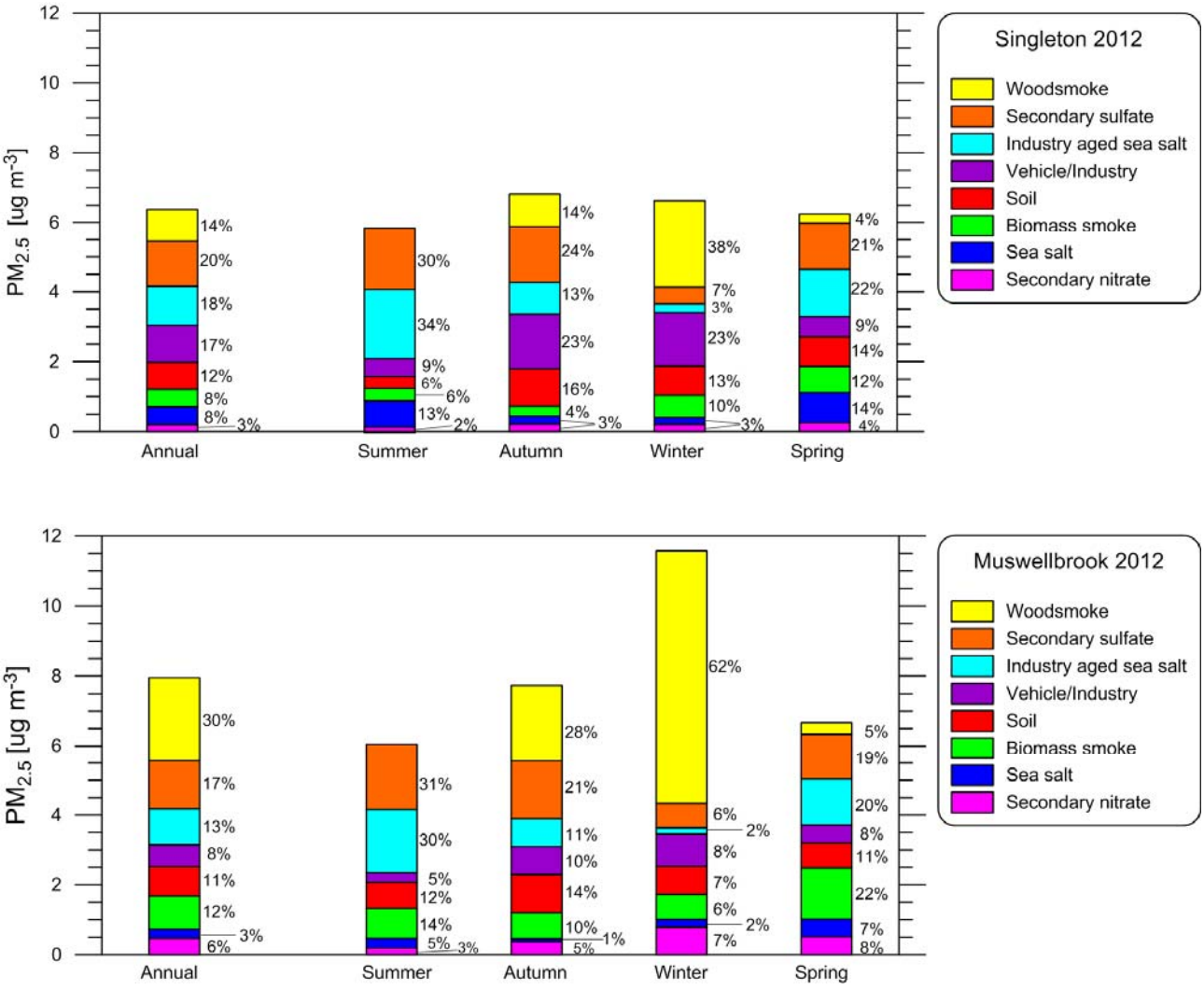

Figure 50. Annual and seasonal source contributions to $PM_{2.5}$ concentrations in Singleton (above) and Muswellbrook (below).

7 Discussion

Table 9 summarises the results from the previous section, listing the main species in each factor and the potential sources of emissions contributing to each factor. The uncertainty in the contribution by each factor to total $PM_{2.5}$ includes uncertainties from the PMF analysis (the uncertainty in the mathematical factor analysis procedure), estimates of uncertainties from the differences between the main CSIRO EPA PMF analysis described in Section 6 and ANSTO PMF2 DOS analysis described in Appendix C and a minimum uncertainty of 10% as an estimate of inherent uncertainty in field studies of the atmosphere.

The results of an independent PMF analysis of the speciated data undertaken by ANSTO are presented in Appendix C . Although there were slight differences between the CSIRO and ANSTO analyses, the final results showed good agreement in the source apportionment for all major sources. The results are compared in Table A 3 of Appendix C

Table 9 Summary of the PMF factors (from the EPA PMF 3.0 analysis), main species, contributions of these factors at each site and potential sources

Factor	Main Species in Factor	Contribution of the factor to total annual PM2.5 mass at:		Potential Sources
		Singleton	Muswellbrook	
Factor 1 Woodsmoke	levoglucosan, mannosan, OC1	14 ± 2%	30± 3%	Domestic woodheaters
Factor 2 Vehicle/Industry	BC, OC1, OC2, SO_4^{2-} Fe, Zn, Mn, Cu	17 ± 2%	8 ± 1%	Vehicles, industry
Factor 3 Secondary Sulfate	NH_4^+, SO_4^{2-}	20 ± 2%	17 ± 2%	Local and regional sources of SO_2 such as power stations
Factor 4 Biomass Smoke	OC2, OC3, OC4, K, SO_4^{2-}, Al, Si, Ti, BC	8 ± 2%	12 ± 2%	Wildfires, hazard reduction burns
Factor 5 Industry Aged Sea Salt	Na^+, Mg^{2+}, SO_4^{2-} and with almost no Cl^-	18 ± 3%	13 ± 2%	Sea salt, local and regional sources of SO_2 such as power stations
Factor 6 Soil	Al, Si, Ca, Ti and Fe	12 ± 2%	11 ± 1%	Soil dust, fugitive coal dust
Factor 7 Sea Salt	Na^+, Cl^-, and Mg^{2+}	8 ± 1%	3 ± 1%	Sea salt
Factor 8 Secondary Nitrate	NO_3^- and includes some NH_4^+, Cl^-, Na^+, OC	3 ± 2%	6 ± 1%	Motor vehicle NO_2, power station NO_2

Notes: Al – aluminium; BC – black carbon; Ca – calcium; Cl^- – chloride; Cu – copper; Fe – iron; K – potassium; Mg^{2+} – magnesium; Mn – manganese; Na^+ – sodium; NH_4^+ – ammonium; NO_3^- – nitrate; OC1-OC4 – fractions of organic carbon distinguished by the volatility of the organic compounds, OC1 is the most volatile, as organic aerosol ages its OC becomes less volatile; Si – silicon; SO_4^{2-} – sulfate; Ti – titanium; Zn – zinc.

This Upper Hunter Valley Particle Characterisation Study focused on determining components and sources of ambient (airborne) $PM_{2.5}$ at the Singleton and Muswellbrook UHAQMN sites.

Additional information is provided by the NSW EPA's 2008 Calendar Year Air Emissions Inventory which lists sources of $PM_{2.5}$ emissions for the Upper Hunter region as a whole, showing: coal mining (66% of emissions), industrial vehicles and equipment (13.5%), coal fired power stations (13%) as the main sources

of emissions, with other sources contributing less than 5% including woodheating at 0.6% *(http://www.epa.nsw.gov.au/air/airinventory2008.htm).*

There are a number of reasons that the information provided by the results from the current study differ from the information in the Air Emissions Inventory.

Whereas the Air Emissions Inventory comprises estimates of total emissions for the whole Upper Hunter, this study is based on the airborne $PM_{2.5}$ concentrations observed at the Singleton and Muswellbrook monitoring sites. For emissions from a source to be detected at a measurement site (receptor), they must be transported (blown by the wind) from the source to the receptor. As the distance from the source to the receptor increases, so the concentration decreases due to mixing and dilution, and an increasing amount of $PM_{2.5}$ is removed by deposition to the ground, vegetation, etc.

For example, the emissions inventory calculates $PM_{2.5}$ emitted from a range of dust generating sources, such as unsealed roads. As these $PM_{2.5}$ emissions are transported from the source, they mix in the atmosphere and become more dilute. They can also mix with other sources of $PM_{2.5}$. Measurements of $PM_{2.5}$ at Singleton and Muswellbrook contain both the dilute emissions transported from distant sources, as well as more concentrated emissions from sources closer to the monitoring.

Additionally, the Air Emissions Inventory only includes 'primary' $PM_{2.5}$ emitted directly from sources, whereas the airborne $PM_{2.5}$ measured in this study includes both primary particles as well as secondary particles formed in the atmosphere via chemical reactions and gas-to-particle conversions. There is also some transport of particles from distant sources into the region, for example, sea salt.

7.1 Coal dust contributions

Open cut coal mines are one of the major industrial activities in the Upper Hunter Region. A break-down of the 2008 Upper Hunter emissions inventory (NSW EPA 2012) provided by the EPA shows coal dust as 5% of total $PM_{2.5}$ emissions. We note that the main goal of this project is the identification of the particle sources that contribute to $PM_{2.5}$ in Singleton and Muswellbrook. If the aim of the project had been to quantify the total contribution of coal dust to the particle loadings, the sampling regime would have differed in that we would have collected PM_{10} samples as a greater proportion of fugitive coal dust emissions are in the coarser $PM_{2.5\text{-}10}$ fraction than in $PM_{2.5}$.

A unique fingerprint for fugitive coal dust emissions was not found in the analysis used in this study. While BC (black carbon) is a component of coal dust, it is also produced by various other sources and processes, especially combustion. Combustion processes result in the formation of very small particles (less than 1 µm), which remain suspended for much longer and travel further from the source than $PM_{2.5}$ coal dust. The Upper Hunter emissions inventory lists 13% of $PM_{2.5}$ particles as emitted from non-road vehicles (almost all from diesel mining vehicles).

In this study the soil fingerprints at both Singleton and Muswellbrook includes BC. This is in contrast to other studies carried out in Australia e.g. Richmond NSW (Cohen et al., 2012) and Liverpool NSW. (Cohen et al., 2011). The BC in the soil fingerprint appears with other elements that are associated with mechanically derived particles such as wind-blown dust, so the BC in the soil fingerprint identified at Singleton and Muswellbrook may result from the contribution of fugitive coal dust emissions. The amount of BC in the soil factor is 1% of total $PM_{2.5}$ at Singleton and 4% of total $PM_{2.5}$ at Muswellbrook. However, the BC in the soil fraction could also be contributed by the re-suspension of non-road diesel vehicle emissions during mining activity.

7.2 Power station contributions

Several power stations operate in the Hunter Valley and the Greater Sydney Basin. Primary $PM_{2.5}$ emissions from power stations make up 13% of the Upper Hunter emissions inventory, but there is also significant generation of secondary particles. The combustion of coal in a power stations results in the emission of SO_2 as does the combustion of other fossil fuels e.g. in motor vehicles. As discussed in section 6.3, in the

presence of sunlight SO_2 will oxidise to form sulfuric acid (H_2SO_4), which is subsequently neutralised by NH_3 to produce $(NH_4)_2SO_4$. The particles generated in this process are less than 1 µm in diameter and these sulfate particles have a residence time of 3-5 days in the atmosphere (Seinfeld and Pandis 2006). This means that they represent a well-mixed population of particles.

In this study a secondary sulfate fingerprint was identified at both Singleton and Muswellbrook. However it is not possible to directly attribute this fingerprint to powers stations alone or to power stations in the Hunter Valley. There is evidence that the sulfur is derived from a mixture of many regional SO_2 emitters. Firstly, the average SO_4^{2-} concentrations measured at Muswellbrook and Singleton are not higher than those found in other Australian locations. For example, Chan et al. (2008) measured average S concentrations of S ≈ 300 ±300 ng m^{-3} at eight urban and suburban sites in four Australian cities (Melbourne, Sydney, Brisbane and Adelaide) that are similar to those in the Upper Hunter Valley (S = 282 ± 240 ng m^{-3} in Muswellbrook and 255 ± 230 ng m^{-3} in Singleton). Secondly, the CPF plot for factor 3 for Singleton (Figure 28) shows a significant lobe to the south-east, i.e. when the winds are not directly from the Upper Hunter power stations. Additionally, despite summer wind directions at Singleton being almost exclusively south-easterly (Figure 11), which puts the Upper Hunter power stations downwind of Singleton, the time series of factor 3 (Figure 27) show similar amounts of this factor in summer at both monitoring sites. This evidence shows that regional rather than just local SO_2 emitters make a major contribution to the locally observed secondary sulfate factor.

This result also provides support for significant regional transport of the primary $PM_{2.5}$ emitted from the power stations stacks. This is also underpinned by knowledge of dispersion meteorology for these tall stack emissions (e.g. Perry et al., 2005). It can be concluded that although primary $PM_{2.5}$ emissions from power stations make up 13% of the Upper Hunter emissions inventory, they would contribute much less than this to $PM_{2.5}$ concentrations measured in this study.

8 Conclusions

This study provides detailed analysis of the composition of $PM_{2.5}$ in the two main population centres in the Upper Hunter during 2012. The study has described the contributors to fine particles in the Upper Hunter and identified the most important sources and their relative contributions. Seasonal changes in both total $PM_{2.5}$ and the contribution of different sources to $PM_{2.5}$ were also described.

During 2012 the dominant factors at Singleton were identified as:

- Secondary Sulfate, 20 ± 2%
- Industry Aged Sea Salt, 18 ± 3%
- Vehicle/Industry, 17 ± 2%
- Woodsmoke, 14 ± 2%
- Soil, 12 ± 2%,

and at Muswellbrook:

- Woodsmoke, 30 ± 3%
- Secondary Sulfate, 17 ± 2%
- Industry Aged Sea Salt, 13 ± 2%
- Biomass Smoke, 12 ± 2%
- Soil, 11 ± 1%.

Two sets of PMF analysis conducted by CSIRO and ANSTO yielded very similar results, and provide confidence in the veracity of these results. The fingerprints of the factors identified in this study compare well with factors identified and described in other characterisation studies conducted at sites in NSW such as Richmond and Liverpool.

There is some significant seasonal variation in the contributions from some factors.

Woodsmoke is the dominate source of fine particles at both sites during the winter making up an average of 62% of the $PM_{2.5}$ in Muswellbrook and 38% of the $PM_{2.5}$ in Singleton. The Woodsmoke factor is very well defined and a strong seasonal signal is evident with no contribution from this factor to particle levels during summer.

Secondary Sulfate makes the highest contributions during the summer months along with Industry Aged Sea Salt. Both of these factors include secondary particles formed as a result of photochemical reactions in the atmosphere. The sulfate levels measured in this study are comparable to levels found in other Australian locations. The study provides evidence of sulfate as a pollutant at regional scales with considerable regional and inter-regional transport.

A unique fingerprint for fugitive coal dust emissions was not found in this study. However the Soil fingerprints at both Singleton and Muswellbrook identified in this study include BC. This is in contrast to other studies carried out in Australia. The BC in the Soil fingerprint identified at Singleton and Muswellbrook may result from the contribution of fugitive coal dust emissions. However, the BC in the Soil factor could also be contributed by the re-suspension of non-road diesel vehicle emissions during mining activity. Nevertheless the amount of BC in the Soil factor is 1% of total $PM_{2.5}$ at Singleton and 4% of total $PM_{2.5}$ at Muswellbrook.

Some factors such as Factor 2 (Vehicle/Industry) and Factor 4 (Biomass Smoke), provided less definitive identification of sources. However even in these factors likely dominant sources were identified. Further work may be needed to more completely describe the sources embedded in these factors.

This study demonstrates that there are some complex interactions between source emissions, meteorology, particle transport and transformation, and observed ambient concentration. Detailed analysis of specific events such as the elevated BC observed in Singleton in late May could provide additional information about these complex inter-relationships.

References

Chan, Y. C., D. D. Cohen, O. Hawas, E. Stelcer, R. Simpson, L. Denison, N. Wong, M. Hodge, E. Comino and S. Carswell (2008). "Apportionment of sources of fine and coarse particles in four major Australian cities by positive matrix factorisation." Atmospheric Environment **42**(2): 374-389.

Cheung, K. L., L. Ntziachristos, T. Tzamkiozis, J. J. Schauer, Z. Samaras, K. F. Moore and C. Sioutas (2010). "Emissions of Particulate Trace Elements, Metals and Organic Species from Gasoline, Diesel, and Biodiesel Passenger Vehicles and Their Relation to Oxidative Potential." Aerosol Science and Technology **44**(7): 500-513.

Chow, J. C., J. G. Watson, L. W. A. Chen, M. C. O. Chang, N. F. Robinson, D. Trimble and S. Kohl (2007). "The IMPROVE-A temperature protocol for thermal/optical carbon analysis: maintaining consistency with a long-term database." Journal of the Air & Waste Management Association **57**(9): 1014-1023.

Chow, J. C., J. G. Watson, H. Kuhns, V. Etyemezian, D. H. Lowenthal, D. Crow, S. D. Kohl, J. P. Engelbrecht and M. C. Green (2004). "Source profiles for industrial, mobile, and area sources in the Big Bend Regional Aerosol Visibility and Observational study." Chemosphere **54**(2): 185-208.

Cohen, D. D. (1993). "Applications of simultaneous IBA techniques to aerosol analysis." Nuclear instruments & methods in physics research. Section B, Beam interactions with materials and atoms **79**(1-4): 385-388.

Cohen, D. D. (1996). "Elemental analysis by PIXE and other IBA techniques and their application to source fingerprinting of atmospheric fine particle pollution." Nuclear instruments & methods in physics research. Section B, Beam interactions with materials and atoms **109-110**: 218-226.

Cohen, D. D. (1998). "Characterisation of atmospheric fine particles using IBA techniques." Nuclear instruments & methods in physics research. Section B, Beam interactions with materials and atoms **136-138**: 14-22.

Cohen, D. D., J. Crawford, E. Stelcer and A. J. Atanacio (2012). "Application of positive matrix factorization, multi-linear engine and back trajectory techniques to the quantification of coal-fired power station pollution in metropolitan Sydney." Atmospheric Environment **61**: 204-211.

Cohen, D. D., J. Crawford, E. Stelcer and V. T. Bac (2010). "Characterisation and source apportionment of fine particulate sources at Hanoi from 2001 to 2008." Atmospheric Environment **44**(3): 320-328.

Cohen, D. D., E. Stelcer, D. Garton and J. Crawford (2011). "Fine particle characterisation, source apportionment and long-range dust transport into the Sydney Basin: a long term study between 1998 and 2009 " Atmospheric Pollution Research **2**(2): 182-189.

Goncalves, C., C. Alves, M. Evtyugina, F. Mirante, C. Pio, A. Caseiro, C. Schmidl, H. Bauer and F. Carvalho (2010). "Characterisation of PM10 emissions from woodstove combustion of common woods grown in Portugal." Atmospheric Environment **44**(35): 4474-4480.

Hennigan, C. J., A. P. Sullivan, J. L. Collett, Jr. and A. L. Robinson (2010). "Levoglucosan stability in biomass burning particles exposed to hydroxyl radicals." Geophysical Research Letters **37**.

Iinuma, Y., E. Brüggemann, T. Gnauk, K. Müller, M. O. Andreae, G. Helas, R. Parmar and H. Herrmann (2007). "Source characterization of biomass burning particles: The combustion of selected European conifers, African hardwood, savanna grass, and German and Indonesian peat." Journal of Geophysical Research: Atmospheres **112**(D8): D08209.

Joly, A., J. Lambert, C. Gagnon, G. Kennedy, D. Mergler, A. Adam-Poupart and J. Zayed (2011). "Reduced Atmospheric Manganese in Montreal Following Removal of Methylcyclopentadienyl Manganese Tricarbonyl (MMT)." Water Air and Soil Pollution **219**(1-4): 263-270.

Kim, E. and P. K. Hopke (2004). "Comparison between conditional probability function and nonparametric regression for fine particle source directions." Atmospheric Environment **38**(28): 4667-4673.

Malm, W. C., J. F. Sisler, D. Huffman, R. A. Eldred and T. A. Cahill (1994). "Spatial and seasonal trends in particle concentration and optical extinction in the United-States." Journal of Geophysical Research-Atmospheres **99**(D1): 1347-1370.

NICNAS (2003). Methylcyclopentadienyl Manganese Tricarbonyl (MMT):Priority Existing Chemical Assessment Report No. 24**:** 151.

Norris, G., R. Vedantham, K. Wade, S. Brown, J. Prouty and C. Foley (2008). EPA Positive matrix factorization (PMF) 3.0 - Fundamentals and User Guide. US EAP/600/R-08/108 www.epa.gov/heasd/research/pmf.html.

NSW EPA (1999). Selecting, installing and operating domestic solid fuel heaters.

NSW EPA (2012). Air emissions inventory for the greater metropolitan region in New South Wales: 2008 Industrial Emissions. N. E. P. Authority. Sydney, NSW.

Paatero, P. (1997). "Least squares formulation of robust non-negative factor analysis." Chemometrics and Intelligent Laboratory Systems **37**(1): 23-35.

Perry, S. G., A. J. Cimorelli, R. J. Paine, R. W. Brode, J. C. Weil, A. Venkatram, R. B. Wilson, R. F. Lee and W. D. Peters (2005). "AERMOD: A dispersion model for industrial source applications. Part II: Model performance against 17 field study databases." Journal of Applied Meteorology **44**(5): 694-708.

Poirot, R. L., P. R. Wishinski, P. K. Hopke and A. V. Polissar (2001). "Comparative application of multiple receptor methods to identify aerosol sources in northern Vermont." Environmental Science & Technology **35**(23): 4622-4636.

Russell, L. M. (2003). "Aerosol organic-mass-to-organic-carbon ratio measurements." Environmental Science & Technology **37**(13): 2982-2987.

Seinfeld, J. H. and S. N. Pandis (2006). "Atmospheric chemistry and physics: from air pollution to climate change." Atmospheric chemistry and physics: from air pollution to climate change: xxviii + 1203 pp.

Sternbeck, J., A. Sjodin and K. Andreasson (2002). "Metal emissions from road traffic and the influence of resuspension - results from two tunnel studies." Atmospheric Environment **36**(30): 4735-4744.

Taha, G., G. P. Box, D. A. Cohen and E. Stelcer (2007). "Black carbon measurement using laser integrating plate method." Aerosol Science and Technology **41**(3): 266-276.

USEPA (2012). Report to Congress on Black Carbon, Appendix 1: Ambient and Emissions Measurements of Black Carbon.

Appendix A Data quality: Sampling

While both samplers were operated with $PM_{2.5}$ size selective inlets, because of the closeness of the $PM_{2.5}$ cut point to the fine mode in the typical ambient particle size distribution (Figure A 1), any deviation from the correct flow rate will result in a change in the inlet cut size and thus the mass of particles collected. For species that occur in the fine particle range (i.e. less than 1 µm typically from combustion processes such as smoke, vehicle emissions, industrial emissions) this will not be an issue however for species that occur in the coarse mode (derived from mechanical process e.g. wind blown dust and sea salt) this can have a significant effect.

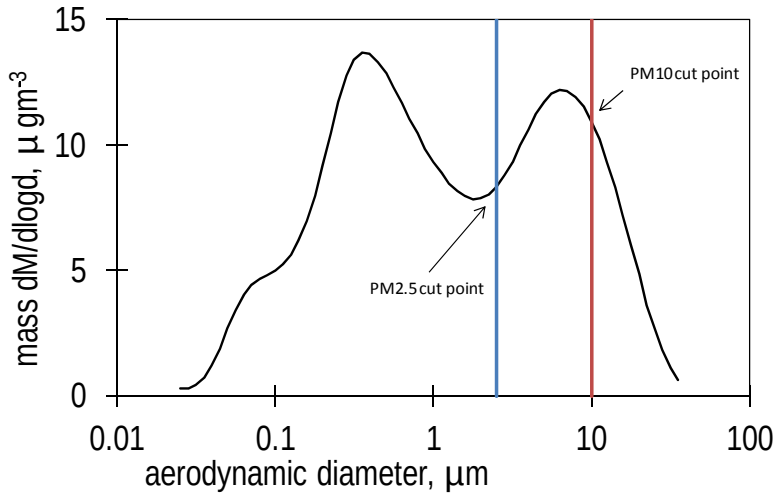

Figure A 1 Size distribution measured at Liverpool in Sydney during the Australian Fine Particle Study (Keywood et al., 1999).

Comparison of species measured by both samplers revealed this to indeed be the case. For species found mostly in the fine particle size range (less than 1 µm) we found good agreement between data measured by PIXE on the 25 mm Teflon filters and by IC on the high volume quartz filters (e.g. S by PIXE and SO_4^{2-} by IC as shown in Figure A 2). However, for species expected to be in the coarse particle range the agreement was poor (e.g. Ca^{2+} by IC and Ca by PIXE). Consequently IC was performed on the $PM_{2.5}$ Teflon filters collected by ANSTO. This removes the uncertainty in the coarse particle species introduced with the use of two different samplers.

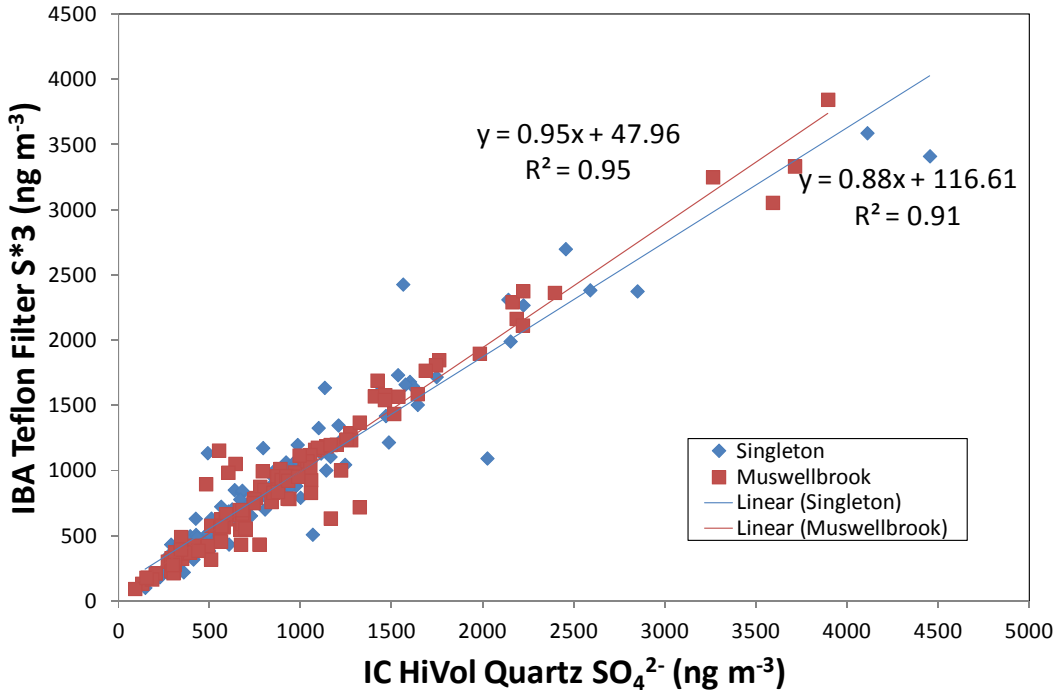

Figure A 2 Comparison of S measured by PIXE on 25 mm Teflon filters and SO_4^{2-}

During the second half of the collection program marks on the high volume quartz filters indicated that the high volume sampler inlet may not have been correctly sealed, allowing the ingress of particles onto the filter that were able to bypass the size selective inlet. This was revealed in the data set when data were compared between the BC measured on the 25 mm Teflon filter by the integrated plate method and EC measured on the high volume quartz filters measured by thermal desorption. Because BC and EC occur in the mode less than 1 µm we would not expect to see a difference caused by inlet cut sizes discussed above. However the time series presented in Figure A 3 shows deterioration in the agreement between the measurements in the second half of the sampling program. The comparison of Ca and Ca^{2+} measured on the 25 mm Teflon filters by PIXE and the high volume quartz filters by IC also shows deterioration in the relationship during the second half of the sampling program. We hypothesis that the enhanced Ca^{2+} on the quartz filters was associated with carbonate which produced an artefact in the EC thermal desorption method, particularly by adding to the OCpyro fraction thus effecting the EC1 fraction. Subsequently we have chosen to use BC for the PMF analysis and have excluded OCpyro and EC1, EC2 and EC3 from the PMF analysis.

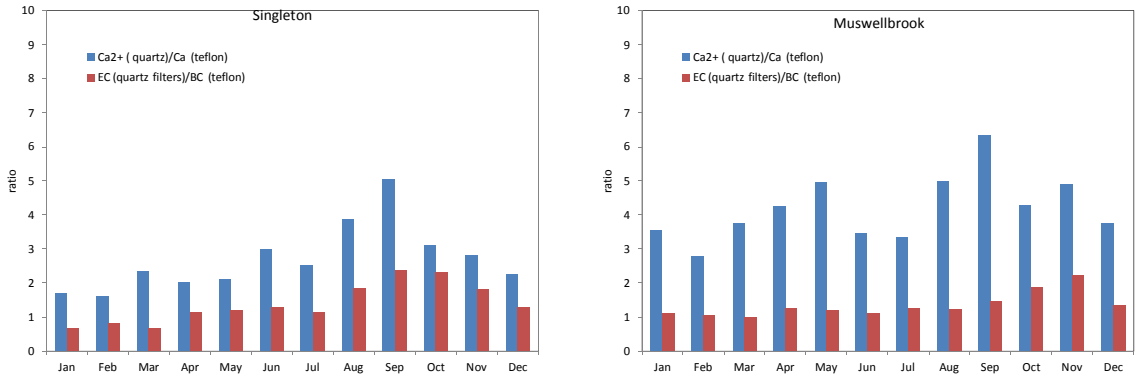

Figure A 3 Monthly averaged ratios of Ca^{2+} (measured on high volume quartz filters by IC) to Ca (measured on 25 mm Teflon filters by PIXE) and EC (measured on high volume quartz filters by thermal desorption) to BC (measured on 25 mm Teflon filters by the integrated plate method). The ratios should be close to 1.

Appendix B Data quality: Analysis

NATA Accreditation

The wet chemistry laboratory at CSIRO Aspendale has National Association of Testing Authority (NATA) accreditation, No 245, for IC analysis. As part of the NATA accreditation a check standard is analysed in each analysis run after the 7 calibration standards and then every 20 samples. The samples are reanalysed if:

- Two or more of the control or replicate standards exceed the ”warning” limit, which means the measured value is greater than 2 standard deviations from the true value.
- One or more control or replicate standards exceed the “recal” limit, which means the measured value is greater than 3 standard deviations from the true value.

Blank Filters

Blank filters were analysed throughout the study. The average of the blank concentration is subtracted from each measurement. The blanks are also used to calculate the method detection limit (MDL). We followed the Standards Australia procedures which are those of the International Standard ISO 6879 Air quality – Performance characteristics and related concepts for air quality monitoring methods. Section 5.2.7 of the Standard states that a zero sample has a 5 % probability of causing a measured concentration above the detection limit, so that:

$$MDL = t_{0.95} \times s_{c(0)} \quad (1)$$

where:

$S_{c(0)}$ is the standard deviation of the blanks, and
$t_{0.95}$ is value of the 1-tailed t distribution for P<0.05 (i.e. the 95 % confidence limit).

Ion Balance

The ion balance (IB) gives an indication of the aerosol chemistry data quality in that the total cation equivalents (positive charged ions) should equal the total anion equivalents (negative charged ions). The Global Atmospheric Watch Program (GAW) which is part of the World Meteorological Organisation (WMO) gives the IB equation and criteria for assessing valid data results in its technical report 160, ”Manual for the GAW Precipitation Chemistry Programme”.

Note that a poor IB does not always indicate bad data quality. For example pH is not measured in this project and samples with high pH levels might have a poor IB due to high levels of bicarbonate; these samples usually also have high levels of calcium. Similarly, samples with low pH may have excess anions. Samples that have been flagged as invalid have been reanalysed. The IB plot for both sites is shown in Figure A 4.

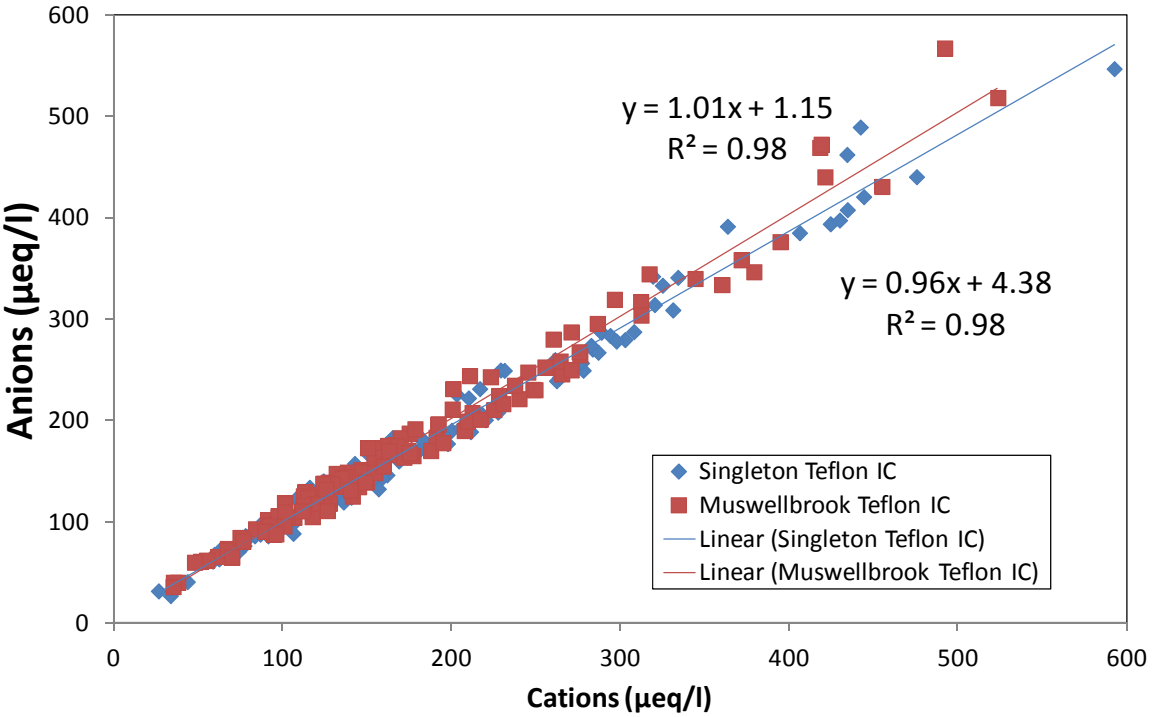

Figure A 4 Ion Balance for the ion chromatography measurements with the anions and cations listed in Section 3.3

WMO Laboratory Inter-comparison

Each year the Wet Chemistry Laboratory at CMAR Aspendale participates in the WMO synthetic rainwater inter-comparison. This involves the analysis of a range of cations and anions on three separate synthetic rainwater samples two times each year. The analytical values for each sample are then compared to the true values. The results of the inter-comparison shown in Figure A 5 indicate that the CMAR Aspendale Wet Chemistry Laboratory performs well in this laboratory inter-comparison. The ring diagram results for CMAR (lab id 700007) are shown for samples 1, 2 and 3. Below the results is the ring diagram overview of the current analyses and the key to the ring diagrams.

Lab 700007 Australia, LIS 2011 45 Ring Diagrams

Sample #1 Sample #2 Sample #3

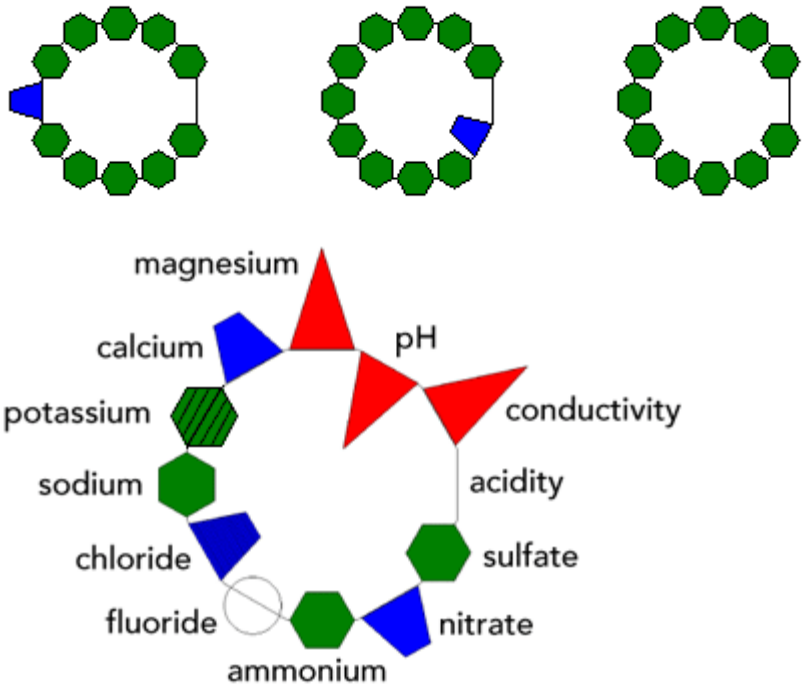

GOOD - Green Hexagon

Measurement is within the interquartile range (IQR), defined as the 25th to 75th percentile or middle half (50%) of the measurements. This applies to sulfate, ammonium, sodium, and potassium.

SATISFACTORY - Blue Trapezoid

Measurement is within the range defined by the median ± IQR/1.349. The ratio, IQR/1.349, is the non-parametric estimate of the standard deviation, sometimes called the pseudo-standard deviation. This applies to nitrate, chloride, and calcium.

UNSATISFACTORY - Red Triangle

Measurement is outside the range defined by the median ± IQR/1.349. This applies to pH, conductivity, and magnesium.

Figure A 5 WMO Inter-Comparison Results and ring diagram overview (see text for more details).

Comparison of Species from IC and IBA analysis

The IC and IBA have some common species which can be compared. Chlorine and sulfur measured by IBA are mostly water soluble and can be compared to chloride and sulfate measured by IC (Figure A6). The sulfur concentrations from IBA analysis have been multiplied by 3 to account for the difference in molecular weight of sulfate. The two analysis methods show very good agreement in mass concentrations and correlations for both comparisons.

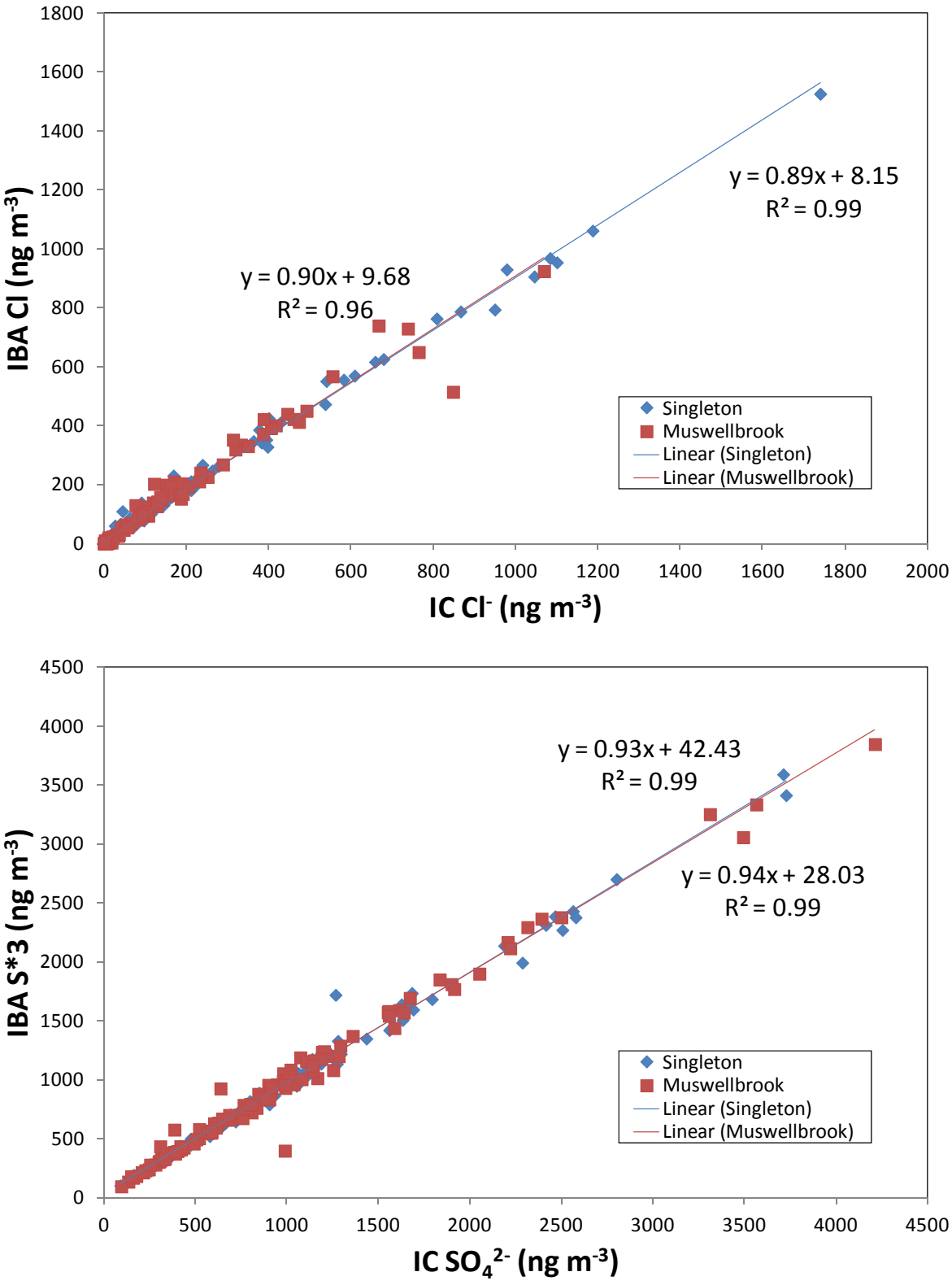

Figure A 6Comparison of IC and IBA analyses for Cl (top) and S (bottom)

Correlation of the eight factors from the EPA PMF analysis

Figure A 7 and Figure A 8 shows the correlation plots between the fingerprints at Singleton and Muswellbrook. These G-Space plots show the independence of the eight factors and is one of the diagnostics when running the EPA PMF program.

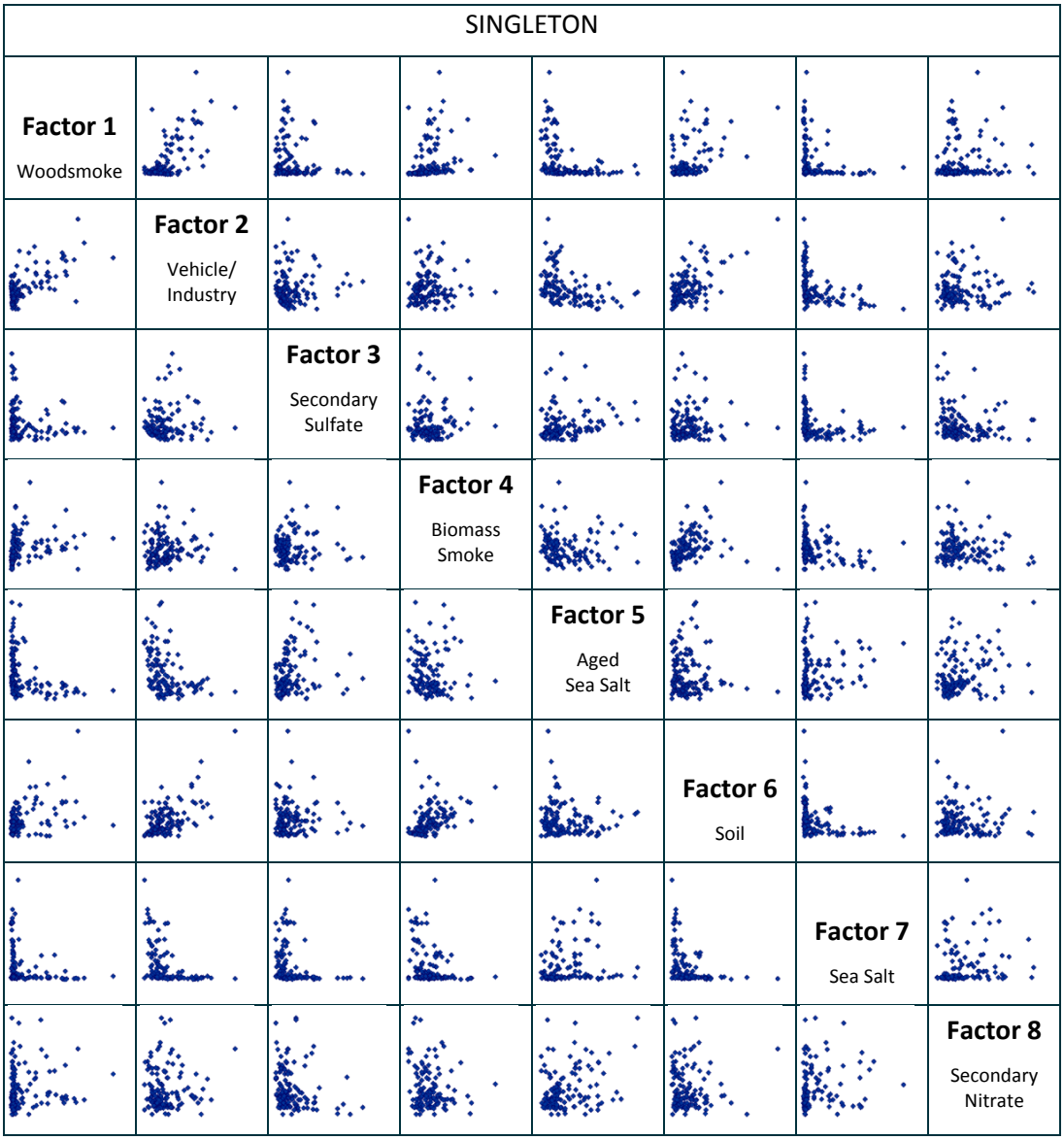

Figure A 7 Correlation plots between the eight EPA PMF factors at Singleton. The left-hand plot on the top line shows the values for each sampling day of the Factor 1 contribution on the y-axis versus the Factor 2 contribution on the x-axis.

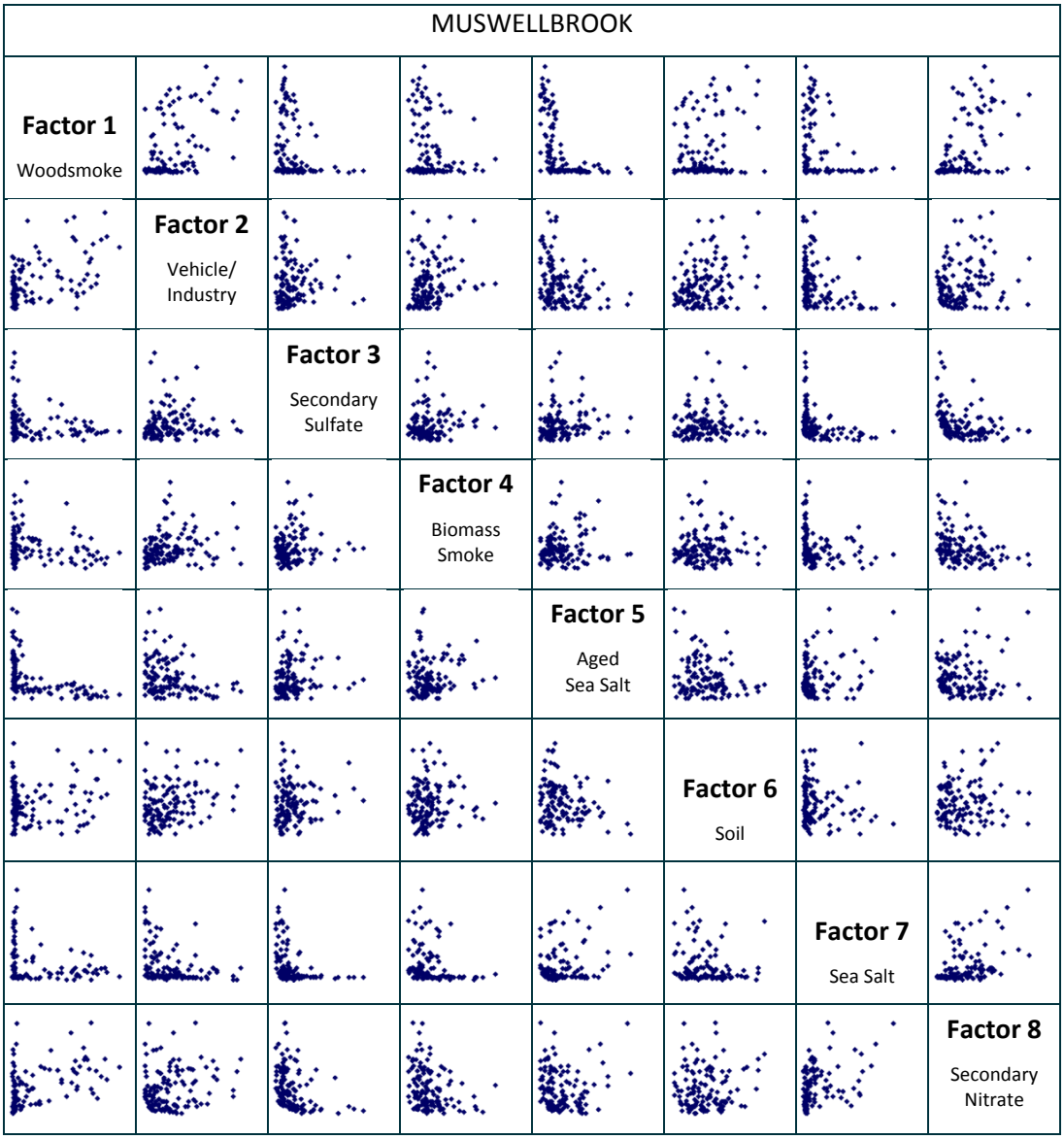

Figure A 8 Correlation plots between the eight EPA PMF factors at Muswellbrook.

Appendix C Data Quality: PMF

The PMF analysis presented in the main body of this report was carried out using the US EPA software package EPA PMF 3.0 (Norris et al, 2008) and the species listed in Tables 4 and 5 for Singleton and Muswellbrook respectively. The PMF analysis was also carried using the PMF2 DOS version and combining the data sets for Muswellbrook and Singleton combined into one data set (to increase the number of samples in the analysis) and the species listed in Table A 1.

Table A 1. Species used in the PMF2 DOS analysis

H	K	Ni	Mg^{2+}
Na	Ca	Cu	Levoglucosan
Al	Ti	Zn	Mannosan
Si	V	Se	Glacatosan
P	Cr	Br	NH_4^+
S	Mn	Pb	NO_3^-
Cl	Fe	BC	Phosphate
	Co	F^-	Oxalate

The ANSTO PMF2 DOS analysis using 31 elements from the IBA and IC analyses revealed nine sources characterised by the profiles shown in Figure A 9 to Figure A 12. These are identified as soil, sea salt (sea), industry sulfur nitrate (IndSNO3), secondary sulfate (2ndryS), Auto1, Smoke1, seasalt aged nitrate (Seaaged NO3), Smoke2 and AutoNO3 using the naming conventions adopted by ANSTO.

As we would expect there is reasonable agreement between these profiles and those identified using the EPA PMF analysis codes presented in the main body of the report (Table A 3). In particular Sea, 2ndryS, soil, Smoke1 and Smoke2 correspond with sea salt, soil, secondary sulfate, soil, biomass smoke and woodsmoke identified in the EPA PMF analysis. AutoNO3 and SeaagedNO3 in the PMF2 DOS analysis when combined may correspond with secondary nitrate in the EPA PMF analysis and Auto1 may correspond with the vehicle/industry factor identified in the EPA PMF analysis. The industry aged seasalt profile identified in the EPA PMF analysis may be similar to the industry sulfur nitrate (IndSNO3) identified in the PMF2 DOS analysis.

Table A 3 compares the relative contribution of the profiles determined from the two PMF analyses to $PM_{2.5}$ mass at each site. Generally there is good agreement with smoke making the greatest contribution to $PM_{2.5}$ mass at Muswellbrook in both analyses and secondary nitrate (AutoNO3) making the lowest contribution at both sites in both analyses. The contribution of secondary sulfate (2ndryS) at each site is similar for both analyses (around 20%). The contribution of seasalt and industry aged seasalt (IndSNO3) are also similar in the two analyses at both sites. Soil and secondary nitrate (AutoNO3) have slightly greater contribution in the EPA PMF analysis. The smoke factor at Singleton is greater in the PMF2 DOS analysis.

This brief comparison shows that despite using different PMF software tools and different species in the PMF analyses, the PMF results can produce similar results. This gives us confidence in the overall PMF results and analysis.

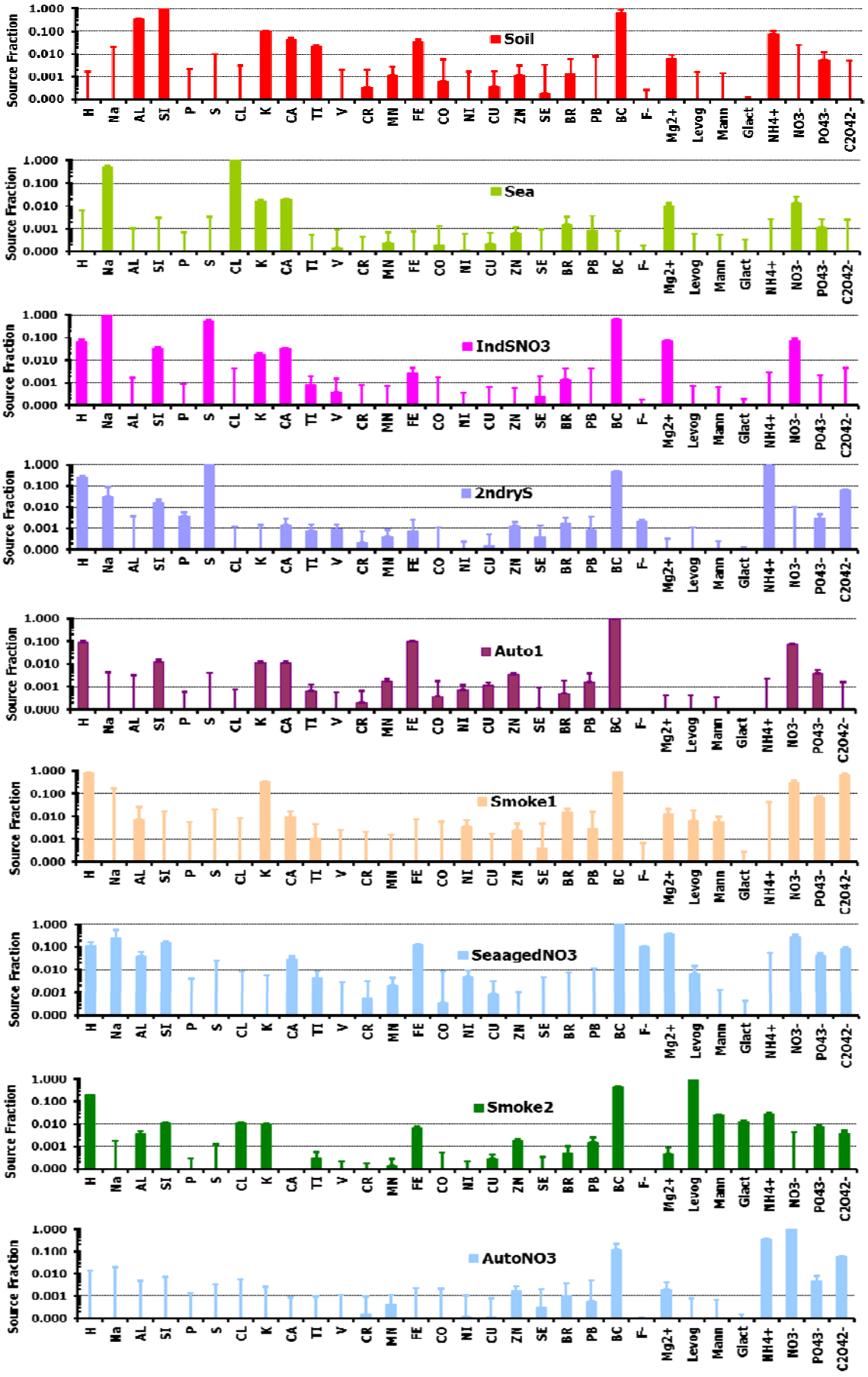

Figure A 9 Fingerprint from the PMF2 DOS analysis

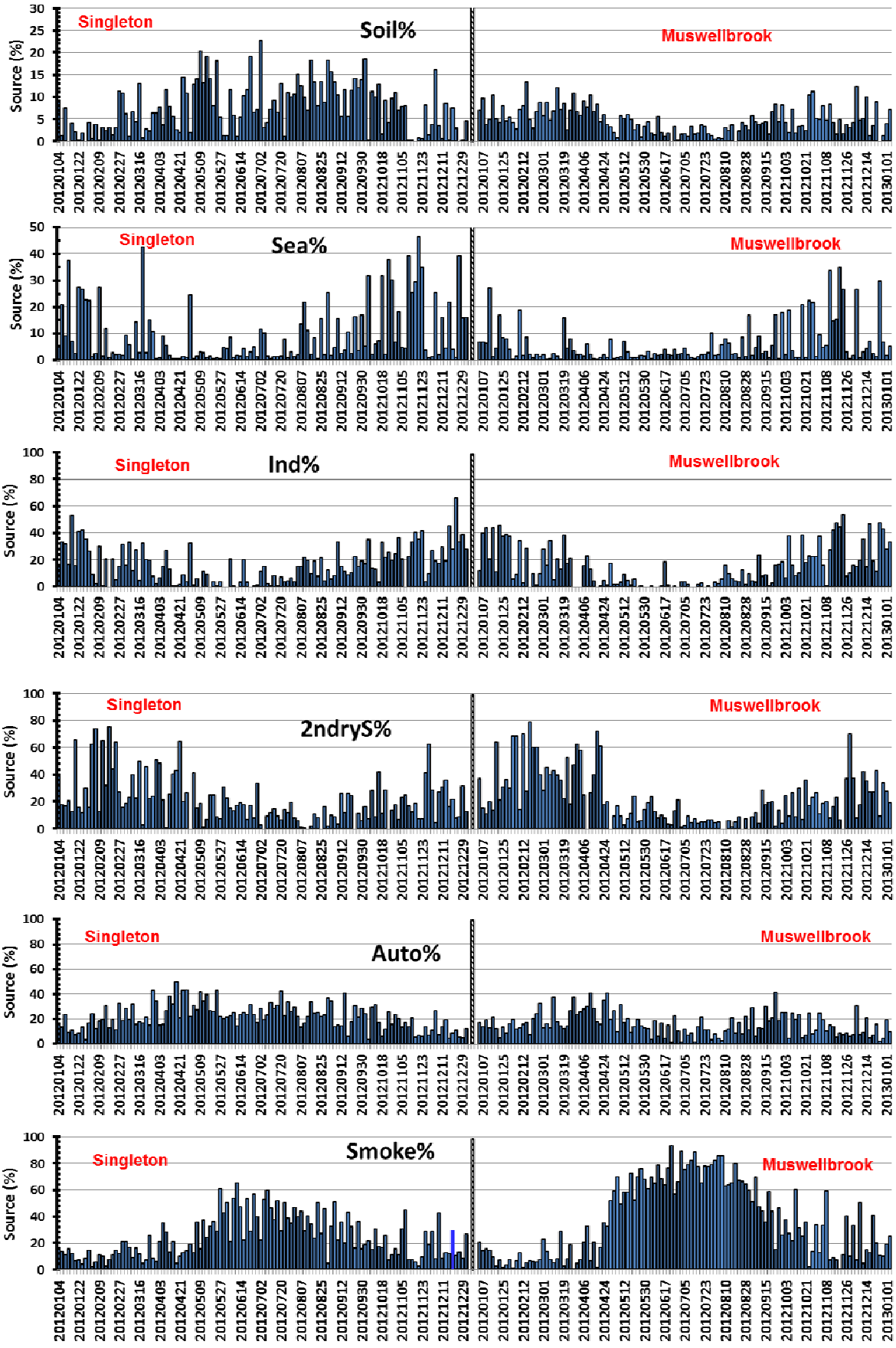

Figure A 10 Source fingerprint contributions with time (each day) from the ANSTO IBA PMF2 DOS analysis

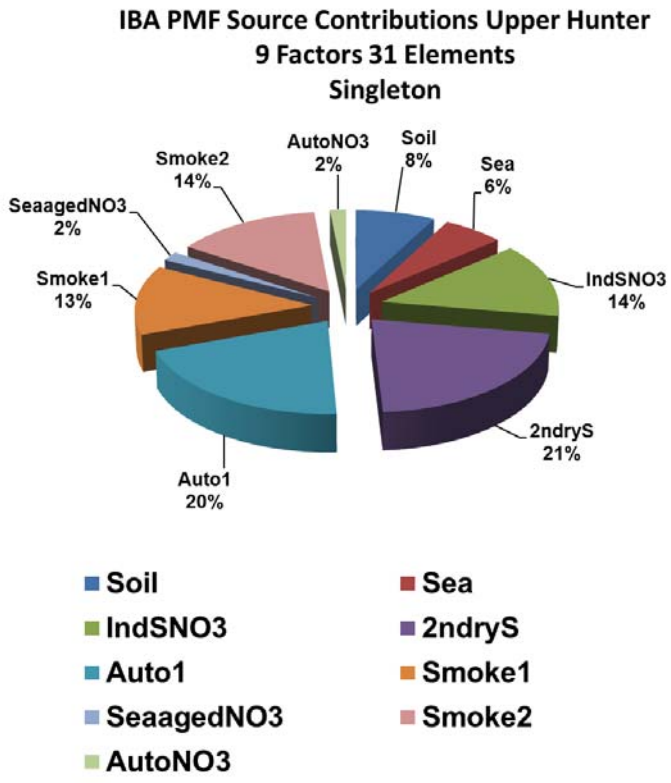

Figure A 11. Percentages are average contributions to the total $PM_{2.5}$ mass over the study period.

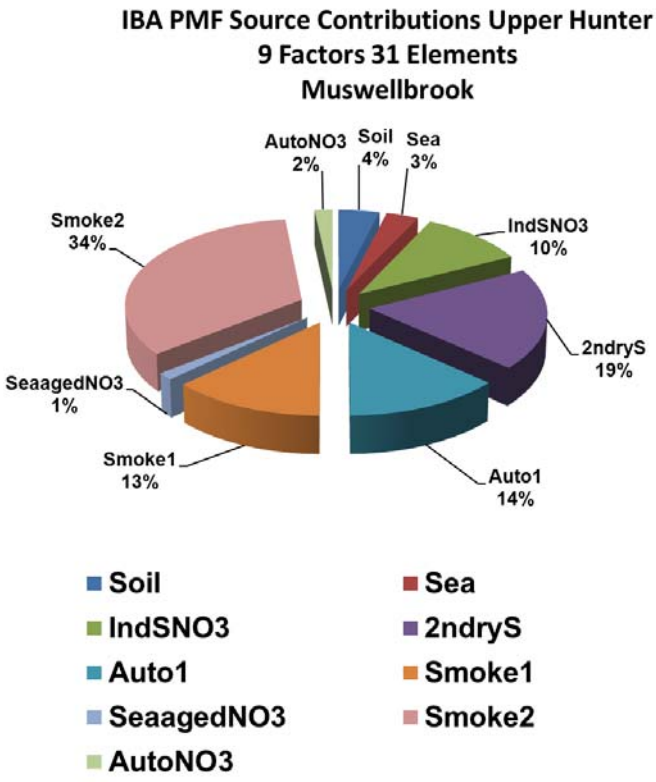

Figure A 12 Percentages are average contributions to the total $PM_{2.5}$ mass over the study period.

Note that although all the data from both sites (245 samples) were combined to generate the fingerprints in the ANSTO PMF2 DOS analysis, separate daily contributions were obtained for each site.

Figure A 13 shows slight correlation between F1 (Soil) and F5 (Auto) due to both having BC, Si and Al components, probably due to retrained soil kicked up by industrial vehicles. Other factors F1 to F9 are the same as those listed in Table A 2.No other significant correlations so this particular solution is producing reasonably unmixed factors or source fingerprints.

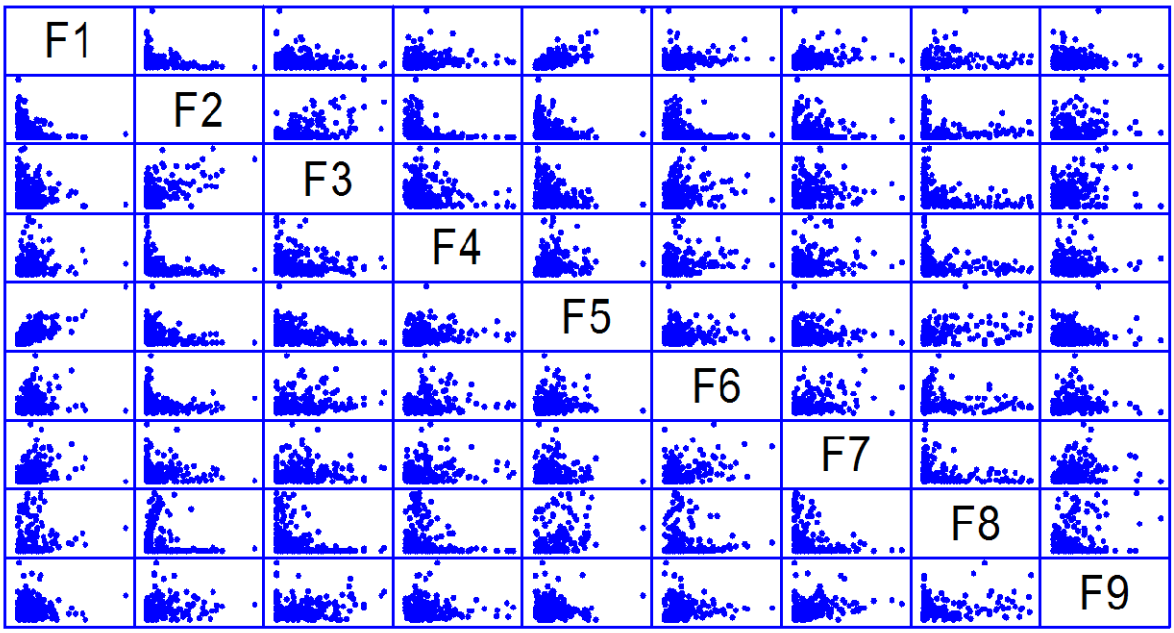

Figure A 13 The correlation plot for the nine factor ANSTO IBA PMF2 DOS analysis.

Figure A 15 shows excellent agreement between the PMF mass and the measured mass. Figure A 15 shows the daily time series plot of the predicted ANSTO IBA nine factor PMF2 DOS mass and the $PM_{2.5}$ gravimetric mass for both Singleton and Muswellbrook. The excellent agreement demonstrates that the nine factor ANSTO solution fits the 99% of the study days!

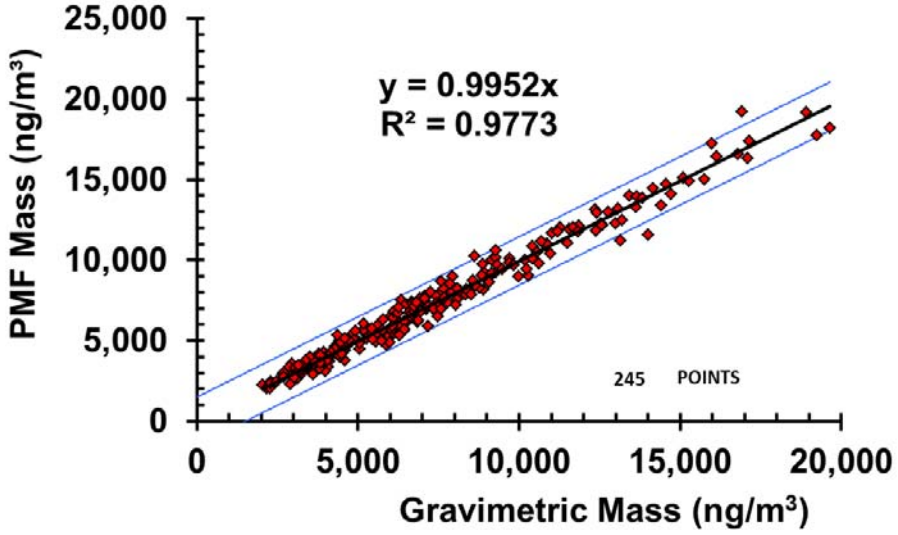

Figure A 14 A Plot of the sum of all nine PMF fingerprint masses versus the gravimetric mass for all the 245 ANSTO $PM_{2.5}$ Teflon filters for the study period. The tramlines either side of the linear fit represent the four standard deviation spread around this least squares fitted line.

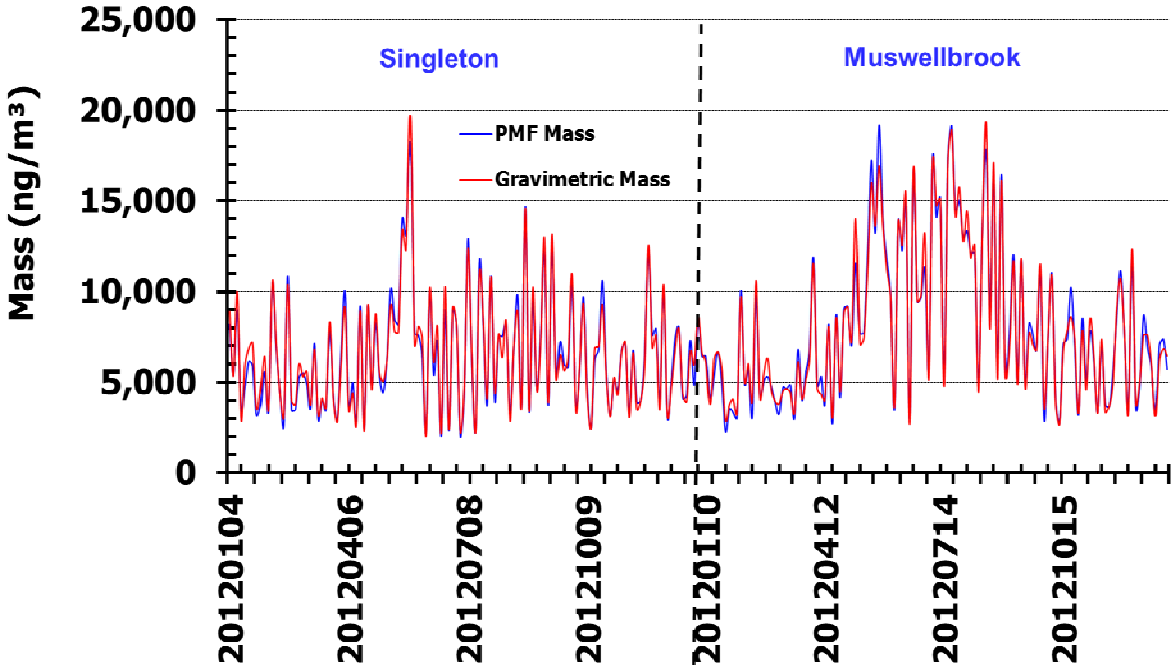

Figure A 15 A daily time series plot for both Singleton and Muswellbrook data of the predicted ANSTO IBA nine factor PMF2 DOS mass and the $PM_{2.5}$ gravimetric mass.

Table A 2 Average mass and percentage contribution to the $PM_{2.5}$ mass of each of the nine fingerprints from the PMF2 DOS analysis for the Singleton and Muswellbrook sites during the study period.

	Singleton	Muswellbrook		Singleton	Muswellbrook
	ng m^{-3}	ng m^{-3}		%	%
$PM_{2.5}$ Mass	6509±200	8106±250		100±3	100±3
F1 Soil	502±100	322±60		7.8±1.6	4.0±0.8
F2 Sea	387±40	255±25		6.0±0.6	3.1±0.3
F3 IndSNO3	898±45	845±41		13.9±0.8	10.4±0.5
F4 2ndryS	1392±50	1545±55		21.5±0.6	19.0±0.6
F5 Auto1	1316±120	1089±110		20.3±1.7	13.4±1.1
F6 Smoke1	842±50	1061±55		13.0±0.7	13.1±0.7
F7 SeaagedNO3	112±50	111±45		1.7±0.7	1.4±0.6
F8 Smoke2	918±30	2745±90		14.2±0.5	33.8±1.1
F9 AutoNO3	100±30	141±45		1.5±0.45	1.7±0.5
PMF Mass	6467±200	8112±250		100±3	100±3

Table A 3 Comparison of factors determined from the EPA PMF analysis (by CSIRO) and PMF2 DOS analysis (by ANSTO)

EPA PMF					PMF2 DOS			
Factor	**Species**	**Contribution at Singleton**	**Contribution at Muswellbrook**		**Factor**	**Species**	**Contribution at Singleton**	**Contribution at Muswellbrook**
Factor 1 Woodsmoke	levoglucosan, mannosan , OC1	14 ± 2%	30 ± 3%		Smoke2	BC, levo, H	14.2 ± 0.5%	33.8 ± 1.1%
Factor 2 Vehicle/Industry	BC, OC1, OC2, SO_4^{2-} Fe, Zn, Mn, Cu	17 ± 2%	8 ± 1%		Auto1	BC, Fe	20.3 ± 1.7%	13.4 ± 1.1%
Factor 3 Secondary Sulfate	NH_4^+, SO_4^{2-}	20 ± 2%	17 ± 2%		2ndryS	H, S, BC, NH_4^+	21.5 ± 0.6%	19.0 ± 0.6%
Factor 4 Biomass Smoke	OC2, OC3, OC4, K, SO_4^{2-}, Al, Si, Ti, BC	8 ± 2%	12 ±2%		Smoke1	H, K, BC, NO_3^-, oxalate	13.0 ± 0.7%	13.1 ± 0.7%
Factor 5 Industry Aged Sea Salt	Na^+, Mg^{2+}, SO_4^{2-} and with almost no Cl	18 ± 3%	13 ± 2%		IndSNO3	Na, S, BC	13.9 ± 0.8%	10.4 ± 0.5%
Factor 6 Soil	Al, Si, Ca, Ti and Fe	12 ± 2%	11 ± 1%		Soil	Al,Si, BC, K	7.8 ± 1.6%	4.0 ± 0.8%
Factor 7 Sea Salt	Na^+, Cl^-, and Mg^{2+}	8 ± 1%	3 ± 1%		Sea	Na, Cl, BC	6.0 ± 0.6%	3.1 ± 0.3%
					SeaagedNO3	Na, BC, Mg^{2+}, NO_3^-,H, Si, Fe, F^-	1.7 ± 0.7%	1.4 ± 0.6%
Factor 8 Secondary Nitrate	NO_3^- and includes some NH_4^+, Cl^-, Na^+, and OC	3 ± 2%	6 ± 1%		AutoNO3	NH_4^+, NO_3^-	1.5 ± 0.5%	1.7 ± 0.5%

CONTACT US

t 1300 363 400
+61 3 9545 2176
e enquiries@csiro.au
w www.csiro.au

YOUR CSIRO

Australia is founding its future on science and innovation. Its national science agency, CSIRO, is a powerhouse of ideas, technologies and skills for building prosperity, growth, health and sustainability. It serves governments, industries, business and communities across the nation.

FOR FURTHER INFORMATION

CSIRO Marine & Atmospheric Research
Mark Hibberd
t +61 3 9239 4400
e mark.hibberd@csiro.au
w www.csiro.au/cmar

CSIRO Marine & Atmospheric Research
Melita Keywood
t +61 3 9239 4400
e melita.keywood@csiro.au
w www.csiro.au/cmar